

# Bio-induced solid selenium for recovery from water

Simon Petrus Wilhelmus Hageman

## **Thesis committee**

### **Promotor**

Prof. Dr C.J.N. Buisman  
Professor of Biological Recovery and Re-use Technology  
Wageningen University

### **Co-promotors**

Dr R.D. van der Weijden  
Researcher, Sub-department of Environmental Technology  
Wageningen University

Prof. Dr A.J.M. Stams  
Personal chair at the Laboratory of Microbiology  
Wageningen University

### **Other members**

Prof. Dr J. van der Gucht, Wageningen University  
Dr M. Lenz, University of Applied Sciences and Arts Northwestern, Muttentz,  
Switzerland  
Prof. Dr N.A.J.M. Sommerdijk, Eindhoven University of Technology  
Dr PA González Contreras - Paques BV, Balk

This research was conducted under the auspices of the Graduate School Socio-Economic and Natural Sciences of the Environment (SENSE)

# Bio-induced solid selenium for recovery from water

Simon Petrus Wilhelmus Hageman

## **Thesis**

submitted in fulfilment of the requirements for the degree of doctor  
at Wageningen University  
by the authority of the Rector Magnificus  
Prof. Dr A.P.J. Mol,  
in the presence of the  
Thesis Committee appointed by the Academic Board  
to be defended in public  
on Friday 23 October 2015  
at 11 a.m. in the Aula.

S.P.W. Hageman  
Bio-induced solid selenium for recovery from water  
148 pages.

PhD thesis, Wageningen University, Wageningen, NL (2015)  
With references, with summary in English

ISBN 978-94-6257-510-3



## Table of contents

1 Introduction	page 1
2 Microbiological selenate to selenite conversion for selenium removal	page 23
3 Bio-production of selenium nanoparticles with diverse physical properties	page 47
4 Selenate reduction to produce recoverable elemental selenium at 50°C by granular sludge from an anaerobic reactor	page 73
5 Microbial selenium sulphide reduction for selenium recovery from wastewater	Page 91
6 General Discussion and outlook	page 127
7 References	page 139
Summary	page 147
List of Publications	page 149
Acknowledgements	page 151
About the author	page 153



# 1 Introduction

The main focus of this research was on removing selenium from wastewater, emphasising the potential for its microbial recovery. In this introduction, we first mention briefly the main selenium chemicals and selenium valences that are important in the context of this thesis. We go on to discuss the economic value and toxicity of selenium, and waste streams as a potential source of selenium – all good reasons to improve the bio-recovery of selenium from wastewater streams. Further, we explain selenate bio-reduction and the complexities involved in controlling the reduction process in the bioreactors as well as the stability of the selenium particle. Finally, we present two possible microbial reduction routes which we researched with the aim of obtaining larger selenium particles from wastewater.

## 1.1 Motivation for biological selenium recovery

### 1.1.1 Selenium

Selenium, element 34 in the periodic table, which is classified as a metalloid or a non-metal, belongs to the chalcogenide group. The chemical properties of selenium resemble those of sulphur (Wessjohann et al. 2007) and selenium, like sulphur, can be oxidized and reduced. It has four main redox valences: +6, +4, 0 and -2. The most important selenium chemicals discussed in this thesis are shown in Figure 1.1.

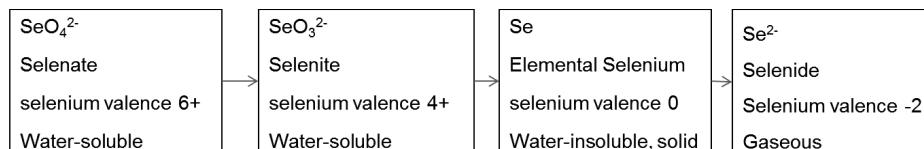


Figure 1.1: The four main selenium compounds discussed in this thesis.

### 1.1.2. Selenium applications

Selenium is used in a wide range of products. For an overview of uses of selenium see Table 1.1. Annual global production is estimated to be around 2500 tonnes (Group 2014, George 2014). In 2012 an estimated 40% was used for metallurgy processes and 25% in the manufacturing of glass (George 2014).

Elemental selenium, redox valence 0, has some metallic properties such as a metallic appearance. The main application of elemental selenium is for colouring and decolouring glass. Furthermore, it has photovoltaic and photoconductive properties (photovoltaic means that light is converted to electric energy and photoconductive means that light reduces electrical resistance). For both properties selenium is used in optical electronic devices, and for manufacturing these devices high-quality (pure) selenium is required. Selenium sulphide ( $\text{SeS}_2$ ) is the working compound in anti-dandruff shampoos and it may be present in concentrations of up to 2.5% w/v (Sanfilippo and English, 2006). Bioavailable selenate (6+) and selenite (4+) are used in the food industry, because selenium is an essential trace element for organisms including human beings. The human body needs an amount of 50-70  $\mu\text{g}$  Se per day (Högberg and Alexander 2007). A shortage of selenium intake causes complications such as infectious diseases and cardiovascular diseases. An overview of selenium shortage and related diseases is provided by Högberg and Alexander (Högberg and Alexander 2007). Selenide – selenium in its most reduced form (-2) – is a reactive compound and highly toxic in gaseous form. Selenide is used in combination with other elements such as copper and gallium in photovoltaic systems.

**Table 1.1: Products and applications for selenium**

	<b>Name of compound</b>	<b>Product/application</b>	<b>Source</b>
<b>1</b>	Sodium selenate	-Fertilizers	(Group 2014)
<b>2</b>	Sodium selenite	-Flat glass industry; Ceramic industry -Animal feed industry -Glass	(Group 2014) (Scalet et al. 2006)
<b>3</b>	Zinc selenite Barium selenite	-Container glass -Glass -Pigment industry	(Group 2014) (Scalet et al. 2006)
<b>4</b>	Selenium dioxide	-Galvanic industry -Manganese production	(Group 2014)
<b>5</b>	Selenium metal (Selenium with Tellurium, Chlorine, Arsenic, and others)	-Glass decolouring (<2 ppm) ,Glass colouring (above 20 ppm) -Pigments -Battery production -Solar cells -rectifiers -Photocopier drums -Digital x-ray techniques -Selenium micro-tubes (potential use in micro-photo devices) -electro optical applications - Improve machinability of copper, lead, and steel alloys	(Scalet et al. 2006) (Group 2014, George 2014)
<b>6</b>	Selenium (di)sulphide	Anti-dandruff shampoos - up to 2.5% w/v; variable – labels of several shampoo brands	(Sanfilippo and English 2006)
<b>7</b>	Cadmium sulphoselenide	Colouring plastics, ceramics and glass	(George 2014)

### **1.1.3. Selenium price and production**

The price of selenium varies with changes in global supply and demand. The supply of selenium is closely correlated with the production of other elements, such as copper and nickel, because selenium is an important by-product from mining. Sometimes the demand for selenium is strongly affected by increased demand in other industries, such as manganese production in China (George 2014) or the production of solar cells. In the period from 2010 to 2013, prices for selenium have fluctuated from 77-146 U\$ dollars per kg (George 2014)).

Most selenium is extracted during copper mining. The world's reserve selenium supply in copper mines is estimated to be around 120,000 tonnes (George 2014). Based on estimated current selenium production of 2500 tonnes per year (Group 2014), existing methods will only allow selenium to continue to be produced from copper mines for a period of approximately 48 years, so its potential extraction from waste streams is very interesting economically in the long run.

### **1.1.4 Selenium toxicity and selenium waste streams**

An amount of several mg of selenium oxyanions per kg of bodyweight per day is fatal for many animals (Högberg and Alexander 2007). A recommended upper limit for selenium in drinking water is 0.040 µg / litre (WHO 2011). Exceeding the standard intake of selenium, 50-70 µg per day (Högberg and Alexander 2007), results in selenosis, which leads to deformed hair, nails, teeth and skin lesions. The effects of selenium toxicity are reviewed by Högberg et al (Högberg and Alexander 2007), the link between selenium toxicity and cancer is described by Brozmanová et al (Brozmanová et al. 2010) and the impact of selenium on biological functions in the environment is discussed by Mehdi et al., (Mehdi et al. 2013).

Selenium can be released into the environment by the selenium processing industry. But agricultural use of selenium and burning fossil fuels, for example in coal-based power plants, also results in higher selenium concentrations in certain areas. Under certain conditions selenate and selenite can be formed. These compounds are mobile in water leading to harmful accumulations in the environment. The global cycles of selenium, including industrial influences and dangerous accumulations, are

documented in detail by Winkel et al., 2011 (Winkel et al. 2011).

Fortunately, most industries are required to limit discharges of selenium. The advised maximum for selenium discharge in industrial wastewater streams is 1 to 5 µg/L (Sandy and Disante, 2010). However, not all the wastewater streams or even natural water streams can meet this requirement. Table 1.2 briefly reviews some of these selenium waste streams.

**Table 1.2** Selenium waste streams

Source	Selenium amount	Remark
1 Selenium refinery plant Shinko Chemical Co. Ltd. Amagasaki City, Hyogo Prefecture.	two samples: 13.2 and 74 mg/L (mainly Selenite )	with pH 0.8 and 1.0 (Soda et al. 2011)
2 Autoclave leach solutions (Copper slimes)	0.197 to 4.00 g/L.	H <sub>2</sub> SO <sub>4</sub> varied between 26.8 and 112.9 g/l (Wang et al. 2003)
3 Coal mine waters Coal contains 0.5 to 12 ppm of selenium (George 2014)	Coal mining waste streams 22 to 500 µg/L Se	Variable flow, variable concentration, contain nitrate, low levels BOD and COD (Envirogen 2011)
4 Commonly in mining wastewater 3 to more than 12,000 µg/L (Envirogen 2011)		Gold mines 33 mg Se/L (McCloskey et al. 2008)
5 Petroleum refinery	Up to 1.8 mg/L Se	Several selenium compounds, including selenite and selenate. (de Almeida et al. 2009)
6 Effluent from refinery:	0,043 mg Se/L	(treated water) (Siddique et al. 2007)
7 Groundwater	Up to 0.34 mg Se/L	75-meter deep groundwater (Bajaj et al. 2011)
8 Secondary lead smelter effluent	2,75 mg/L Se(VI) 0,379 mg/L Se (IV)	Also Pb, Fe, Sb (McCloskey et al. 2008)



### **1.1.5 Examples of biological selenium removal systems**

Currently, several biological water treatment options with a focus on removal are known. To give an impression of the dimensions of these systems, we describe two examples in some detail: (1) A plug flow bioreactor filtration system with facultative anaerobic bacteria accumulated selenium solids, which uses molasses as an electron donor. The accumulated selenium solids are removed from the reactor with high back flush wash. Effluent is below 5 ppb. (Pickett and Harwood, 2012). (2)

Fixed-film fluidized bed reactors treating coal mine waters (line 3 Table 1-2).

Hydraulic retention time (HRT) is around 10 minutes per reactor vessel and the flow is 15,261 m<sup>3</sup>/day. Reactors can be placed in series and the working temperature is around 4° to 10°C. Important factors are the dissolved oxygen concentration 11-13 mg/L, pH value 7-8-9, nitrate concentration 6 to 40 mg/L (Envirogen 2011). Both examples involve the removal but not the recovery of selenium.

### **1.1.6 Key objective**

The key objective of this thesis is to increase the amount of recoverable selenium by producing larger bio-selenium particles.

## 1.2 Selenium reduction in (bio)reactors

To understand the effects of process conditions on biological selenium reduction processes, knowledge of both chemical and biological selenium reduction is required.

### 1.2.1 Chemical selenium reduction

With chemical selenate or selenite reduction the valence of the selenium atom is reduced (Figure 1.1) and electrons are accepted by the selenium atom. Such selenium reduction is a half reaction and, to complete the redox reaction, electrons need to be accepted from an oxidation reaction. The electron donor in chemical selenite reduction can be H<sub>2</sub>S (Pettine et al. 2011) and ascorbic acid (Pettine et al. 2013). For balanced redox reactions the number of electrons which are transferred in both the reduction and oxidation reaction should be equal. The energy release in the redox reaction is affected by conditions such as the concentration of the substrates, concentration of the products and the pH could also be involved.



In redox reactions the total energy of the full redox reaction is the result of the energy release from both the oxidation and the reduction reaction. The standard enthalpy of formation at 25°C for selenate is -441 kJ mol<sup>-1</sup> and for selenite -370 kJ mol<sup>-1</sup> (Amend and Shock, 2001). This means that the reduction of both compounds to elemental selenium reduces the energy release of the full redox reaction. The energy release in the full redox reaction is generated by the oxidation of the electron donor.

For selenium reduction reactions the energy release and the activation energy are important. For complete redox reactions, the selenate reduction to elemental selenium yields more energy compared to selenite reduction to elemental selenium. However, in many cases selenite is a more reactive compound and therefore the reaction with selenite will occur more readily. For example, this is true for selenite reduction using ascorbic acid (eq. 1.1) (Pettine et al. 2013) or sulphide, (eq. 1.2) (Pettine et al. 2011).

### 1.2.2 Biological selenium reduction

In biological systems, the enzymes involved in the redox reaction have the ability to reduce the activation energy and to affect the preference for reduction of the

selenium substrates. Selenate and lactic acid do not react at room temperature, even though the Gibbs free energy change of reaction is negative. However, this reaction can be catalysed with micro-organisms. The electron donor can be an organic compound such as lactic acid that is oxidized to  $\text{CO}_2$ , or partly oxidized to acetate (see Fig.1.2). The electron donor and the (partly) oxidized electron donor affect the energy release of the full redox reaction in which selenium is reduced. See Table 1.3 for biological conversions and the effect of pH on the Gibbs free energy.

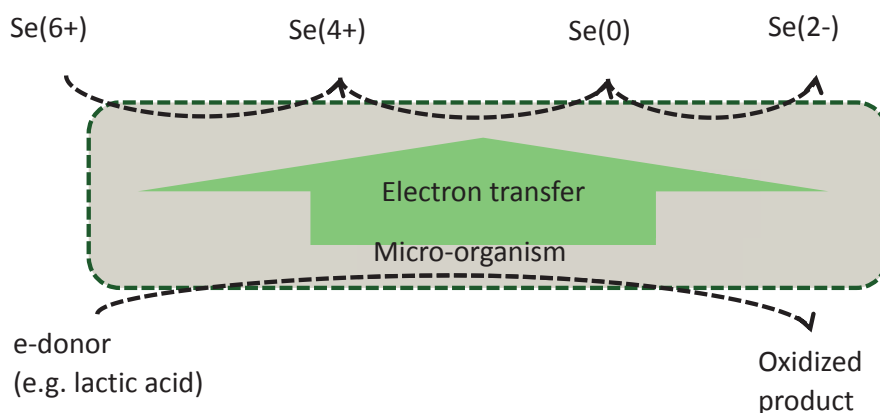


*Figure 1.2: Micro-organisms transfer electrons to selenium atoms. Upper side: selenium reduction. Lower side: electron donor oxidation.*

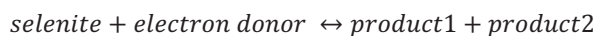
**Table 1.3** Selenium reduction reactions with organic compounds

Reaction	$\Delta G^\circ$ (kJ mol <sup>-1</sup> ) pH=0	$\Delta G^{\circ'}$ (kJ mol <sup>-1</sup> ) pH=7	$\Delta G^{\circ'}$ (kJ e <sup>-</sup> mol <sup>-1</sup> )
Fully oxidized electron donors			
1 3 acetic acid(aq)+4SeO <sub>4</sub> <sup>2-</sup> + 8H <sup>+</sup> ↔ 4 Se (s)+ 6 CO <sub>2</sub> (aq) + 10 H <sub>2</sub> O(l)	-1733	-1413	-59
2 3 lactic acid(aq) + 6SeO <sub>4</sub> <sup>2-</sup> +12H <sup>+</sup> ↔ 6Se(s) + 9CO <sub>2</sub> (aq) + 15 H <sub>2</sub> O(l)	-2779	-2299	-64
Partially oxidized electron donors			
3 lactic acid(aq)+2 SeO <sub>4</sub> <sup>2-</sup> ↔ acetic acid(aq)+ 2SeO <sub>3</sub> <sup>2-</sup> + CO <sub>2</sub> (aq) + H <sub>2</sub> O(l)	-342	-342	-86
4 3 lactic acid(aq)+2 SeO <sub>4</sub> <sup>2-</sup> +4H <sup>+</sup> ↔3 acetic acid(aq) + 2Se(s) + 3CO <sub>2</sub> (aq) + 5H <sub>2</sub> O(l)	-1046	-886	-74
5 lactic acid(aq)+SeO <sub>3</sub> <sup>2-</sup> +2H <sup>+</sup> ↔ acetic acid(aq)+Se+CO <sub>2</sub> (aq)+2H <sub>2</sub> O(l)	-352	-272	-68

*$\Delta G^\circ$  and  $\Delta G^{\circ'}$  values of selenium reduction reactions with organic electron donors at 25°C. Data obtained from Amend and Shock 2001. At 298 K, comparing biochemical conditions (pH=7) corresponds with an energy shift of 40 kJ per H<sup>+</sup> involved in the reaction.*

### 1.2.3 Control of chemical and biological selenite reduction

Because selenite is reactive and is involved in many reactions, the difference between how the chemical and biological controls work is explained below. Both the chemical and biological reactions can be described as follows:



The products can be for example elemental selenium, selenium sulphide or a partly oxidized electron donor. As an example, the reaction rate as a function of the temperature for both chemical and biological processes is described below. When a chemical reaction follows the Arrhenius equation, the reaction has a higher rate at a higher temperature. Every temperature corresponds to a certain reaction rate. However, the biological rate is the highest at a certain temperature (optimal). The more the temperature has a set-off (either lower or higher) from the optimal T, the less selenium is reduced and the reaction rate is reduced. The example of temperature in combination with the Arrhenius equation is illustrative for other controls, Fig. 1.3).

In biological selenium reduction processes in a bioreactor, selenite can also react chemically with biomass as electron donor (Falcone and Nickerson 1963) or with a biologically produced sulphide.

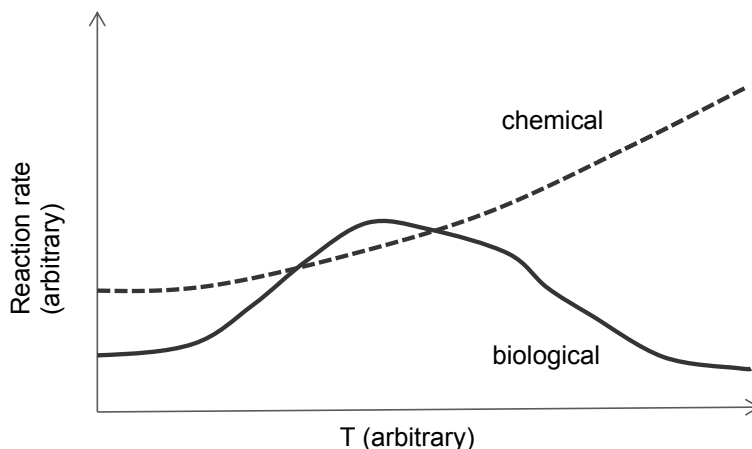


Figure 1.3: Difference between biological and chemical control with Arrhenius kinetics. Biomass has an optimum temperature and reaction rates are controlled differently.

#### 1.2.4 Possible microbial selenium products

Various micro-organisms can reduce selenium and produce a variety of selenium products. Here is a brief overview: (1) Micro-organisms reduce selenium oxyanions and conserve energy for growth (Oremland et al. 1994). (2) In some cases, micro-organisms reduce selenate and selenite to elemental selenium for detoxification. This process is not coupled to growth. (3) Another detoxification route is via the methylation of selenium compounds. Methylated selenium compounds are volatile and can be released into the air (Chasteen and Bentley 2003). (5) Selenate is also reduced by sulphate-reducing bacteria, for example *Desulfovibrio desulfuricans* (DSM 1924) (Tomei et al. 1995) and (6) nitrate-reducing bacteria, for example *Desulfurispirillum indicum* S5<sup>T</sup> (Rauschenbach et al. 2011). So biomass type and metabolic activity should be controlled to avoid selenium losses to unwanted products.

### 1.2.5 Control of microbial selenium products in an open bioreactor

The type of micro-organism is selected according to the process conditions. The micro-organisms with the highest net growth rate will outcompete other micro-organisms in the reactor. Often this results in a mixed culture in which substrates are degraded by physiologically different micro-organisms. In an open reactor methanogenesis, sulphate reduction, and denitrification may interfere with selenium reduction. Control can be achieved by the choice and concentration of the electron donor, pH, temperature, redox, (solid retention time) SRT, up-flow velocity, and hydraulic retention time (HRT). Based on energy calculations, the electron donors will be used first for selenate reduction, then for sulphate reduction and finally for methane production.

Temperature control or the addition of chemicals to the reactor can be easily controlled technically during operation. On the other hand, some process conditions are difficult to control, especially the composition of the selenium waste streams: e.g. the low pH of acid main drainage or if the wastewater has a high salt content. Selenate reduction in sediments was observed by Steinberg and Oremland at salinity ranges between 1 to 250 g/L, but not at 320 g/L, (Steinberg and Oremland 1990). Selenate reduction by sediment cultures can be inhibited by compounds such as  $\text{NO}_3^-$ ,  $\text{NO}_2^-$ ,  $\text{MoO}_4^{2-}$ ,  $\text{WO}_4^{2-}$  (Steinberg and Oremland 1990). On the other hand some of these elements, applied in low concentrations, are beneficial for selenate reduction since the reduction process is catalysed by a molybdenum-dependent, membrane-bound enzyme in *Enterobacter cloacae* SLD1a-1 (Watts 2003). The appearance of Fe(III) in the medium costs electron donor when *Anaeromyxobacter dehalogens* is used as a biocatalyst because selenite and Fe(III) can be simultaneously reduced (He and Yao, 2010). Ca and Mg as divalent cations could affect the bioavailability of selenate and selenite (Torres et al. 2010), hindering their reduction. These examples show the complexity of the controls.

### **1.2.6 Advantage of biological removal above chemical removal**

For chemical processes, when sulphate is present in waste streams it interferes with chemical selenate removal because of selenate's chemical similarities with sulphate, (McCloskey et al. 2008). This results in low selenium purity (mixed product) and high electron donor costs (ineffective reagent addition). For selenate removal an unselective chemical is often needed. The chemical and the selenate need to make contact with each other during the reduction process, and this is a disadvantage at low selenate concentrations and expensive at high selenate concentrations. The advantage of biological selenium removal is the ability to control the selectivity of the micro-organisms to reduce a certain substrate.

Various chemical selenium reduction reactions are possible and a variety of selenium products can be obtained. Here are three examples of reduction steps that are important in this thesis: Brimmer et al., 1987 demonstrated the conversion of selenate to selenite in 6 mol HCl in 30 minutes and 91°C, Mondal et al, 2004., described selenate conversion directly to elemental selenium with Fe and FeNi, whereby selenite can be reduced to elemental selenium using NaHSO<sub>3</sub> as reducer (Harańczyk et al. 2002) (Wang et al. 2003). These examples demonstrate that, although chemical treatment is possible, the compounds that are added need to be neutralized afterwards. For this reason, environmentally friendly biological treatment has a considerable advantage.

## **1.3. Formation of bio-selenium particles**

### **1.3.1 Desired selenium particles for recovery**

Selenium particles can be recovered by liquid solid separation. Filtration can be used, depending on the size of the selenium particles. When applying a sedimentation method, the difference between the density of the liquid and the particles is important (see Appendix 1A). It would benefit the selenium recovery process if it were possible to produce selenium with a high density and with particles as large as possible. The density of trigonal selenium is 4.819 g cm<sup>-3</sup> and the density of the amorphous structure is 4.270 g cm<sup>-3</sup> (Minaev et al. 2005). This is why the preferred method of producing crystalline hexagonal selenium was adopted in this research.

### 1.3.2. Bio-selenium product stability

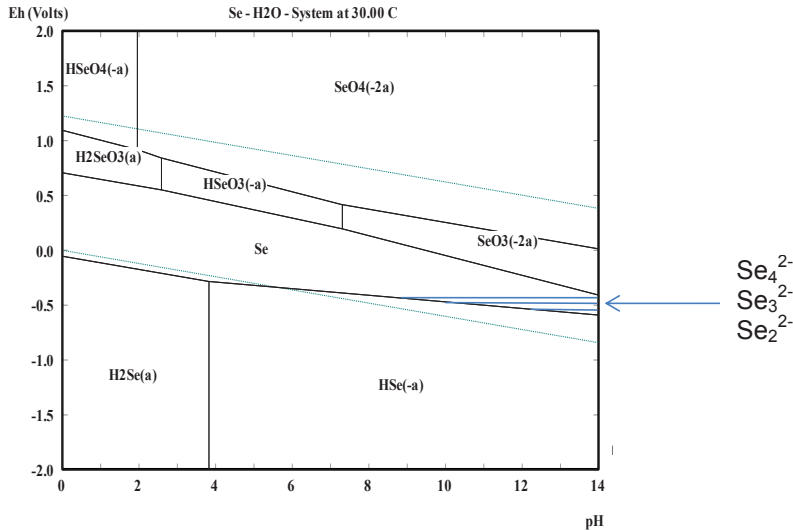


Figure 1.4: Pourbaix diagram of selenium species in water. Calculations were made with 10 mM selenium at 30°C with the program HSC chemistry 6 (source Ourtotec). Polyselenides exist and are more reduced than the solid structure. Polyselenide areas ( $\text{Se}_4^{2-}$ ,  $\text{Se}_3^{2-}$ ,  $\text{Se}_2^{2-}$ ) are drawn manually from an example presented by Iida et al., 2010 and the areas are indicative. The  $\text{Se}_4^{2-}$  is the dominant species at pH between 9 and 13, (Iida et al. 2010).

Microbial reduction and chemical reduction are the two reduction options for selenium in reactors. Thermodynamics still influences the product's final stability. An interesting tool for demonstrating this is the pH vs. redox diagram, the Pourbaix diagram. The Pourbaix diagram displays the chemically main stable selenium compound at a certain pH and redox value.

The effect of pH on the selenate and selenite speciation is visible. When the redox potential in the reactor is low, selenium can be further reduced to selenide (Fig. 1.4). In its most reduced state, selenium ( $\text{Se}^{2-}$ ) can form solid selenides with for example Zn (Pearce et al, 2008) and it can be immobile, but also volatile and mobile. Selenide ( $\text{H}_2\text{Se}$ ) is a volatile, highly toxic compound. In addition, it is very reactive and can be oxidized to elemental selenium by the addition of oxygen.

Selenite reduction to elemental selenium in the presence of oxygen by *Zoogloea*



*ramigera* (Srivastava and Mukhopadhyay 2013), *Pseudomonas alcaliphila* (Zhang et al. 2011), *Bacillus cereus* (Dhanjal and Cameotra 2010) and *Bacillus* species NS3 EU573774.1 (Tejo Prakash et al. 2009) has been reported. The disadvantage of these reactions at aerobic conditions is that the elemental selenium produced under such high redox conditions tends to oxidize again since selenate is energetically the most stable selenium form under these conditions (Fig. 1.4).

### 1.3.3 Principle of selenium particle formation

Elemental selenium is insoluble in the water phase. Consequently, bio-produced elemental selenium will precipitate to particles in the medium of the bioreactor. During selenate and selenite reduction polyselenium is formed.



The exact mechanism is unclear and a combination of these reactions is possible.

Polyselenium molecules grow and selenium chains elongate further.

During the selenium chain elongation some of these molecules are more stable than others. When  $n=6$  or  $n=8$ , selenium molecules can form a ring. This ring is a relatively stable form of a selenium molecule (Hohl et al., 1987).

The production of either uniform selenium molecules or molecules that enable a repetition in a solid structure increases the probability of crystal formation. Crystal structures have the ability to grow in size, which is desirable in the recovery process. So one of the aims of this research was to produce large, uniform selenium molecules. An example of how selenium molecules are built and finally form a crystalline structure is shown in Figure 1.5.

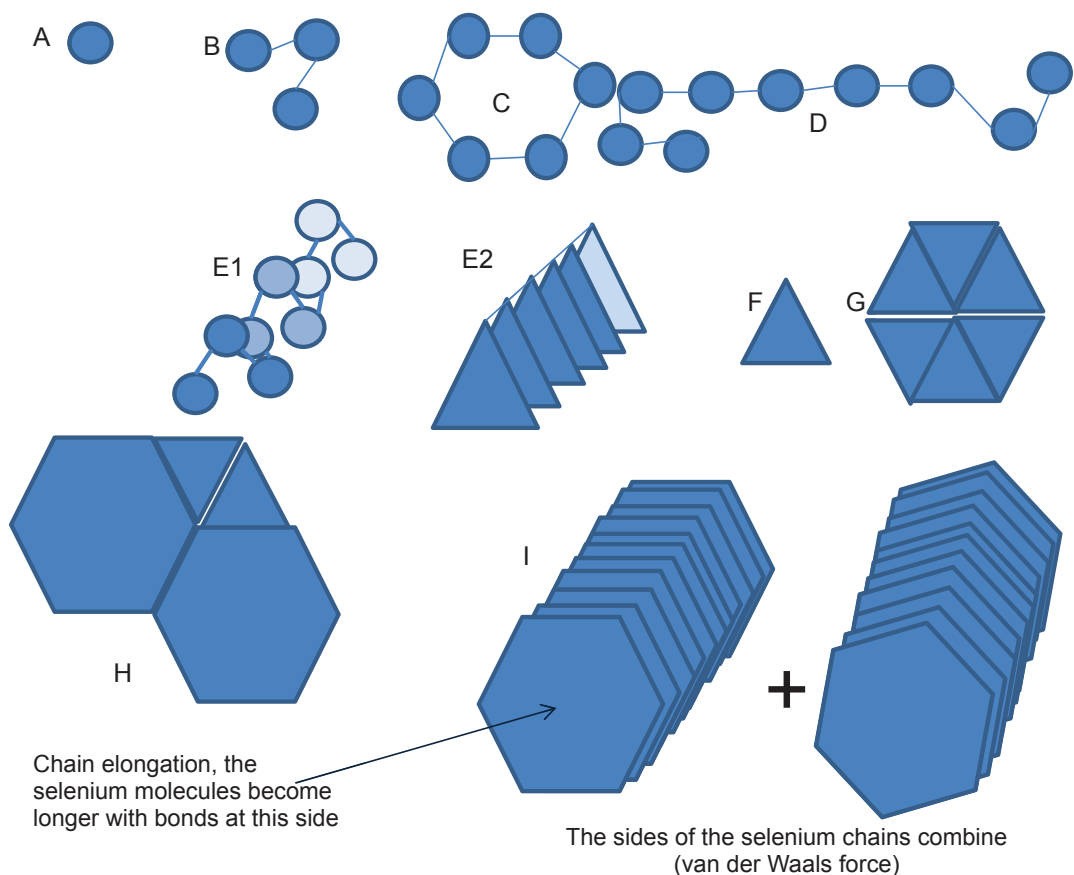


*Figure 1.5: Building selenium structures. A, single selenium atom. B, triatomic selenium molecule. C, selenium ring of 6 atoms. D, selenium chain. E1, Most stable form of a selenium chain, the trigonal structure like a winding staircase. E2, abstract form of the trigonal structure. F, side surface of trigonal selenium. G, trigonal selenium sticks together, energetically favourable. A hexagonal structure can be formed. H, combinations of trigonal selenium growing thicker (Mondal et al., 2008). I, trigonal or hexagonal selenium with indicated particle growth places. The arrow indicates a tip-end, at which molecules grow longer (Xi et al., 2006). The “+” indicates the growth in size of the selenium particles (van der Waals force).*

## **Hexagonal crystalline selenium**

The most stable forms of selenium is hexagonal (trigonal). Selenium atoms form a long chain and are structured like a winding staircase in which three selenium atoms are needed to make one winding (Mondal et al., 2008). A long selenium molecule is formed in a triangular shape and the chain can be elongated at the end of both selenium tips. As a result the (poly)selenium molecules can grow (Figure 1.5).

## **Red amorphous selenium**

Selenium occurs as mixed molecules in amorphous particles, and the polyselenium molecules often have different sizes. Among these are  $\text{Se}_8$ ,  $\text{Se}_6$  rings and longer chain structures (Minaev et al., 2005). The transformation temperature required for the transition towards a more crystalline structure is room temperature.

### **1.3.4 Biological selenium particle production rate**

Precipitation of selenium is the result of supersaturation. Fast precipitation can result in an amorphous structure. However, slow precipitation can result in a crystalline structure, since the selenium atoms or molecules are then likely to be positioned in a crystal structure.

The volumetric selenium production rate is important for particle formation (saturation) and it also affects the morphology of the selenium particles (Harańczyk et al. 2002). When the microbial biomass is doubled, the volumetric production rate in the reactor can be doubled. However, when the microbial biomass is doubled, the volumetric production rate per biomass remains unchanged. In this case selenium particle formation may be unchanged regardless of the amount of biomass in the reactor.

### **1.3.5 Abiotic control**

Once selenium nanoparticles have been formed and the reduction capacity of the biomass is no longer important, the particles and biomass can be removed from the bioreactor. Process conditions can be changed to bring about selenium particle modifications. Several techniques can be used to achieve the desired particle properties. For example, the solution can be heated to start phase transformation from amorphous selenium to hexagonal selenium (Lenz et al. 2009).

### **1.3.6 Particle formation and time**

All of the steps from selenate reduction to particle formation require time. In short: you start with the reduction of selenate to selenium, followed by the formation of molecules, the formation of particles and end with the stabilisation of these particles. All of these processes need time and need to be properly controlled to improve product stability and finally form sufficiently large, dense selenium particles, which is the aim of this research.

Se-oxyanion → Se-atom → Se molecules → Se-particle formation → growth and stabilization

### **1.3.7 Influence of the organic compounds**

Selenium has hydrophobic properties and can attract other hydrophobic molecules such as organic molecules. These molecules may cover the selenium molecules in such a way that selenium particle growth is altered or even blocked (Mondal et al., 2008). Amorphous spherical selenium particles are stabilized by biomolecules. This means that the ratio of selenium to biomass should be as high as possible.

The start of selenium particle formation can also be influenced by biomolecules, as the biomolecules act as seeds and selenium particles start to grow with the biomolecule as the starting point. This has been demonstrated in several chemical selenium reduction experiments in which the addition of organic compounds alters the final selenium particle shape (Mondal et al., 2008)

## 1.4 Main hypothesis and outline

The main objective in this thesis is to improve the recovery of bio-selenium from selenate or selenite waste streams, by producing selenium particles that are as large as possible. Two routes are examined: (1) selenate reduction directly to elemental selenium, (2) from selenate via selenite and  $\text{SeS}_2$  to elemental selenium (Fig. 1.6).

For the bio-recovery route via selenite it is essential that all selenate can be bio-converted into selenite (**Chapter 2**). Since the reduction of selenate to selenite gains more energy per electron compared to direct selenate reduction to elemental selenium, it might be possible to reduce selenate to selenite using a low amount of electron donor. At high electron donor concentrations the reducing capacity could be strong enough to reduce selenite further to elemental selenium. It is hypothesized in Chapter 2 that at low electron donor concentrations selenite will be the main product during selenate reduction.

Selenate can also be converted directly to elemental selenium. **Chapters 3 and 4** focus on the direct production of elemental selenium particles from selenate. **Chapter 3** focuses on the influence of temperature and pH on particle formation. In this chapter it is hypothesized that at a higher temperature phase transformation from amorphous to hexagonal selenium can be induced and a higher pH could change the formation of the selenium molecules as building blocks. Based on the outcome of **Chapter 3**, settings are arranged to produce crystalline selenium particles continuously in a long experiment lasting eight months to allow crystalline selenium particles to grow at  $50^\circ\text{C}$ . This is described in **Chapter 4**. It is hypothesized that crystalline selenium particles can grow in that time period at  $50^\circ\text{C}$ .

Literature study indicates that there is an interaction between sulphur and selenium in several processes (Frenkel et al. 1991, Ball and Milne 1995, Kice et al. 1980). Selenite is a reactive compound and it reacts with sulphide to form selenium sulphide ( $\text{SeS}_2$ ) (Geoffroy and Demopoulos 2011). It would be interesting to explore whether it is possible to further reduce the sulphur or selenium. If elemental selenium could be obtained in this way, a new method for the recovery of selenium would be achieved. Moreover, selenium particle formation follows a different route. This can provide valuable information about the selenium reduction mechanisms in the direct route for selenium reduction. Biological  $\text{SeS}_2$  reduction is described in **Chapter 5**.

In the general discussion in **Chapter 6** ways of improving the particles size of recovered bio-selenium are discussed. Within this discussion direct selenium particle formation (**Chapters 3 and 4**) and the route via  $\text{SeS}_2$  (**Chapters 2 and 5**) are compared. Finally a vision for future research on biological selenium recovery from waste streams is provided. The experimental outline is visualised in Figure 1.6.

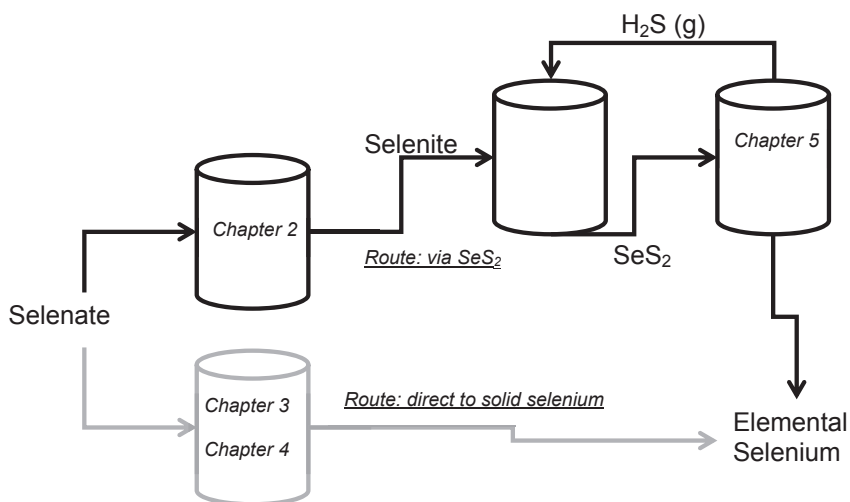


*Fig 1.6: Selenium bioreactors and chapters. The bio-reduction of selenate to selenite is discussed in **Chapter 2**. The direct bio-reduction of selenate to elemental selenium is discussed in **Chapters 3 and 4**. **Chapter 3** deals with the effect of pH and temperature on selenium particle structure. **Chapter 4** describes an attempt to improve selenium particle growth in a long-term experiment. **Chapter 5** describes the result of an alternative biological reduction route via selenite and selenium sulphide to elemental selenium.*

## Appendix 1A Effect of particle size on the sedimentation velocity

Sedimentation velocity of a particle in liquid ( $\text{m s}^{-1}$ ) can be calculated

$$v_{\text{sedimentation}} = \frac{2(p_p - p_l)g}{9u_l} r^2 \quad (1)$$

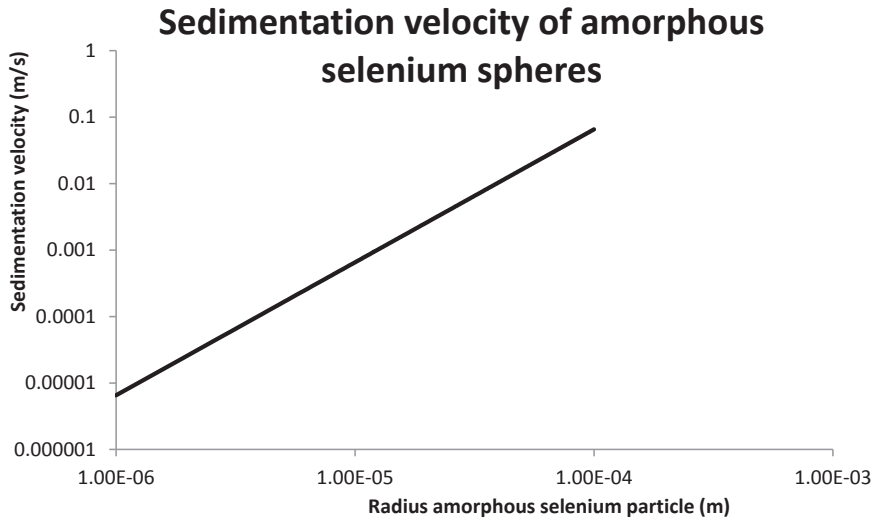
$p_p$  = particle density ( $\text{kg m}^{-3}$ )

$p_l$  = liquid density ( $\text{kg m}^{-3}$ )

$g$  = acceleration by gravitation ( $9.81 \text{ m}^{-1} \text{ s}^{-2}$ )

$u_l$  = dynamic viscosity ( $\text{kg m}^{-1} \text{ s}^{-1}$ )

$r$  = radius of the sphere (m)



Given for amorphous selenium:  $p_a = 4280 \text{ kg/m}^3$  and  $p_l = 1000 \text{ kg/m}^3$  and the water dynamic viscosity  $= 1 \cdot 10^{-3} \text{ kg m}^{-1} \text{ s}^{-1}$  the plot is constructed according to:

$$v_{\text{sedimentation}} = \frac{2(p_p - p_l)g}{9u_l} r^2$$

$V = \frac{4}{3}\pi r^3$  Volume of a sphere ( $\text{m}^3$ )

$p_{p=\frac{M}{V}}$  Density as mass per volume ( $\text{kg m}^{-3}$ )

$M$  = Mass (kg)

$V$  = Volume ( $\text{m}^3$ )

With a certain amount of mass  $M$ , the radius of a round particle can be expressed as a function of the density. With the recrystallisation of amorphous selenium to the crystalline structure, the total mass remains the same, while the radius of the particles decreases as the density increases.

$$r = \left( \frac{M}{\frac{4}{3} p_p \pi} \right)^{\frac{1}{3}}$$

Substitution of the radius in the sedimentation velocity equation results in the ratio between the sedimentation velocity of the amorphous particles and the crystalline particles:

$$\frac{v_{amorphous}}{v_{crystalline}} = \frac{(p_a - p_l) p_a^{\frac{2}{3}}}{(p_c - p_l) p_c^{\frac{2}{3}}}$$

Given for amorphous selenium  $p_a = 4270 \text{ kg/m}^3$ , and  $p_c = 4819 \text{ kg/m}^3$  and for the liquid it is  $p_l = 1000 \text{ kg/m}^3$  the maximum increase for sedimentation rate by selenium recrystallisation from amorphous to hexagonal selenium is:

$$\frac{v_{amorphous}}{v_{crystalline}} = \frac{(p_a - p_l) p_a^{\frac{2}{3}}}{(p_c - p_l) p_c^{\frac{2}{3}}} \approx 0.8$$

Through recrystallisation the sedimentation velocity of amorphous selenium can be increased by 25%.



## **Chapter 2**

### **Microbiological selenate to selenite conversion for selenium removal**

This chapter has been published as:

Microbiological selenate to selenite conversion for selenium removal

Simon P.W. Hageman,  
Renata D. van der Weijden,  
Jan Weijma,  
Cees J.N. Buisman

Water Research

Volume 47, Issue 7, 1 May 2013, Pages 2118–2128

doi:10.1016/j.watres.2013.01.012

## Abstract

Removal of the toxic selenium compounds selenite and selenate from waste water before discharge is becoming increasingly imperative in industrialized countries. Bacteria can reduce selenate to selenite, but also further to elemental selenium, selenide or organic selenium. In this paper, we aim to exclusively bio-reduce selenate to selenite in an open high-rate bioreactor. This conversion could be part of a two-stage process in which the selenite is subsequently reduced by chemical means under optimal conditions to produce a biomass-free selenium product. In the process, yield and reduction rate of biological selenate to selenite should be maximized, while formation of elemental selenium, selenide and organic selenium compounds should be avoided. Fed-batch experiments with a liquid volume of 0.25 to 0.75 litre at different temperatures 20-30-40-50°C, pH settings 6-7-8-9, initial biomass concentration of 1 or 5 g wet weight granular Eerbeek sludge and various lactic acid concentrations were performed to determine their effect on the biological conversion of selenate to selenite. Furthermore, the effect on selenite losses by further biological reduction or, if present, chemical reduction was investigated as well. Optimal selenate reduction to selenite was found at 30°C and pH 6 or 7 or 8 with 25 mM selenate and 13.75 mM lactic acid in the influent, with a selenite yield of 79-95%. In all the other conditions, less selenate was reduced to selenite. Also a 5 times higher electron donor concentration resulted in less selenite production, with only 22% of the selenate converted to selenite. The high yield and the high biological reduction rate of at least 741 mg Se/g initial VSS/day detected in the 1 g initial biomass experiment implicate that biological selenate conversion to selenite is a feasible process.

## 2.1 Introduction

Increased energy prices, depletion of valuable resources and stricter environmental policies are forcing industries to look for alternative or improved processes to remove harmful and valuable compounds from waste waters: Bioconversions could help to remove or recover components and have therefore received more attention from the metal mining and metal processing industries in the last decades. Microbes can reduce or oxidize elements from metallurgical waste streams and compete with chemical reduction and oxidation processes regarding chemical and energy consumption.

For industries, one such element in waste water is selenium. Selenium pollution is worldwide and is associated with human activities (Lemly, 2004). The LD<sub>50</sub> for many Se-compounds ranges between 1.5 and 6 mg/kg body weight for different animal species (Högberg and Alexander, 2007). For humans, adverse effects of clinical selenosis were detected at an intake of 1200 µg Se/day (Högberg and Alexander, 2007). Therefore, selenium in waste water has to be removed before discharge. Selenium is often speciated as the highly toxic selenium oxyanions selenate and selenite (Torres et al., 2010). Selenate containing streams can be treated with methanogenic or sulfate reducing reactors (Lenz et al., 2008a), through which the produced elemental selenium particles were mainly retained in the biomass. Due to this, the selenium product is not very pure. When selenate is converted exclusively to selenite, this would allow alternative processes to subsequently remove selenite. For example by further bio-conversion to reduce selenite to solid selenium (Soda et al., 2011), chemical adsorption (Zhang et al., 2008), chemical reduction by ferric salts (Murphy, 1988), chemical reduction with hydrogen (Puranen et al., 2010) or sulphide (Geoffroy and Demopoulos, 2011; Hockin and Gadd, 2003). This has the advantage that the selenium precipitation can be controlled independent from the bioreactor conditions, possibly resulting in faster reaction kinetics and a purer product.

Selenate can be reduced to selenite chemically. Chemical selenate reduction needs a strong reducing agent that reduces selenate to selenite, e.g.  $\text{SeO}_4^{2-} + 4\text{H}^+ + 2\text{Cl}^- \rightarrow \text{H}_2\text{SeO}_3 + 2\text{H}_2\text{O} + \text{Cl}_2(\text{g})$  in 10 M HCl at 60°C (Bye and Lund, 1988), or directly to selenium, e.g. reduction with ferrous hydroxide (Murphy, 1988). The strong reducing agent is not directly reusable after it has been oxidized in the chemical process. The

alternative, biological selenate reduction to selenite, has the advantage that the biomass uses a renewable organic electron donor as reducing agent, e.g. lactic acid. Furthermore, the biological reaction proceeds under mild environmental conditions requiring less energy and chemicals than the chemical reduction.

Selenate can be reduced to selenite mainly for respiratory processes for sustaining metabolic activity, e.g. by strain SES-3 (Oremland et al., 1994). However, in mixed cultures such as in open bioreactors, elemental selenium is the common end product of selenate reduction, with volatile methylated selenium or selenide as side products (Lenz et al., 2008b; Zehr and Oremland, 1987). These microbial reductions should be avoided if the aim is to maximize selenite production. In general, the reduction of selenate yields more Gibbs free energy per electron than the reduction of selenite to selenium (Table 2.1). This indicates that the selenate to selenite conversion may outcompete the selenate/selenite to selenium conversion under substrate limiting conditions.

**Table 2.1**-Free energy change of reactions with different Se electron acceptors using hydrogen as electron donor.

Reaction	$\Delta G$ (kJ / mol electron) <sup>a</sup>						
	pH=6 T=30°C	pH=7 T=30°C	pH 8 T=30°C	pH 9 T=30°C	pH=7 T=20°	pH=7 T=40°C	pH=7 T=50°C
(1) $\text{SeO}_4^{2-} + 3\text{H}_2 + 2\text{H}^+ \rightarrow \text{Se} + 4\text{H}_2\text{O}$	-67.0	-65.1	-63.2	-61.2	-65.9	-64.3	-63.5
(2a) $\text{SeO}_4^{2-} + \text{H}_2 \rightarrow \text{SeO}_3^{2-} + \text{H}_2\text{O}$	-80.5	-78.1	-76.9	-76.7	-78.7	-77.4	-76.9
(2b) $\text{SeO}_4^{2-} + \text{H}_2 + \text{H}^+ \rightarrow \text{HSeO}_3^- + \text{H}_2\text{O}$	-80.5	-78.1	-76.9	-76.7	-78.8	-77.4	-76.7
(3a) $\text{SeO}_3^{2-} + 2\text{H}_2 + 2\text{H}^+ \rightarrow \text{Se} + 3\text{H}_2\text{O}$	-60.3	-58.6	-56.3	-53.5	-59.5	-57.7	-56.8
(3b) $\text{HSeO}_3^- + 2\text{H}_2 + \text{H}^+ \rightarrow \text{Se} + 3\text{H}_2\text{O}$	-60.2	-58.6	-56.3	-53.5	-59.4	-57.7	-56.8

<sup>a</sup> $\Delta G$  values were calculated with data from (Amend and Shock, 2001) Calculations were corrected for temperature, pH, and concentrations of the chemical compounds: partial hydrogen pressure  $\text{H}_2$  was 0.010 atm, selenate concentration was 5 mM, Se concentration was 5 mM and  $\text{SeO}_3^{2-}$  concentration was calculated with  $pK^*a=7.306$  and a total  $\text{HSeO}_3^- + \text{SeO}_3^{2-}$  concentration of 5 mM.

The Gibbs free energy per electron for the Se reduction reactions mentioned in table 2.1 increases with higher pH and higher temperature. Additionally, the difference in  $\Delta G$  between reaction 2 and reaction 3 in table 2.1 becomes greater at a higher pH and higher temperature. Although the  $\Delta G$  differences in table 2.1 is small, from an energetic point of view, a smaller amount of selenite losses by further reduction is expected in the high pH-range and high temperature-range.

The reduction of selenate to selenite is pH-neutral if  $\text{SeO}_3^{2-}$  is formed (Table 2.1). According to equations 3a and 3b in table 2.1, further reduction of  $\text{HSeO}_3^-$  or  $\text{SeO}_3^{2-}$  to elemental selenium results in acid consumption. The reduction rate of selenite with  $\text{Na}_2\text{S}$  (Geoffroy and Demopoulos, 2011), Yeast (Falcone and Nickerson, 1963),  $\text{NaHSO}_3$  (Harańczyk et al., 2002) or  $\text{H}_2\text{S}$  (Pettine et al., 2011) was repressed or incomplete at pH=8-10 range. From a kinetic point of view, less selenite losses by further chemical selenite reduction is expected in the higher pH-range. From another chemical kinetic point of view, higher chemical reaction rates are expected at higher temperatures, therefore less selenite losses are expected in the lower temperature range.

In this study, a fed-batch system was used to investigate selenate reduction to selenite around the optimum range of conditions for the biocatalyst; pH=6-9 and  $T=20\text{-}50\text{ }^\circ\text{C}$ . The electron donor concentration was varied as well; 6.6 or 33 electrons from lactic acid oxidation per selenate molecule. The goal was to maximize selenite production and to minimize the generation of other selenium substances by investigating which parameters control the selenium bioconversion processes.

## **2.2 Material and methods**

### **2.2.1 Biomass**

Granular anaerobic sludge from a full-scale reactor treating paper mill waste water in Eerbeek, the Netherlands was used to inoculate Fed-Batch reactors. The bacterial cultures in the Eerbeek sludge have previously been described by Roest (Roest et al., 2005). Methane production, selenate reduction to mainly elemental selenium and sulphate reduction with this biomass was found by Lenz (Lenz et al., 2008a) and a small amount of selenite production and reduction with this biomass was found by Astratinei (Astratinei et al., 2006). Only granules were used as inoculum and suspended biomass appeared during the experiments. The granules were not acclimated to selenium.

### **2.2.2 Fed-Batch reactor use**

Unless stated otherwise, all reactor runs were carried as follows: a fed-batch system (Fig. 2.1) was used and cultivation started with a liquid volume of 250 mL medium

with a composition according to Stams (Stams et al., 1992) but without sodium selenite, sodium hydrogen carbonate and sodium sulphide (as to prevent other pH controls and the reaction between sulphide and selenite (Geoffroy and Demopoulos, 2011)). The medium consisted of (in grams per liter):  $\text{Na}_2\text{HPO}_4 \cdot 2\text{H}_2\text{O}$  (0.53),  $\text{KH}_2\text{PO}_4$  (0.41),  $\text{NH}_4\text{Cl}$  (0.3),  $\text{CaCl}_2 \cdot 2\text{H}_2\text{O}$  (0.11),  $\text{MgCl}_2 \cdot 6\text{H}_2\text{O}$  (0.10), and acid- and base trace elements and vitamin solution (Stams et al., 1992). The feed consisted of medium with 25 mM selenate and 13.75 mM lactic acid. The feed volume, 300 mL  $\pm$  30 mL, was added in 10  $\pm$  2 days and followed by a batch period of 11  $\pm$  1 days. The inoculum was 5 g wet weight Eerbeek sludge that had been stored at 4°C and that had not been adapted to the reactor conditions. The temperature was controlled with a water bath and the pH was kept constant with 0.1 M NaOH or 0.1 M HCl. Redox potential was measured vs Ag/AgCl. The total volume of the reactor was 1000 mL and the headspace was continuously flushed with 2000 mL/h  $\text{N}_2$  to avoid accumulation of toxic selenium compounds. The effluent gas was washed with ethylglycol to trap produced methylated selenium compounds and 3M KOH with pH indicator thymolblue to trap selenides. The  $\text{N}_2$  flush was increased to 25000 mL/h for at least 10 minutes before liquid sampling. The reactor liquid was mixed with a magnetic stirring rod (100 rpm) that was suspended in a Teflon construction to keep the rod 0.5 cm above the reactor bottom.

The effect of temperature was studied at T=20°C, T=30°C, T=40°C, T=50°C. The feed for the 50°C experiment was 500 mL. The effect of pH was studied at 30°C and pH=6, pH7, pH=8, pH=9. The effect of extra electron donor was studied with 5 x 13.75 mM lactic acid in the feed and T=30°C pH 7. Finally, the effect of less initial biomass was studied by starting the experiment with 1 g biomass instead of 5 g biomass.

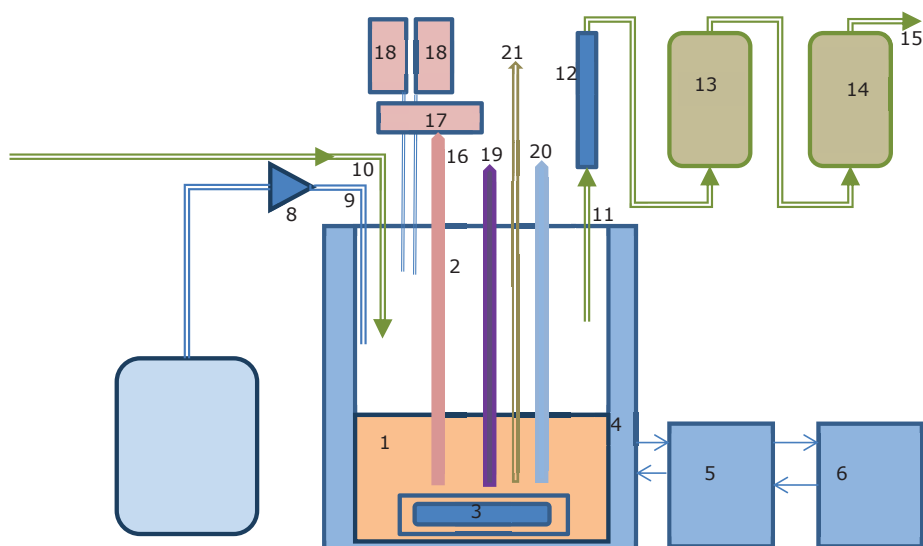


Fig. 2.1 – Schematic overview of the Fed-Batch reactor: 1. Reactor liquid volume; 2. Reactor headspace; 3. Suspended magnetic stirrer; 4. Reactor water jacket; 5. Temperature controlled heating bath; 6. Cryostat; 7. Influent vessel; 8. Influent Stepdos pump; 9. Influent port; 10. N<sub>2</sub>-in; 11. Gas out; 12. Condenser (connected to the cryostat 6); 13. Gas effluent ethylglycol washer; 14. Gas effluent base washer; 15. Gas exit; 16. pH-sensor; 17. pH-controller; 18. Base and acid supply barrels for pH control; 19. Redox sensor; 20. Temperature sensor; 21. Sample port;

### 2.2.3 Analytical methods

Liquid samples were taken with a syringe and selenate concentration ( $C_{\text{selenate}}$ ) and selenite concentration ( $C_{\text{selenite}}$ ) were analysed by ion chromatography (IC-CD). The IC-CD system was based on Lenz (Lenz et al., 2006) and consisted of an Autosampler AS-3000, a Dionex ICS-2100 equipped with an IonPac AS19 column (4 mm x 250 mm) at 30°C, an ASRS 4mm suppressor (75 mA) and an electrochemical conductivity detector at 35°C. The flow rate was 1.0 mL min<sup>-1</sup> and sample loop of 5  $\mu$ L was used. Low chain fatty acids were determined using Gas Chromatography according to Weijma (Weijma et al., 2000) with the following modifications: acetate and propionate were analysed with a column temperature of 130°C and the column pressure was 2 bar. At the end of each experiment, the reactor content was sieved (1

mm) to remove (parts of) the initial granules from the liquid reactor content. The granules were washed twice with ultrapure water. The total amount of elemental selenium attached to the granules ( $M_{\text{Se,gran}}$ ) was analysed by Inductively Coupled Plasma-Optical Emission Spectroscopy (ICP-OES). A sample of the granules was dissolved in 10 mL aqua regia in a Teflon tube. Subsequently the Teflon tube was closed and destruction of the sample continued by heating the solution in a microwave. After cooling down, the samples were diluted with ultrapure water to 100 mL 10% aqua regia prior to analyses with ICP-OES for  $M_{\text{Se,gran}}$  (mmol) determination. The sieved reactor liquid with suspended biomass was further analysed for disperse precipitated selenium ( $C_{\text{Se(s)}}$ ) and total selenium concentration ( $C_{\text{Se(aq+s)end}}$ ). For total selenium concentration, samples of 1 mL were destructed and analysed with ICP-OES. For disperse precipitated selenium concentration, 25 mL reactor liquid was centrifuged (10 min 10.000 rpm) and subsequently the solid pellet was treated with aqua regia microwave destruction prior to ICP-OES analyses. The pellet was washed twice with ultrapure water. Both, ( $C_{\text{Se(aq+s)end}}$ ) and  $C_{\text{Se(s)}}$ ) were measured twice. Samples from the gas wash bottles (1 mL) were also treated with micro wave aqua regia destruction to determine the total amount of selenium in the base and ethylglycol. The end liquid volume of each experiment ( $V_{\text{reactor,end}}$ ) was determined with a graduated 1 litre cylinder with 10 mL ruler.

#### **2.2.4 Calculations**

The liquid volume of the fed-batch at the start of each experiment was 250 mL and increased due to the addition of 300 mL +/- 30 mL of feed solution. About 80 mL of the volume was used for sampling and the liquid volume also changed by addition of base and acid for pH control (10-50 mL). As granular sludge was used in the experiments the reactor was not completely homogeneously mixed with respect to biomass concentrations. To overcome complex calculations of sampling volume and acid/base addition for pH control the following calculation and assumption were made to estimate the amount of selenium that was lost during sampling. The total selenium concentration was assumed homogeneously mixed in the reactor and the theoretical estimated total selenium concentration could be calculated using equation (1). At  $t=0$  the estimated selenium concentration is 0.



$$\text{Estimated } C_{Se,t+\Delta t} = \frac{\text{Estimated } C_{Se,t} * V_{reactor,t} + Q * C_{Se,in} * \Delta t}{Q * \Delta t + V_{reactor,t}} \quad (\text{mol / L}) \quad (1)$$

With:

t = time (h)

Δt = time interval (h)

Q = feed rate (mL / h)

C<sub>Se,in</sub> = selenium concentration in the influent (mol/L)

V<sub>reactor,t</sub> = liquid volume in the reactor at time t (mL)

The estimated total selenium losses during sampling, *Estimated M<sub>se,sampling</sub>*, could be calculated with *Estimated C<sub>Se,t</sub>* and the sampling volume at each time.

$$\text{Estimated } M_{se,sampling} = \sum_0^t V_{sampling,t} * \text{Estimated } C_{Se,t} \quad (\text{mmol}) \quad (2)$$

Selenium was neither detected in the ethylglycol wash bottle nor in the base wash bottle. The selenium recovery was calculated with the selenium that was added with feed, lost during sampling, measured from the granules and the measured total selenium concentration as soluble and insoluble selenium (C<sub>Se(aq+s)</sub><sub>end</sub>) at the end of each experiment.

$$\text{Se recovery} = \frac{\text{Estimated } M_{se,sampling} + M_{Se,gran} + V_{reactor,end} * C_{Se(aq+s)}_{end}}{\Delta t * \phi V * C_{Se,in}} * 100 \quad (\%) \quad (3)$$

The red insoluble (C<sub>Se(s)</sub>) concentration and the selenium attached to the granules (M<sub>Se,gran</sub>) in the reactor was assumed to be elemental selenium. Selenate, selenite and elemental selenium at the end of the experiment were calculated separately according the following equations.

$$M_{Selenate} = V_{reactor,end} * C_{Selenate} \quad (\text{mmol}) \quad (4a)$$

$$M_{Selenite} = V_{reactor,end} * C_{Selenite} \quad (\text{mmol}) \quad (4b)$$

$$M_{Elemental\ Selenium} = V_{reactor,end} * C_{Se(s)}_{end} + M_{Se,gran} \quad (\text{mmol}) \quad (4c)$$

With:

C = Concentration (mol / L)

The total of these three selenium compounds was verified with the total amount of

selenium detected at the end of each experiment to see if another selenium compound was produced. The verification is expressed:

$$Verification = 100 * \frac{M_{Selenate} + M_{Selenite} + M_{Elemental\ Selenium}}{V_{end, reactor} * C_{Se(aq+s)}_{t, end} + M_{(Se, gran)}} \quad (\%) \quad (5)$$

The outcome of the verification was around 100% in most experiments and it is assumed that the selenium content in the reactor was mostly selenate, selenite and elemental selenium. The selenate, selenite and elemental selenium amount was fractionated from the total to evaluate different experiments with each other. As an example the selenite fraction calculation is given below.

$$P_{Selenite} = 100 * \frac{M_{Selenite}}{M_{Selenate} + M_{Selenite} + M_{Elemental\ Selenium}} \quad (\%) \quad (6)$$

The yield of selenite from selenate was calculated as the percentage of reduced selenate that was converted to selenite at the end of the experiment.

$$Y_{Selenite} = 100 * \frac{P_{Selenite}}{P_{Selenium} + P_{Selenite}} \quad (\%) \quad (7)$$

The efficiency of electron donor use for selenite production was calculated as follows: every lactate molecule can donate 12 electrons for selenium reduction if it is fully oxidized to CO<sub>2</sub> and H<sub>2</sub>O. However, when acetate or propionate is produced, the electrons that could have been used for selenite production are still stored in these products: 8 electrons for acetate and 14 electrons for propionate. A correction for the produced amount of acetate and propionate at the end of each experiment was made. Produced elemental selenium and selenite effectively used two electrons for selenate to selenite conversion.

$$Y_{electron\ donor} =$$

$$100 * \frac{2 * C_{Selenite} + 2 * (C_{Se(s)} + \frac{M_{Se, gran}}{V_{end, reactor}})}{(C_{Se(aq+s)}_{t, end} + (\frac{M_{Se, gran}}{V_{end, reactor}}) * n * 12 - 12 C_{Lactic\ acid} - 14 C_{Propionate} - 8 C_{Acetate}} \quad (\%) \quad (7)$$

With:

n = the ratio between selenate and lactic acid in the influent (mol/mol)

C<sub>Lactic acid</sub> = the lactic acid concentration (mol/L)

C<sub>Acetate</sub> = the acetate concentration (mol/L)

C<sub>Propionate</sub> = the propionic acid concentration (mol/L)

## 2.3 Results

### 2.3.1 Effect of temperature on selenite production

In all the experiments, the selenate concentration increased after the start due to the addition of selenate to the reactor. At 30°C, the first decrease in selenate concentration and simultaneous increase in selenite concentration was detected between 23 hours and 95 hours. From this period onwards, the selenate was mainly converted to selenite (Fig. 2.2.A and 2.2.B). The selenite concentration remained around 680 mg Se/L during the batch period and the selenite yield was 83% at the end of the 30°C experiment (Table 2.2). The 30°C experiment also showed the highest selenate to selenite conversion rate compared to other temperatures. Around 300 mL 25 mM  $\text{SeO}_4^{2-}$  feed was added to the reactor and the selenate was depleted at 240 hours, the average selenate reduction rate was roughly 2.5 mg Se/h from  $t=0$  to  $t=240$  hours. At 40°C, selenite formation and selenate depletion was slower in the fed-batch phase. The selenate to selenite reduction continued during the batch period until a selenite concentration of 398 mg Se/L and a selenate concentration of 376 mg Se/L at  $t=360$  h. At this moment the concentrations of the electron donors, lactate, acetate and propionate, were below 10 mg/L and this could have stopped the reduction process. The final yield of selenite from selenate was 69% in the 40°C experiment (Table 2.2). At 20°C, a small amount of selenite, less than 60 mg Se/L, was detected from  $t=260$  h and this concentration remained stable. In the 50°C experiment, no selenite was detected. The selenate concentration decreased after the fed-batch phase, this could be caused by the biological selenate reduction to elemental selenium and also by dilution caused by the addition of base or acid.

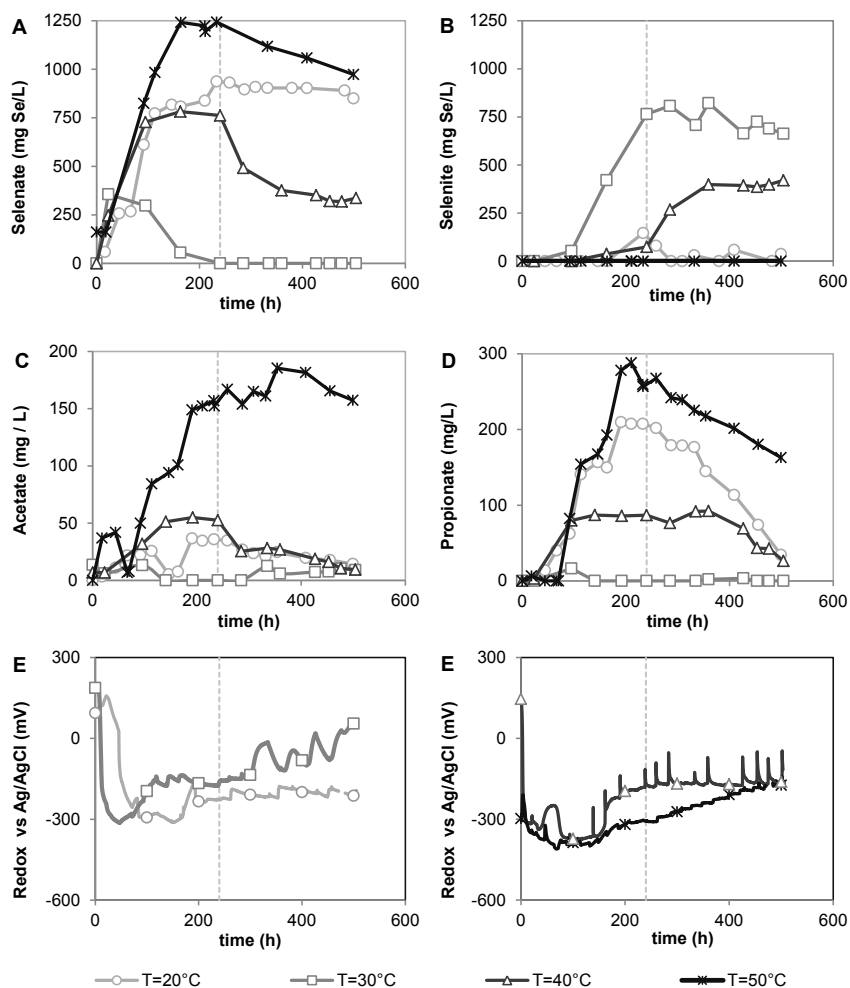


*Fig. 2.2 – Reactor experiments at pH=7 and at four different temperatures: The dotted vertical line at 240 hours represents the switch from fed-batch to batch mode. Displayed are the concentrations in the reactor of selenate (A), selenite (B), acetate (C) and propionate (D). Each symbol is a data point and direct lines connect the points. Redox potential (E) is constructed with data points only.*

**Table 2.2-Balance and yield of selenium conversions after each experiment**

Description experiment	Recovery (%)	Verification (%)	P <sub>Selenate</sub> (%)	P <sub>Selenite</sub> (%)	P <sub>Selenium</sub> (%)	Y <sub>Selenite</sub> (%)	Y <sub>electron</sub> (%)
20°C, pH=7	91	116	92	4	4	52	3
30°C, pH=7	93	91	0	83	17	83	28
40°C, pH=7	94	106	36	45	20	69	22
50°C, pH=7 <sup>a</sup>	94	105	86	0	14	0	9
30°C, pH=6	100	107	0	85	15	85	40
30°C, pH=8	100	105	0	79	21	79	36
30°C, pH=9	95	100	93	0	7	0	4
30°C, pH=7 <sup>b</sup>	96	92	67	23	9	72	6
30°C, pH=7 <sup>c</sup>	98	106	0	95	5	95	34

<sup>a</sup> Feed was 500 mL instead of 300 mL

<sup>b</sup> Lactic acid concentration in the feed was 68.75 mM instead of 13.75

<sup>c</sup> initial biomass concentration was 1 g wet weight instead of 5 g wet weight

Lactate concentrations peaked to maximum of around 70 mg / L in all reactors during the first days (data not shown). Only small amounts of propionate and acetate (around 10 mg/L) were detected at 30°C, showing that the biomass was substrate limited. For the 20, 40 and 50°C experiments, the acetate and propionate concentrations decreased further after the fed-batch phase, indicating that the biomass was still active in the batch mode (Fig. 2.2C 2.2D).

In all the experiments, the redox potential dropped from the start to reach the redox minimum in the fed-phase, -305 mV vs Ag/AgCl for the 20°C experiment, -330 mV vs Ag/AgCl for the 30°C experiment, -372 mV vs Ag/AgCl for the 40°C experiment and -421 mV vs Ag/AgCl for the 50°C experiment. After the redox potential had reached the minimum redox value a small increase of redox-potential occurred to an end value of -209 mV vs Ag/AgCl for the 20°C experiment, 41 mV vs Ag/AgCl for the 30°C experiment, -160 mV vs Ag/AgCl for the 40°C experiment and -257 mV vs Ag/AgCl for the 50°C experiment. Fluctuations were partly caused by sampling and acid base addition by the pH- controller (Fig. 2.2E).

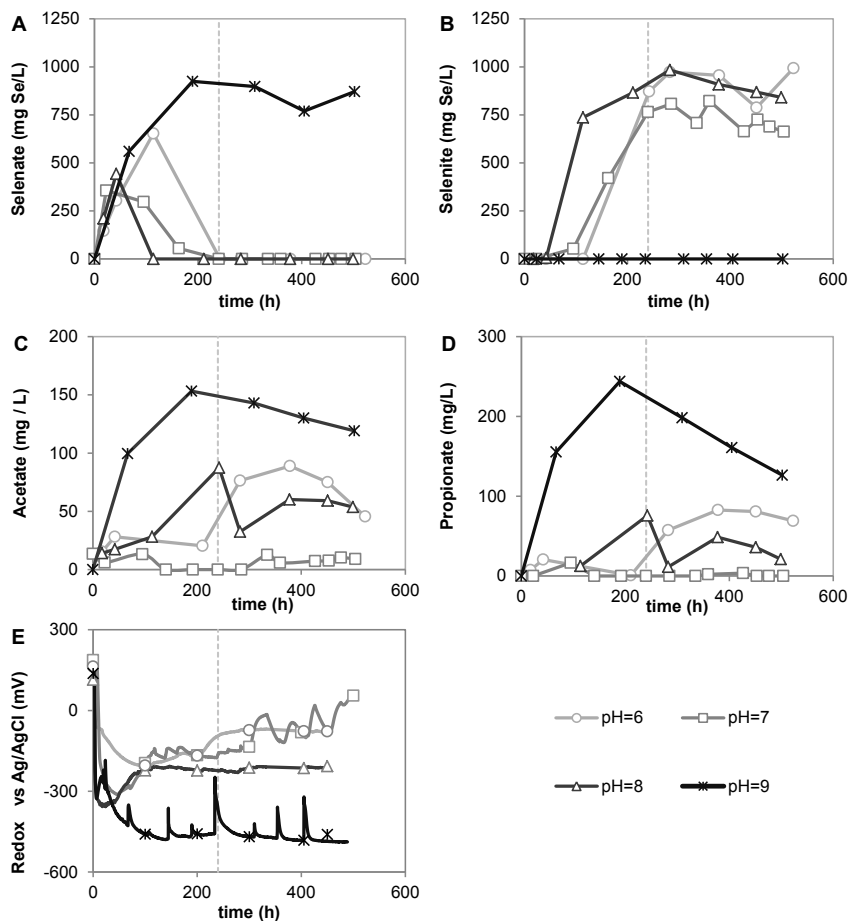


*Fig. 2.3 – Fed-batch experiments at 30°C and at four different pH-settings. The dotted vertical line at 240 hours represents the switch from fed-batch to batch mode. Displayed are the concentrations in the reactor of selenate (A), selenite (B), acetate (C) and propionate (D). Each symbol is a data point and direct lines connect the points. Redox potential (E) is constructed with data points only. At pH=6 and pH=8 data points are missing from 450 hour till the end of the experiment.*

In all experiments red or orange precipitates were formed, resembling typical selenium solids. ICP analysis confirmed the presence of selenium. No selenium

compounds were found in the ethylglycol or in the base flushing system.. An overview of the yields is given in table 2.2. The yield of selenite on the electron donor at pH 7 was maximum 28% at 30°C (Table 2.2). Under these conditions, all lactate was consumed and acetate and propionate concentrations were below 10 mg/l. This indicates that the majority of electrons had been shuttled to unidentified electron acceptors, most likely CH<sub>4</sub> or CO<sub>2</sub>. A relatively high amount of solid selenium (14%) and no selenite production was detected in the 50°C experiment (Table 2.2).

### **2.3.2 Effect of pH on the selenite production**

At pH=9, no selenite was detected and the selenate fraction at the end of the experiment was 93%, (Table 2.2). For pH=8, no selenate was detected from t=113 hours. At pH=7, almost all the selenate was converted in selenite at t=163 hours. At pH 6, all the selenate was converted and mainly into selenite at the end of the batch (Fig. 2.3B).

In all pH experiments, the lactic acid was partly or totally converted in propionate and acetate. The concentration of propionate and acetate was relatively low (about maximum between 0-89 mg/L) at pH 6, 7 and 8 while at pH=9, the propionate concentration reached a maximum of around 244 mg/L and acetate concentration reached a maximum of around 154 mg/L. Redox potential monitoring for the pH=6, pH=7 and pH=8 experiments gave a similar trend as in the temperature experiments; first the potential drops till a minimum during the fed-phase. From the minimum value the redox potential rises slowly during the experiment. At pH=9, the redox potential dropped to -479 mV vs Ag/AgCl and remained around this number during the experiment. Experiment pH=9 ended with a high concentration of electron donor and also a high concentration of selenate.

In all pH experiments, solid orange-red selenium was detected. The highest fraction (15%-17%-21%) of solid selenium at the end of the fed-batch experiment was found in the pH-range (6-7-8), (Table 2.2). In the same pH-range, high selenite concentrations were detected (85%-83%-79%).

### **2.3.3 Effect of initial biomass concentration, electron donor concentration on selenite production**

An experiment in which the biomass concentration was one fifth of that in the previous experiments and an experiment in which the electron donor was 5 times higher than that in the previous experiments were performed. This was done to obtain more information about the biomass capacity and the effect of the ratio between selenium oxyanion and electron donor. Both experiments were performed at  $T=30^{\circ}\text{C}$  and  $\text{pH}=7$ . The results are presented in Fig. 2.4.



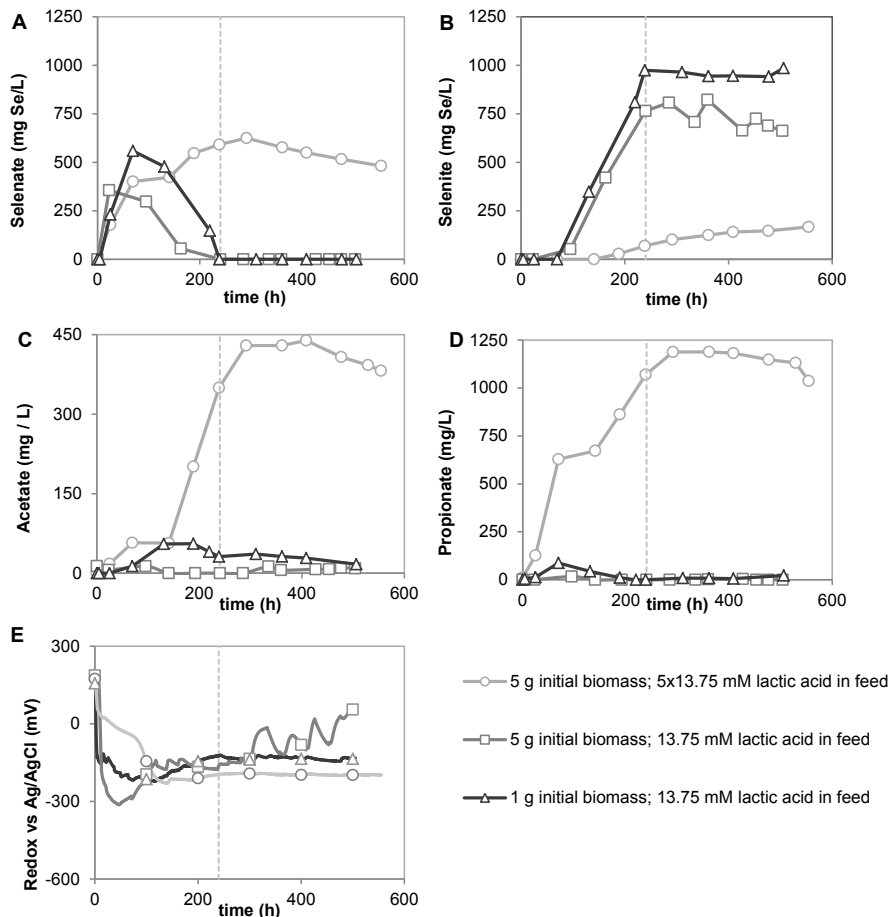


*Fig. 2.4 - Fed-batch experiments with varied biomass concentration and varied lactic acid concentration in the feed. The dotted vertical line at 240 hours represents the switch from fed-batch to batch mode. Displayed are the concentrations in the reactor of selenate (A), selenite (B), acetate (C) and propionate (D). Each symbol is a data point and direct lines connect the points. Redox potential (E) is constructed with data points only.*

With 68.75 mM lactic acid at 30°C and pH=7 , at around t=200 hours the first selenite could be detected. After that, the selenate reduction and the selenite production continued, but the conversion rate was not as fast as in the reference experiment at

pH=7 and T=30°C experiment with 5 times less electron donor. This indicates an inhibition effect, possibly by the fairly high concentrations of propionate and acetate of 1188 mg/L and 440 mg/L, respectively. For the 68.75 mM lactic acid 30°C pH=7 experiment, the redox potential drops till -220 mV vs Ag/AgCl after 4 days and remained around -143 mV vs Ag/AgCl during the rest of the experiment.

The inoculation of 1 gram wet weight biomass in the experiment shows a similar starting time for selenite production compared to the experiment with 5 g biomass at t=30 and pH=7. This lesser amount of biomass was capable of reducing all the selenate and the maximum concentrations of acetate and propionate were only 55 mg/L and 88 mg /L, respectively. The amount of elemental selenium was 5%, and this is very low compared to other experiments with a high selenite production (Table 2.2). The redox potential first reached a minimum of -228mV vs Ag/AgCl in 4 days, next the potential increased to -199 mV vs Ag/AgCl till the end of the experiment. Selenate was converted, but not as fast as in the experiment with 5 g biomass.

## **2.4 Discussion**

### **2.4.1 Effect of temperature on the selenite production**

At 30°C, pH 7 and with 5 g biomass, the average selenate reduction rate calculated over the batch period (10 days and all the selenate was converted) was 148 mg Se/g initial VSS/day (5 g wet weight corresponds to 400 mg VSS). The maximal reduction rate was roughly three times higher at 450 mg Se/g initial VSS/day. To indicate, Astratinei (Astratinei et al., 2006) detected selenate removal rates from 400 to 1500 ug g VSS<sup>-1</sup> h<sup>-1</sup> and Lenz (Lenz et al., 2008a) detected selenate reduction rate of 28 ug Se g VSS<sup>-1</sup> h<sup>-1</sup>. Factors that may have contributed to this large difference are: the higher selenate concentration in this work, the composition of the medium, the mixing intensity in the reactor and the composition of the microbial community of the inoculum. The source of the inoculum, biomass from a full scale bioreactor, had a relatively stable composition of the microbial community over a period of three years, (Roest et al., 2005).

The temperature effect on the electron donor oxidation rate showed a similar pattern as the temperature effect on the selenate reduction rate. The highest oxidation rate

was around 30°C because in this experiment low concentrations acetate (<20 mg/L) and propionate (<70 mg/L) were detected (Fig. 2.2C and 2.2D). For the reduction of selenate to selenite, 28% of the electrons available from electron donor oxidation were used (Table 2.2). Probably some of the electron donor was converted in undetected compounds, for example CH<sub>4</sub> that has been produced by Eerbeek Sludge during related reactor conditions (Lenz et al., 2008a).

The temperature effect can be discussed within one species of micro-organism. Temperature experiments with *P.stutzeri* showed a low selenate and a high selenite reduction rate at 40°C and a high selenate and a low selenite reduction rate at 20°C, (Lortie et al., 1992). Selenate reduction rate was more temperature sensitive than selenite reduction in a *Enterobacter cloacae* SLD1a-1, (Ma et al., 2007). In our 3 weeks experiments, the reduction rate of selenate to selenite at 30°C and 40°C was clearly higher than the selenite reduction rate. In longer time experiments the amount of selenite reducers could develop in the reactor due to the high concentration of selenite and finally decrease the selenite yield. At 50 °C, the growth of se reducing biomass was probably inhibited by 50 °C.

Besides biological selenite reduction also selenite losses may occur due to chemical reduction of selenite. Selenite can be reduced chemically with thiols (Frenkel et al., 1991; Kice et al., 1980), H<sub>2</sub>S (Geoffroy and Demopoulos, 2011; Pettine et al., 2011) or biomass compounds (Falcone and Nickerson, 1963; Frenkel et al., 1991). A higher process temperature increases a chemical selenite reduction rate with H<sub>2</sub>S, (Pettine et al., 2011). In the 50°C and the 20°C experiments, the selenate reduction was comparably low, and selenite was detected in the 20°C experiment only (Table 2.2). A possible explanation for no selenite detection at 50°C is that a further chemical selenite reduction with reduced compounds is fast compared to the biological selenite production. These reduced compounds come from the inoculum directly or are metabolites.

Besides reduction, also methylation of selenite can contribute to selenite and electron donor losses. No methylated compounds nor selenide were detected in all our three

weeks experiments. Lenz et al., (2008b) detected in the reactor with Eerbeek sludge dimethylselenide after 13 days and dimethyldiselenide after 17 days of operating, (Lenz et al., 2008b). Our operating time could have been too short for the biomass to develop methylated selenium compounds. Also, in some of our experiments, the relatively low electron donor concentrations could have had a negative effect on selenium methylation since methylation costs electron donor.

#### **2.4.2 Effect of pH on the selenite production**

Like temperature, the pH can select different species of micro-organisms in a reactor. Within one organism the pH can select the selenate reduction or selenite reduction rate: for micro-organism *Pseudomonas stutzeri*, selenate reduction rate and the selenite reduction rate is equal between pH=7 and pH=9, selenate reduction rate is lower than the selenite reduction rate at pH=6, the selenate reduction rate is higher than the selenite reduction rate at pH =9.5 (Lortie et al., 1992). For Eerbeek sludge at pH=6, pH=7 and pH=8, the selenate to selenite conversion rate was higher than the selenite reduction rate. For the pH=9 experiment, no selenite was detected indicating that the selenite production rate was equal to the selenite reduction rate, or all the converted selenate was immediately reduced to selenium without selenite as an intermediate. Selenate reduction occurred under all pH settings, because red elemental selenium was detected in all cases.

The pH also has an effect on chemical selenium reduction of selenite. Reactive reducing elements could have been added to the reactor with the inoculum. The  $pK_{a2}$  value of selenite is 7.3, and at higher pH more  $SeO_3^{2-}$  species are available. In chemical selenite reduction with thiols, the pH has an effect on the mechanism and rate (Kice et al., 1980). Chemical selenium precipitation rate for selenite reduction by sulfide was found to be lower at higher pH range: pH>8 (Pettine et al., 2011) and pH>9.5 (Geoffroy and Demopoulos, 2011). In our pH=6, pH=7 and pH=8 experiments, high selenite concentrations were obtained, , but not more elemental selenium was detected at pH=6 compared to pH=8. The amount of inoculum, thus the amount of other elements, like S, was equal in each pH experiment. This amount of other reducing compounds could be limiting if the chemical reactions contribute to

the reduction of selenite to elemental selenium.

### **2.4.3 Effect of biomass and electron donor concentration on selenite production**

In the 30°C pH=7 and 1 g wet weight biomass experiment, all the selenate was converted in 240 hours. The electron donor concentration was low during the experiment: max 87.6 mg propionic acid and max. 55 mg acetic acid. The average selenate reduction rate was roughly 741 mg Se/ g initial VSS/day over a period of 10 days. This high reduction rate indicates that the 1 g wet weight of biomass was capable of reducing all the selenate and oxidize the majority of the electron donor. This indicates that fluctuations in the feed of 5 gram initial wet weight experiments around the biocatalysts optimum (pH=7 and T=30°C) conditions had no effect on selenite production because the biomass conversion capacity of selenate and electron donor was high enough compared to the addition of the selenate and the electron donor via the feed.

In all experiments, a part of the lactic acid was reduced to propionic acid and a part of the lactic acid was oxidized to acetate. The energy from the lactic acid reduction to propionic acid is calculated with values from Amend and Shock (Amend and Shock, 2001) with partial hydrogen pressure 0.010 atm:



If we compare this energy release with the energy release in table 2.1, we can conclude that selenate and selenite reduction gain more energy per electron than lactate reduction. However, in spite of this higher energy release in selenate reduction compared to lactic acid reduction, the sludge reduces a part of the lactic acid to propionate first: unadapted Eerbeek granules is used in every experiment, it is possible that the granules has to adapt to selenate reduction first or that lactic acid is preferable as an electron acceptor.

The inoculum was granular sludge and limited mass transport over the granules has some protection advantages. On one hand diffusion limitation could have protected

the biomass in the inside of the granule from high selenate concentration. On the other hand, disperse biomass was detected after two or three days in each experiment. The biological activity of Eerbeek sludge alters if it is crushed, (Astratinei et al., 2006). The biological activity could have been changed by the growth of disperse biomass. In our experiments, dispersed growth seemed correlated with the selenate to selenite reduction.

For reduction of selenite to selenium 4 electrons are needed and for the reduction of selenate to selenite only 2. Lenz (Lenz et al. 2008b) also produced elemental selenium with Eerbeek sludge but without detecting selenite. The work was performed at pH=7 and T=30°C and the chemical oxygen demand (COD)/selenate ratio in the influent was 633 (g/g). Astratinei converted 16% of selenate to selenite at pH=7.5 and T=30°C, the COD/selenate ratio was 13.4 (g/g) at the start of the batch. After the addition of extra electron donor in the experiment of (Astratinei et al., 2006) the selenate was still reduced, but also the selenite concentration decreased. In our 13.75 mM lactic acid experiments the ratio between COD/selenate is 0.35 (g/g) in the influent. Probably a low electron donor concentration and biomass in our T=30° experiments stopped the biomass to reduce selenite further towards elemental selenium because: 1 less electrons were available from the electron donor. 2 the conversion rate of selenite to elemental selenium was lower than for selenate to selenite conversion, a low biomass concentration compared to high selenate concentration results in selenite production. 3 Selenite was chemically reduced, less reduced compounds were present in the medium due to the low biomass and electron donor concentration.

For the 68.75mM electron donor concentration the yield of selenite from selenate was 72% and the yield of selenite from the electron donor was 6 %. The ratio between COD/selenate was 1.75 (g/g), the high amount of electron donor resulted in less selenate reduction and less selenite production. The fraction elemental selenium was relatively high compared to the amount of produced selenite.

Lenz (Lenz et al., 2008a) and Astratinei (Astratinei et al., 2006) used sulphur

compounds in their medium. Probably, no selenite could be detected because of bioproduced reduced sulphur compounds, or other reduced compounds, that directly precipitate with selenite. The experiment with only 1 g initial wet weight biomass resulted in less elemental selenium than the experiment with 5 g wet weight initial biomass (Table 2.2). In both experiments all the selenate was converted and yielded high selenite production.

The selenium alkylation route described by Chasteen (Chasteen and Bentley, 2003) has selenite as intermediate. Lenz (Lenz et al., 2008b) found alkylated and methylated selenium compounds but no selenite. For methylated selenium compounds, not only electrons are needed for selenium reduction, but also electron donor is needed for methylation. A possible explanation is that at higher electron donor concentration the micro-organisms have the opportunity to methylated selenium compounds besides reducing selenium.

#### **2.4.4 Effect of redox potential**

Redox potential was followed in all the experiments and showed a minimum value during the first days in the experiments. The lowest redox potential in the temperature experiment was reached in the 50°C experiment and the lowest redox in the pH experiments was reached at pH=9 (Fig. 2.2E and Fig. 2.3E). An explanation for this decrease at high temperature could be the that lactic acid is converted to propionic acid and H<sub>2</sub> or to propionic acid and other reduced compounds, causing the low redox potential. If selenite was produced, then these reduced compounds will react with selenite and the redox potential rises again. This trend of the redox potential is also seen in chemical selenite reduction after the addition of the reducing compound (NaHSO<sub>3</sub> or SO<sub>2</sub>) the redox potential decreases and rises later (Harańczyk et al., 2002). For the pH=9 experiment, a very low redox potential was established for a longer period in the experiment, around -500mV vs Ag/AgCl. No selenite was detected in this experiment.

## **2.5 Conclusions**

This study demonstrates that a high percentage of selenate is rapidly converted in selenite at pH=7, T=30°C and using 1 g wet weight not adapted Eerbeek sludge. A

high average reduction rate of 741 mg Se/ g initial VSS/day was measured and 95% of the selenate was converted to selenite. Unwanted volatile products like methylated selenium compounds and selenides were not detected. After selenate to selenite conversion, selenite losses could be caused by further biological reduction and chemical reduction with other compounds like thiol groups in the biomass. Process conditions like pH and temperature affect the latter reaction and this should be taken into account when choosing optimal settings for selenate to selenite reduction. Experiments at pH 9 combined with a temperature of 30°C and at pH 7 combined with a high temperature of 50°C resulted in elemental selenium but no selenite production. Furthermore, the electron donor concentration should be regulated to control the production of selenite, the redox potential could be used as a monitoring parameter. This is to minimize electron donor costs, minimize inhibition effects and to avoid further reduction and methylation of selenite. The high yield and the high biological reduction rate of selenate to selenite makes the process suitable to remove selenate from waste water.



## **Chapter 3**

### **Bio-production of selenium nanoparticles with diverse physical properties**

This chapter has been prepared for submission as:

Bio-production of selenium nanoparticles with diverse physical properties

Simon P. W. Hageman,  
Renata D. van der Weijden,  
Alfons J.M. Stams,  
Cees J.N. Buisman

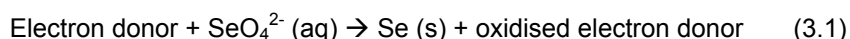
## **Summary**

Biological reduction of soluble selenate to insoluble elemental selenium enables the removal and recovery of selenium from aqueous streams. Economic, efficient biological selenium recovery depends on properties of selenium particle such as size, density, stability, hydrophilic character and attachment to the biomass. The properties of selenium particles are affected by the bioreactor process conditions under which the particles are formed. In batch and fed-batch reactors using anaerobic sludge, the influence of pH (6-9) and temperature (20-50°C) on the morphology, structure and stability of the biologically produced selenium particles properties were studied using SEM, XRD, and light microscopy. At a high pH or a high temperature these experiments resulted in grey crystalline hexagonal acicular selenium particles, while a low pH combined with a low temperature red amorphous nanospheres were dominant. Particle stability tests were carried out by changing the temperature or pH after the particles had formed. Red amorphous selenium spheres (produced at pH=7 and 30°C) transformed gradually towards the grey hexagonal structure at 50°C over a period of three weeks. We show here that biological selenium particle crystallinity, shape and colour can be controlled by temperature and pH. Although the formation of crystalline particles seems possible, the removal efficiency and reduction kinetics of the biomass still needs to correspond with the bioreactor conditions. The production of crystalline particles is an important first step to grow larger selenium particles in the future in order to reduce costs for selenium recovery in bioreactors.

### **3. 1 Introduction**

Selenium removal, recovery and re-use from wastewater streams are of importance, because of its harmful effects on the environment but also because of its use as a valuable compound in many applications. Selenium emissions from several industries contribute to pollution (Lemly 2004, Winkel et al. 2011). The water-soluble forms of oxidised selenium, selenate and selenite, can cause problems due to their mobility and possible toxic accumulation effects (Lemly 2004). But selenium also has considerable economic value, as it is used in, for example, food (as a trace element), paint and electronic products.

The bio-reduction of soluble selenate to form insoluble elemental selenium followed by a liquid-solid separation process is a promising environmentally friendly selenium removal and recovery method. In this process, micro-organisms oxidise organic electron donors using selenate as electron acceptor for dissimilatory reduction (see equation 1) (Steinberg and Oremland 1990). The solid selenium thus produced requires appropriate particle properties for efficient recovery during the solid liquid separation process. The sedimentation rate is influenced by selenium particle size, density, (red amorphous selenium is 4.27 g/mL and crystalline selenium 4.81 g/mL (Minaev et al., 2005)) attachment to biomass and crystal structure. Selenium particle properties might also be relevant to the toxicity effect on the biomass (Fernández-Martínez and Charlet 2009).



Several morphologies of selenium nanoparticles have been described: rods (Mondal et al. 2008, Xi et al. 2006), crystalline spheres (Xi et al. 2006, Mishra et al. 2011), trigonal nanowires (Gates et al. 2002), amorphous spheres (Gates et al. 2002) and trigonal nanotubes (Xi et al. 2006). Unless otherwise stated we use the terms spheres and aciculars. The term rosette is used for spherical particles with acicular parts radiating out from the spherical core.

Several mechanisms for the formation of biological selenium particles have previously been described with models (Xi et al. 2006) (Gates et al. 2002). These models describe

the phenomenon that red amorphous or monoclinic selenium spheres are produced first and later on these spheres are transformed into more acicular hexagonal crystalline structures. This transformation is accelerated by heating (Lenz et al. 2009), sonification, or by replacing the water phase with ethanol (Li and Yam 2006) or a mixture of chloroform and methanol (Tejo Prakash et al. 2009). However, for biological selenate reduction water is indispensable. Heating and sonification have limitations in bioprocesses. , once bio-selenium particles have been formed, the particles can be subjected to changes in the process conditions.

The hexagonal acicular selenium particles can grow along the ends from the acicular particles (Mondal et al. 2008). At a slow crystallization rate, longer selenium particles appear due to a preferred growth at the tips of the acicular hexagonal selenium crystals. At a higher growth rate there is more growth competition between the tips and the side of the selenium particles, resulting in thicker particles. At a higher temperature, the van der Waals force is weaker due to the higher temperature (Mondal et al. 2008) and molecules can diffuse better through the water phase, enabling them to start growing along the tips of the acicular particles. The selenium molecules also diffuse better through the water phase at high pH (Xi et al. 2006). This means that biological acicular selenium particles are expected to be produced at as high as possible temperature and pH, but within the restricted conditions for micro-organisms that are able to reduce selenate.

In this study, the properties of selenium particles were investigated to find a threshold for temperature and pH to differentiate between biological production of amorphous selenium and crystalline selenium. The properties of bio-selenium particles were analysed by taking precipitates from selenate-reducing bioreactors operated under different conditions. The temperature was varied between 20°C and 50°C, in steps of 10°C. The pH was varied between 6 and 9 in steps of 1 pH-unit. In a second step, using red amorphous selenium spheres produced at 30°C and pH=7, a stabilisation test was performed at pH or temperature conditions that had led to more crystalline selenium particles (pH 9 or 50°C).

### **3.2 Material and methods**

Two collections of bio-selenium precipitates were used. Defrosted selenium precipitates from fed-batch experiments (chapter 2) and selenium precipitates from batch experiments. In fed-batch experiments pH and temperature were controlled by a pH and temperature stat. In batch experiments only the temperature was controlled.

#### **3.2.1 Temperature and pH-controlled fed-batch experiments**

In fed-batch experiments pH and temperature were controlled by a pH and temperature stat. Defrosted selenium precipitates from fed-batch experiments were used to compare the properties of selenium particles with the properties detected in the batch experiments. For a description of the experimental setup see Chapter 2. The starting volume was 250 mL without selenate and  $\pm 300$  mL 25 mM selenate was added to the reactor in  $\pm 10$  days. The  $\pm 10$ -day fed-batch was followed by a  $\pm 11$ -day batch mode in which the pH was still controlled and the headspace flushed with nitrogen. The medium was the same as in the batch bottles (3.2.2), but the selenate and the electron donor concentration varied due to addition of the feed. In these experiments Eerbeek sludge from a reactor treating paper mill effluent at pH=6.9 and temperature ranges from 30°C to 37°C (Oude Elferink et al. 1998) was used. Around 10% of the selenate was converted to elemental selenium during the three weeks that the reactor was used. The liquid with small particles was collected from the reactor and stored at -20°C. The properties of the selenium particles thus produced (crystallinity, morphology, sedimentation, size, colour) at reactor settings T=30°C with pH 6, 7, 8, 9 and pH=7 with T=20°C, T=40°C and T=50°C were compared. Samples of sieved (1mm) reactor liquid with a volume of 25 mL (stored at -20°C) were defrosted and made ready for light microscope (LM) analyses. Subsequently the samples were centrifuged and washed twice with 8 mL MilliQ water, 10 minutes 2395 rpm at 20°C with a Firlabo SW12 centrifuge, prior to SEM analyses and XRD analyses. For SEM analyses, samples were dried at room temperature. The samples were placed on a SEM sample holder using carbon adhesive tabs (EMS Washington USA) and subsequently coated with about 10 nm carbon. Samples were analysed at 3 kV, 25 pA, WD 4 mm at room temperature, in a field emission scanning electron microscope (SEM) (Magellan 400, FEI, Eindhoven, the Netherlands). EDX analyses were done using an INCA X ray

analyser (Oxford Instruments Analytical, High Wycombe, England) at an acceleration voltage of 10 kV, 100pA, WD 4mm.

### **3.2.2 Batch experiments with the temperature controlled**

From the fed-batch tests described above, it was concluded that the properties of selenium particles and formation was influenced by pH or/and temperature. To obtain more data points batch tests were performed.

For the batch experiments, medium according to chapter 2 was prepared. Lactic acid was added to a final reactor concentration of 1.25 mM. The pH was adjusted to 6, 7, 8 or 9 by adding 0.1 M NaOH. Crimp seal flasks with a volume of 118 mL (SD=0.77 n=10) were filled with 24 mL of prepared medium. Subsequently 1 mL of a 50 mM sodium selenate solution was added; this resulted in a final selenate concentration of 2 mM. Between 0.25 and 0.30 g of fresh unadapted wet weight granular 'Eerbeek' sludge was added to the flasks. The headspace was degassed to 0.5 atm. and then the pressure was increased to an overpressure of 0.5 atm. with N<sub>2</sub>. This cycle was repeated 5 times, ending with an overpressure of N<sub>2</sub> 0.5 atm. The bottles were shaken at 100 RPM and at temperatures of 20°C, 30°C, 40°C or 50°C. All experiments were carried out in duplicate (A+B). Controls without biomass were prepared for each pH, but only for 20°C and 50°C and not in duplicate.

The colour of the precipitates and the pH were followed over time. On t=15 days extra electron donor was added to the batch bottles (0.3 mL of neutralised NaOH 0.1 M lactic acid). After 30 days the crimp seal flasks were removed from the incubators and placed at room temperature. Liquid samples were taken from the bottle using a syringe, leaving the remainder of the inoculum granules in the bottle. These liquid samples contained coloured Se particles and dispersed biomass. An absorbance spectrum of the liquid from 340 nm to 900 nm was made with a Dr Lange ION-500 spectrophotometer. Light microscope (LM) pictures were made with a NIKON ECLIPSE 400 microscope. The bottles were stored at 4°C. For XRD, samples were washed once with 15 mL MilliQ water (45000 RPM for 10 minutes with Firlabo SW12), subsequently the centrifuge step was repeated and the pellet was resuspended in around 0.2 mL MilliQ. The 0.2 mL was applied onto an object glass

used for microscopy (VWR ECN 631-1550 76×26×1 mm) and dried at room temperature prior to XRD analysis. XRD was performed with a PHILIPS SR 4160, 40 kV 30mA. Raw data were analysed with the program HighScore Plus. Peaks were traced using the following software method: 2<sup>nd</sup> derivate; Minimum significance 1.00; Minimum tip width ( $^{\circ}2\Theta$ ) 0.01; Max. tip width ( $^{\circ}2\Theta$ ) 1.00 and peak base width ( $^{\circ}2\Theta$ ) 2.00.

### **3.2.3 Particle stability test**

Selenium particles that were produced over three weeks at 30°C and pH=7 in fed-batch experiments were also tested for their stability with changing temperature and pH for another three weeks. Reactor samples were shaken at 100 RPM under new process conditions: T=30°C and pH=7, T=30°C and pH8, T=30°C and pH=9, T=40°C and pH=7 and T=50°C and pH=7. At 11 days and at 22 days an absorbance spectrum of the solution was made. After three weeks LM pictures were also taken of the precipitates. Other samples were washed twice with 5 mL MilliQ at 2395 RPM, 20°C 10 min with Firlabo SW12 centrifuge and finally air dried prior to XRD analyses.

### **3.2.4 Sedimentation test**

Sieved (1 mm) samples from all the fed-batch reactors were added to a 30-mL tube at mL scale and the sedimentation was followed visually over time to see if the sedimentation velocity of the selenium particles differed and could be correlated to the selenium particle structure.

## **3.3 Results and discussion**

### **3.3.1 Temperature and pH related to selenium particle morphology**

Selenium precipitates formed in in a pH-controlled bioreactor in three weeks (Chapter 2) were investigated using LM. The LM pictures in Figure 3.1 indicate mainly two different particle morphologies: selenium acicular or selenium particles that are assumed to be spheres (Fig. 3.1). The precipitates with mainly acicular structures were a darker red than the precipitate with mainly spheres.

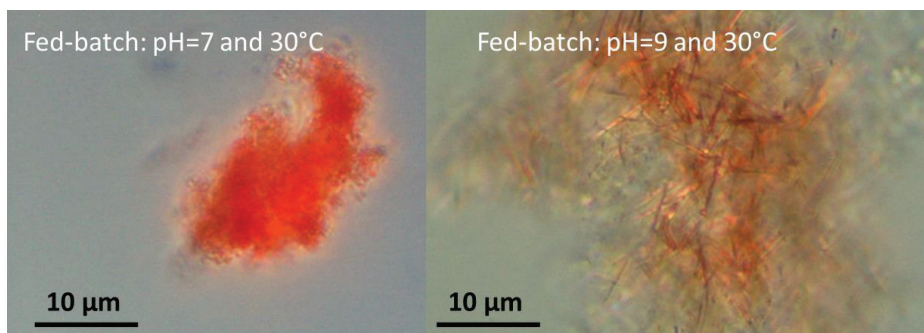


*Figure 3-1: Light microscope photos of two fed-batch precipitates: Both types of precipitates are composed of biomass and selenium particles.*

The LM pictures were not always clear enough to distinguish between several selenium particle morphologies: single spheres were barely visible, but larger acicular selenium structures were clearly visible. SEM pictures were made from the fed-batch experiments (stable pH during the particle formation) to provide more detailed information about the particle morphology.



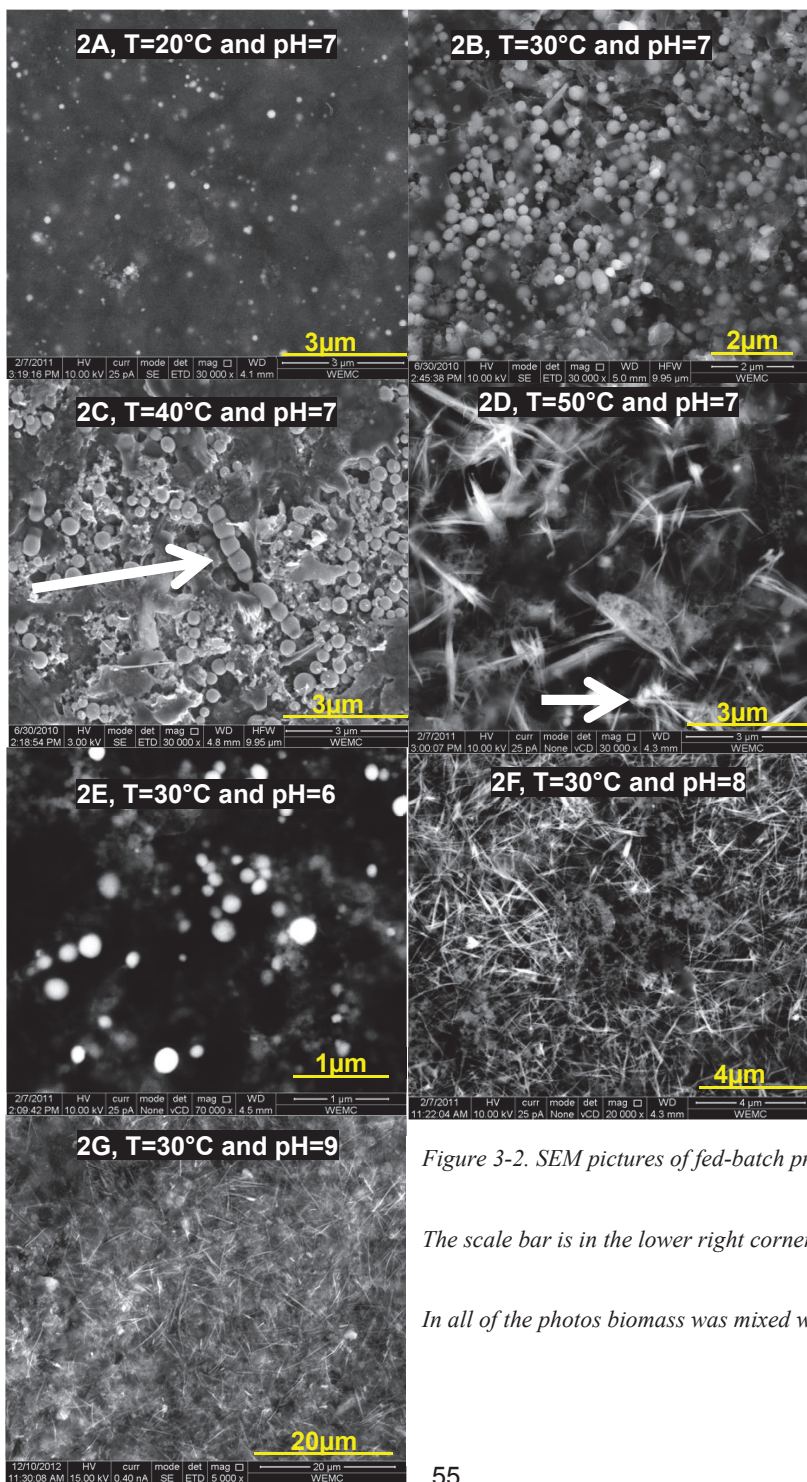


Figure 3-2. SEM pictures of fed-batch precipitates.

The scale bar is in the lower right corner of each picture.

In all of the photos biomass was mixed with selenium particles.

The SEM photos confirmed the morphology that was obtained from the LM-photos. Mainly sphere-like particles were detected at the pH-controlled fed-batch experiments: 20°C, 30°C and 40°C all at pH=7 and also at 20°C and at pH=6. Mainly selenium acicular particles were detected at 50°C and at pH=7 (Fig. 3.2D) and in the two experiments in the higher pH range: T=30°C and at pH=8 (Fig. 3.2F) and pH=9 (Fig. 3.2G). The samples with mainly acicular selenium nanoparticles also revealed rosettes (arrow in Fig. 3.2D). A mixture of particles with diverse structures has also been detected by others (Xi et al. 2006, Pearce et al. 2009) and indicating a selenium phase transformation. At 40°C and pH=7 some spheres were merged with other spheres (arrow in Fig. 3.2C).

The precipitates of the batch experiments were only investigated with the LM and different particle morphologies were revealed, such as acicular structures in grey precipitates (Fig. 3.3). However, the morphology of the particles in the red precipitates was difficult to see using LM because the size of the particles was small, but it was assumed that there were red amorphous selenium nanospheres (Fig. 3.3). Regrettably, the pH of the medium was not stable during the batch processes (Appendix 3A and Table 3.1).

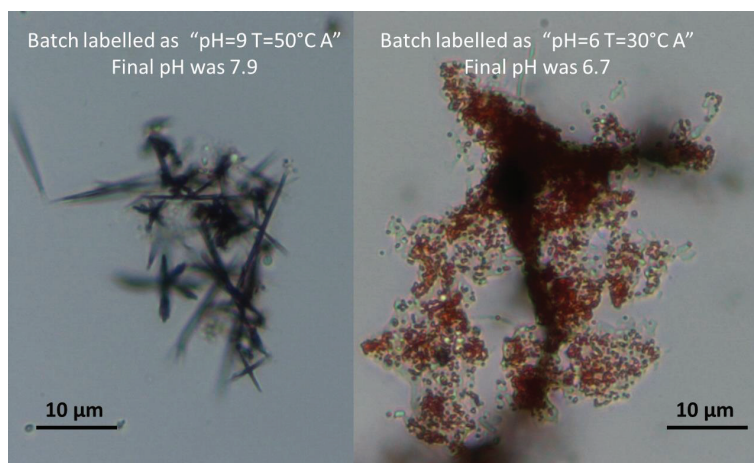


*Figure 3.3: Two precipitates from batch experiments at 30 days; on the left a more acicular-like structure mixed with biomass from batch. On the right, a red coloured precipitate mixed with biomass.*

The size of acicular selenium compared to the size of the micro-organisms suggests that the particles were outside the micro-organisms (Fig. 3.3, Fig. 3.2). Whether the selenium nanospheres were produced epicellularly, extracellularly or intracellularly is not clear from the LM and SEM pictures.

**Table 3.1: Colour and final pH of the batch experiments in duplicate after 30 days**

pH set - point	6		7		8		9	
T (°C)	Label pH: "6 A"	"6 B"	"7 A"	"7 B"	"8 A"	"8 B"	"9 A"	"9 B"
50	<b>6.50</b>	6.31	6.95	6.80	7.5	7.42	7.87	7.82
40	6.63	6.63	7.00	7.03	7.33	7.34	7.68	7.67
30	6.72	6.78	7.03	6.91	7.42	7.47	7.82	7.86
20	6.77	6.73	7.14	7.04	7.53	7.79	8.21	7.74

*The initial pH setting, which is reported in the first row, is used as labelling. The pH shift from initial to final pH was mainly established within the first days of the experiment (data Appendix 3A). Four results of precipitate colour were notable: White = almost no precipitation; Red = red to orange precipitates; Light yellow = yellow precipitates; Grey = grey precipitates.*

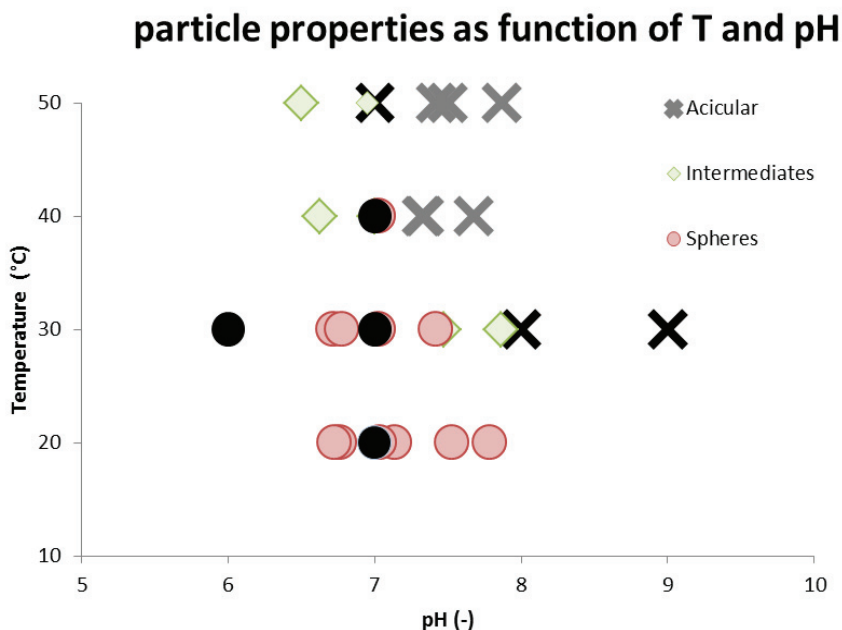


Figure 3.4: Spheres, intermediates and acicular, as function of pH and temperature. In this plot the final measured pH value (30 days) of batch experiment was used. Results from fed-batch (21 days) with controlled pH are expressed in black.

From Figure 3.4 it can be concluded that in the lower pH and temperature range mostly spherical selenium particles can be detected and in the higher pH and higher temperature range acicular selenium can be detected.

### 3.3.2 pH and temperature related to selenium colour precipitates

The four most distinctive liquid colours at the end of the batch experiments were red, orange, yellow and grey (Fig. 3.5). Grey coloured liquid was mostly detected in the 50°C experiments at a pH above 6.9. These colours can be correlated with particle size and morphology. From Table 3.1 and Figure 3.4 it seems that red colour is linked to amorphous spheres and grey colour is linked to acicular particles.

The liquid colour in the experiments changed from light yellow to red, followed by grey. The change from light yellow to red corresponds with the redshift in the absorbance peak that occurs when the amorphous nanospheres particle size increases from 0-18 nm to 220-240 nm (Lin and Wang 2005) (Dauchot and Watillon 1967). The change from red to grey corresponds with a blue shift that occurs when selenium nanospheres transform to more irregular particles (Gates et al. 2002). However, sometimes because of mixtures of particles it was difficult to link colour to selenium particle morphologies. This was also seen in the fed-batch experiments with mainly acicular morphologies; all precipitates were also reddish and composed of spherical and intermediate particles. Colour can be used as an indication, but structure and morphology should be analysed as well.

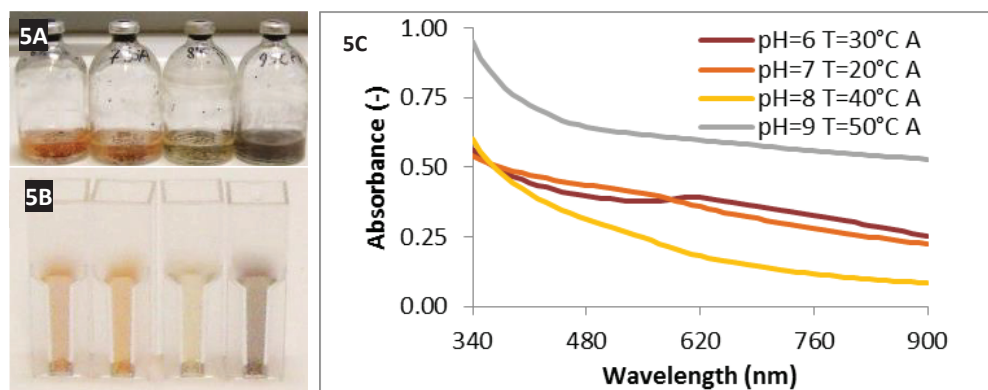


Figure 3.5: Batch bottles and their colour. 5A, batch bottles from left to right “pH=6 T=30°C A”; “pH=7 T=20°C A”, “pH=8 T=40°C A” and “pH=9 T=50°C A”, with the corresponding colours: reddish, red/orange, light yellow and grey. 5B, the corresponding cuvettes of the bottles in 5A. 5C, absorption spectra of the different solutions.

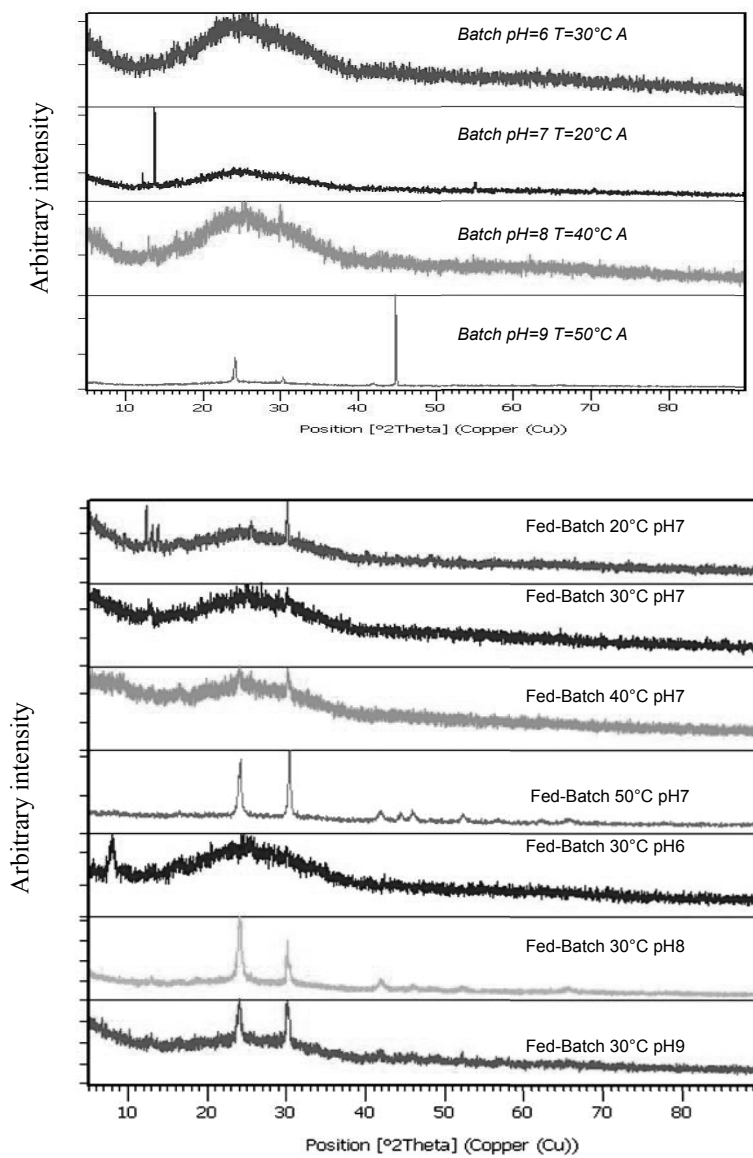


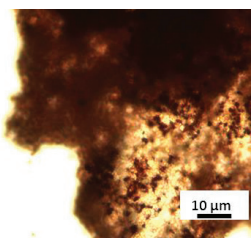
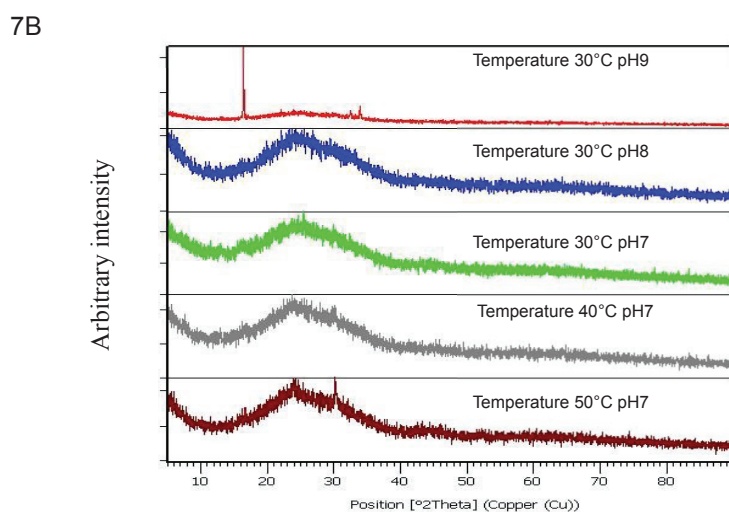
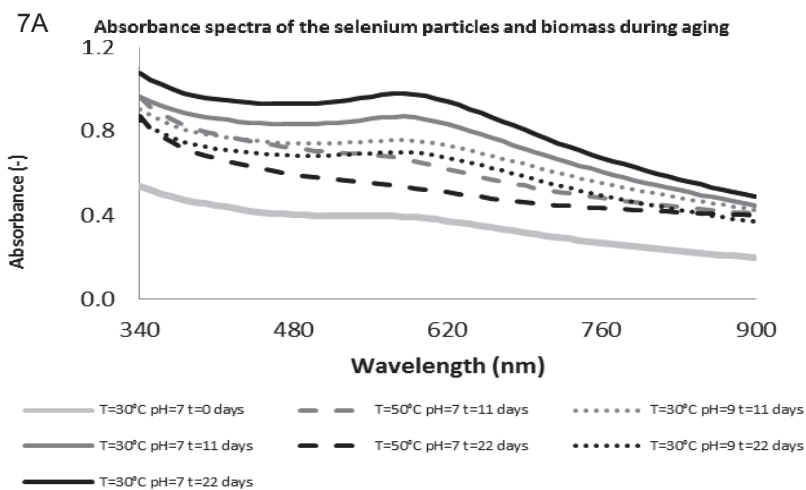
Figure 3.6: XRD of batch and pH-controlled fed-batch experiments.

### 3.3.3 Reactor pH and temperature related to crystal structure formation

Precipitates from the batch and the pH-controlled fed-batch were examined by XRD (Fig. 3.6). At 50°C fed-batch, seven hexagonal selenium peaks were detected and this confirmed the hexagonal structure. The XRD results showed that crystalline hexagonal selenium was formed at a higher pH and temperature range. This is in correlation with the morphology (Fig. 3.4) and colour (Fig. 3.5) of the selenium particles discussed earlier and so the acicular structures and grey colour are linked to crystalline hexagonal selenium.

Deviation between the peak intensities at  $24^\circ 2\theta$  and  $30^\circ 2\theta$  can be observed in Figure 3.6 (All XRD peak tables are in Appendix 3B). In some published XRD patterns the peak intensity at  $24^\circ 2\theta$  was the highest (Xi et al. 2006, Gates et al. 2002, Li and Yam 2006, Tejo Prakash et al. 2009, Wang et al. 2010, Song et al. 2006), while other studies show that the  $30^\circ 2\theta$  peak intensity was highest in the selenium XRD patterns (Mondal et al. 2008, Mayers et al. 2003, Zhang et al. 2004, Shah et al. 2010a, Srivastava and Mukhopadhyay 2013, Shah et al. 2010b, Pejova and Grozdanov 2001). A high peak intensity at  $24^\circ 2\theta$  (*hkl* 100) is explained by the preferential orientation effects of selenium in a certain direction (Li and Yam 2006, Song et al. 2006), also named the 001 direction (Tejo Prakash et al. 2009) or the c-axis (Wang et al. 2010),(Gates et al. 2002). Ding et al. (2002) showed that for long acicular selenium the  $24^\circ 2\theta$  peak was most intense. By grinding these acicular particles and making an XRD the  $30^\circ 2\theta$  peak became most intense (Ding et al. 2002). All together, the relative intensity of the  $24^\circ 2\theta$  increases with acicular length. This is confirmed by our batch experiments at pH=9 and T=50°C where long acicular selenium structures were identified by LM (Fig. 3.3). XRD spectra of this precipitate resulted in a relative intensity at  $24^\circ 2\theta$  that was at least 4.5 times the intensity at  $30^\circ 2\theta$ .

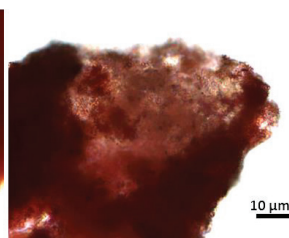




7C pH=7 and  $T=50^{\circ}\text{C}$



7D pH=7 and  $T=30^{\circ}\text{C}$



7E pH=9 and  $T=30^{\circ}\text{C}$

Figure 3-7: Particle stability tests, absorbance spectra, and XRD and LM photos at 22 days



### 3.3.4 Particle stability tests

The amorphous selenium spheres that were produced in the fed-batch experiment at  $T=30^{\circ}\text{C}$  and  $\text{pH}=7$  were incubated under altered temperatures and pH conditions to observe if these particles are stable or undergo changes. The shape of the curve in Figure 3.7a at  $50^{\circ}\text{C}$  changed most compared to the other shapes at 22 days (Fig.3.7a). Broadening of the absorption peak in an absorbance spectrum with ageing time was reported before, (Song et al. 2006). The colour of the  $50^{\circ}\text{C}$  sample became a darker red compared to the other samples. XRD patterns revealed that the selenium crystallization peak at  $30\ 2\theta^{\circ}$  appeared at a higher temperature during the stabilisation tests (Fig. 3.7B). Analyses with LM revealed structural changes in the selenium particles. Darker stretched particles were detected in the  $50^{\circ}\text{C}$  sample (see Fig. 3.7c). This indicates that at  $50^{\circ}\text{C}$  the amorphous selenium spheres had been transformed into a more stable structure.

The particles became more crystalline at  $50^{\circ}\text{C}$ . The same effect was observed at  $40^{\circ}\text{C}$ , but it was less strong. The  $30\ 2\theta^{\circ}$  appeared at a  $\text{pH}=9$  as well (detected by software) and the colour of the liquid seemed a little darkened. The recrystallization effect was less visible compared to  $50^{\circ}\text{C}$ , but recrystallization could have occurred at a higher pH in three weeks. The transformation from amorphous to the more crystalline structure needs energy and this transformation can be enhanced by increasing the temperature. A higher pH can also result in more crystalline selenium particles during the particle stability tests. Xi et al. (2006) proposed that the solubility of selenium increases due to the high pH and that amorphous selenium develops into trigonal selenium (Xi et al. 2006) which is hexagonal. When particles were produced directly at a higher temperature or pH, the precipitates seemed to be more hexagonal, darkened and acicular according to XRD and photos than after the particle stability tests under comparable conditions.

**Table 3.2: The biological properties of selenium particles as a function of pH and temperature in the literature**

Name	e-donor	pH	T	Time (h)	Dominant Morphology	XRD	Remark and morphology defined in the original source
<i>Geobacter sulfurreducens</i>	Acetate	7,5	30	500	Spheres	Amorphous	(a bit acicular structures) Weak peaks visible in XRD. Addition of anthraquinone disulfonic acid creates a crystalline structure.(Pearce et al., 2009)
<i>Shewanella oneidensis</i>	H <sub>2</sub>	7,5	30	500	Spheres	Amorphous	With anthraquinone disulfonic acid crystallinity detected (Pearce et al., 2009)
<i>Veillonella atypica</i>	H <sub>2</sub>	7,5	37	500	Spheres	Amorphous	With anthraquinone disulfonic acid (Pearce et al., 2009)
<i>Pseudomonas alcaliphilia</i>	Citrate	7.5	28	48	Spheres	Amorphous	Monoclinic and trigonal selenium according to Raman. Formation of t-Se-nanorods; transformation is avoided by adding PVP (Zhang et al., 2011)
<i>Geobacter sulfurreducens</i>	H <sub>2</sub>	7,5	30	500	Deformed spheres	Crystalline	With and without anthraquinone disulfonic acid (Pearce et al., 2009)
<i>Bacillus subtilis</i>	Glucose	7	35	48	Spheres (became larger in time) (washed with ethanol)	presumed to be monoclinic nanospheres from Raman data	(monoclinic) m-Se nanoparticles were capped by proteins excreted from <i>B.subtilis</i> (Wang et al., 2010)
<i>Bacillus magaterium</i>	Acetate	7.5	37	8	spheres	Crystalline according to XRD results	Crystalline spheres (Mishra et al, 2011) (reduction of selenite)
<i>Bacillus selenitireducens</i>	Lactate	9.8	30	400 h	Not available	Not available	Black crystalline allotrope (Herbel et al., 2003)
Purple non-sulphur bacterium strain NKPB030619	Phototrophic reaction	8	30	336 h	nanorods	Not available	-the pH increased, starting at 6.8 and was 8 at the end of the experiment. - phototrophic conditions - Amorphous red granules After 2 days - crystalline structure, needle-like structure; after 2 weeks (Yamada et al., 1997) (reduction of selenite)

**Table 3.2** pH and temperature values are from the various references. Sufficient examples were found with a pH around 7 and a temperature around 30°C, so only a selection is presented in this table. Examples of studies at other pH and temperature settings are less common. Sometimes only initial conditions were provided and deviations in the values are sometimes not validated by the authors of these scientific papers.

### 3.3.5 Effect of pH and temperature on particle properties in other studies

From our particle stability tests it is clear that selenium particles can be modified during ageing. To compare our results with other studies we focused on particles with a production time up to 500 hours to exclude ageing effects. The pH and temperature settings used for the production of selenium particles in other studies are summarised in Table 3.2.

The production temperature and the production pH of amorphous spheres are shown in

the first four lines of the Table 3.2. The corresponding pH is around 7.5 and the temperatures vary between 28°C and 37°C. These results are more or less comparable with our pH and temperature values for amorphous spheres production (Fig. 3.4). The production of intermediates is presented in lines 5 to 8 in Table 3.2. The pH is around 7 to 7.5 and the temperature range is from 30°C-37°C. These pH and temperature values are close to the pH and temperature values at which amorphous spherical selenium particles were produced and the particles are also more related to amorphous spheres than to the acicular hexagonal structure. The production of acicular, black or crystalline selenium was reported at T=30°C and a pH ranging from 8 - 9.8 (Table 3.2). Overall, the biological data reported in other studies are in agreement with our findings, though most data were obtained at around pH=7 and T=30°C.

### **3.3.6 Effect of the particle properties on selenium recovery**

Defrosted and sieved effluent from the fed-batch experiments was tested for sedimentation in a 30 mL tube. After a couple of seconds the tubes contained some solid material at the bottom of the tube and a coloured suspension with selenium particles remained (Fig.3.8). These non-precipitated suspensions were composed of heterogeneous structures of particles and biomass, and the medium and amount selenium that was produced varied as well. Only around a centimetre of the top of the suspension discoloured in days due to sedimentation, but this value cannot be quantified.

A particle size distribution curve was constructed from the fed-batch experiment at pH=7 and T=30°C (Fig.3.9). The average calculated selenium particle diameter was 260 nm. The corresponding sedimentation rate in water is in the order of 8 mm/day (see Appendix 1A Chapter 1). The calculated sedimentation rate is in the order of the estimated sedimentation rate in the sedimentation experiment described in the paragraph above.

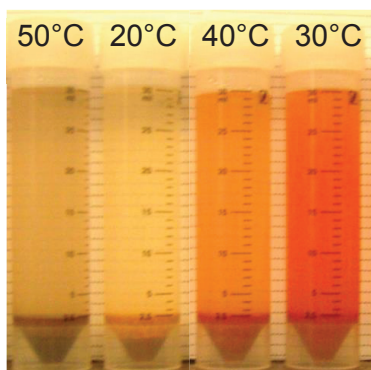


Figure 3.8: Sedimentation of defrosted liquid samples. Fed-batch experiments at pH= 7

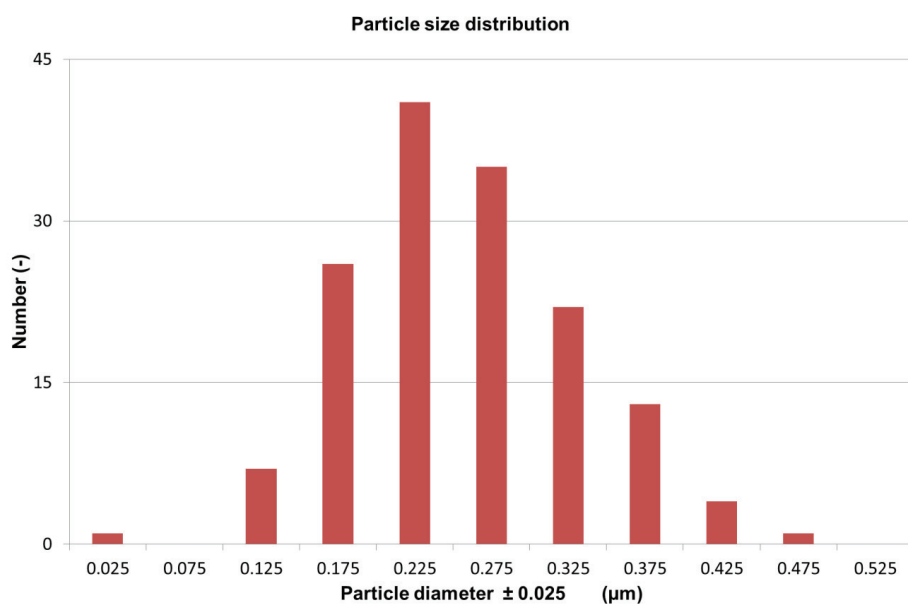


Figure 3.9: selenium particle size distribution curve constructed from a SEM picture of fed-batch experiment pH=7 and T=30°C. 150 particles were analysed using the software “ImageJ”.

A phase transformation from amorphous to more hexagonal selenium was established in the 50°C particle stability test. Although the density of the selenium particles increased,

the density of the biomass with the selenium particles seemed the same. This means that it is essential to grow hexagonal selenium particles to accelerate the sedimentation velocity significantly.

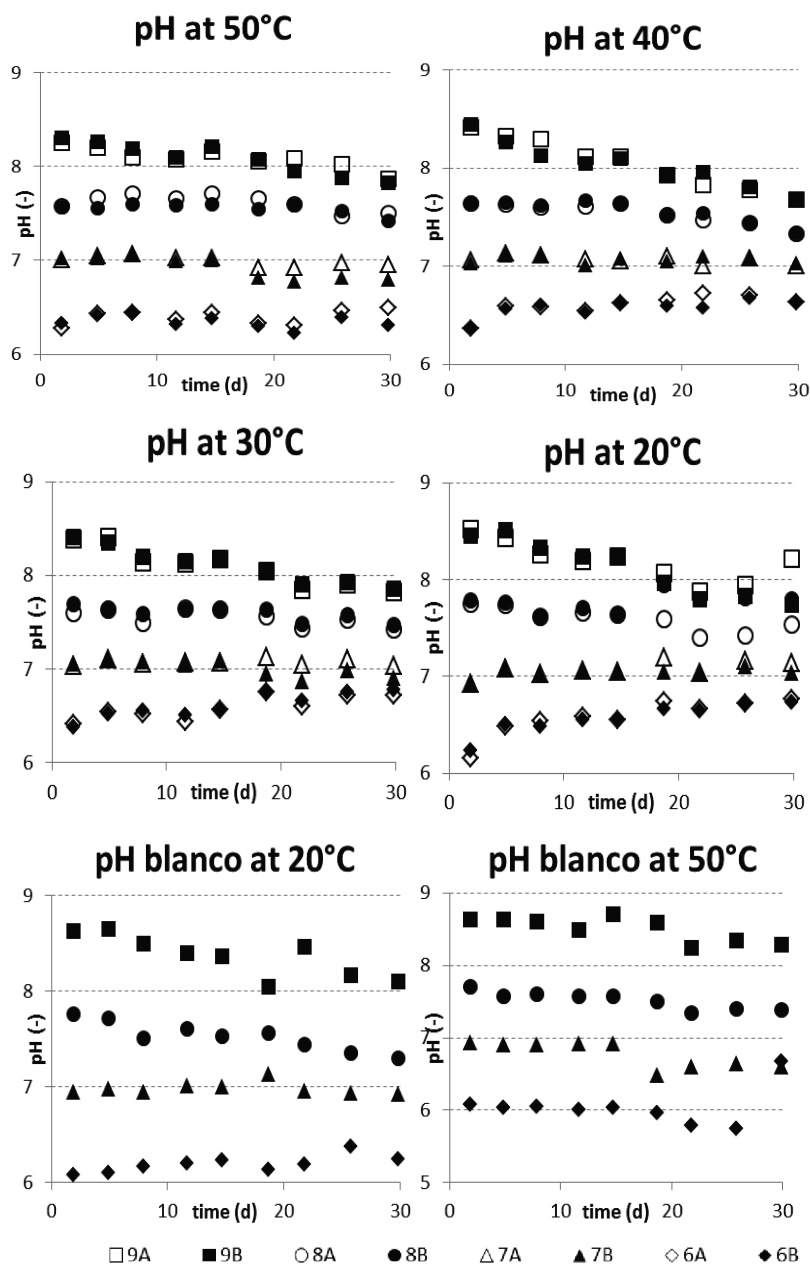
### **3.3.7 Production of recoverable particles**

To achieve an industrially applicable sedimentation rate larger selenium particles are required. Our ability to produce amorphous spherical nanoparticles that can transform to acicular structures corresponds to the description of several models (Xi et al. 2006) (Gates et al. 2002). The particle stability tests prove that the moment selenium particles are formed the particle formation is different compared to a post-treatment step under the same conditions. Amorphous selenium particles are metastable and transform in time to the acicular shape under the same pH, temperature and anoxic conditions. This is important for obtaining recoverable selenium particles. Furthermore, biomolecules such as proteins (Tejo Prakash et al. 2009) or other additives such as poly(vinylpyrrolidone) (Song et al. 2006) stabilise the amorphous selenium particles. It is preferred to grow larger acicular selenium structures instead of the amorphous red phase, because the particles seem to be extracellular and the density is larger and this could finally result in a cheaper selenium recovery system.

## **3.4 Conclusion**

Acicular crystalline hexagonal bio-selenium particles can be produced at a temperature of approximately 40°C or 50°C or/and a pH of approximately 8 or 9. A lower temperature between approximately 20°C and 30°C combined with a pH of 6 or 7 resulted in mostly amorphous selenium particles that seemed to be more connected to the biomass. The effect of temperature and pH on the properties of the selenium particles was more effective when selenium particles were produced than during the post-modification processes used to convert amorphous spheres to the acicular structure. Unfortunately, the majority of the acicular particles did not accelerate the sedimentation process since the mass of the acicular and the amorphous particles were comparable. However, the formation of biological acicular selenium particles can be seen as the first step towards growing compact selenium particles to achieve good cheap selenium recovery through solid liquid separation.

### Appendix 3A: pH measurements during batch experiments



Bottles are labelled as the set-point of the pH. Blanco experiments (without biomass) led to less change in pH compared to the bottles with added biomass.

## Appendix 3B: XRD peak tables

Table B-1: Peaks in the XRD patterns during 4 batch experiments

Batch pH=6	No.	Pos. [°2Th.]	FWHM Left [°2Th.]	Area [cts*°2Th.]	Backgr. [cts]	d-spacing [Å]	Height [cts]	Rel. Int. [%]	Integral Breadth [°2Th.]
T=30°C	#N/A	#N/A	#N/A	#N/A	#N/A	#N/A	#N/A	#N/A	#N/A
Batch pH=7	1	12.1749	0.059	5.33	96.66	7.26984	91.5	16.53	0.05824
T=20°C	2	13.6755	0.0984	53.74	102.2	6.47531	553.6	100	0.097067
	3	16.2665	0.9446	11.64	114.38	5.44927	12.49	2.26	0.93184
	<b><u>4</u></b>	<b><u>54.9904</u></b>	<b><u>0.1968</u></b>	<b><u>9.93</u></b>	<b><u>68.64</u></b>	<b><u>1.66987</u></b>	<b><u>51.16</u></b>	<b><u>9.24</u></b>	<b><u>0.194133</u></b>
	<b><u>5</u></b>	<b><u>70.2668</u></b>	<b><u>0.3149</u></b>	<b><u>6.3</u></b>	<b><u>58.04</u></b>	<b><u>1.33964</u></b>	<b><u>20.29</u></b>	<b><u>3.66</u></b>	<b><u>0.310613</u></b>
Batch pH=8	1	12.8739	0.1181	4.33	93.42	6.87665	37.14	89.62	0.11648
T=40°C	2	25.3776	0.4723	10.86	184.21	3.50976	23.32	56.26	0.46592
	<b><u>3</u></b>	<b><u>29.927</u></b>	<b><u>0.2362</u></b>	<b><u>9.65</u></b>	<b><u>159.25</u></b>	<b><u>2.98577</u></b>	<b><u>41.44</u></b>	<b><u>100</u></b>	<b><u>0.23296</u></b>
Batch pH=9	1	24.0573	0.1181	80.36	182.65	3.6993	689.91	27.19	0.11648
T=50°C	<b><u>2</u></b>	<b><u>29.3077</u></b>	<b><u>0.2362</u></b>	<b><u>9.02</u></b>	<b><u>156.92</u></b>	<b><u>3.04744</u></b>	<b><u>38.73</u></b>	<b><u>1.53</u></b>	<b><u>0.23296</u></b>
	3	30.2247	0.1574	23.41	152.31	2.95704	150.76	5.94	0.155307
	4	41.8621	0.4723	30.54	83.64	2.15801	65.55	2.58	0.46592
	5	44.7204	0.096	324.78	79.33	2.02482	2537.37	100	0.128
	6	44.859	0.048	90.62	79.13	2.02391	1415.95	55.8	0.064
	7	45.9311	0.576	15.37	77.51	1.97423	20.02	0.79	0.768
	8	48.7427	0.768	15.18	73.91	1.86672	14.82	0.58	1.024
	9	52.2162	0.384	8.46	69.52	1.75042	16.53	0.65	0.512
	10	65.7914	0.768	23.75	66.65	1.41831	23.2	0.91	1.024

*XRD peaks from 4 batch experiments: Italic and underline lines correspond with hexagonal selenium peaks according reference pattern 96-901-2502, according to the software used. FWHM =Full width at half maximum.*

**Table B-2: XRD Peak table in 7 fed-batch experiments**

Fed-Batch pH=7	No.	Pos. [°2Th.]	FWHM Left [°2Th.]	Area [cts**2Th.]	Backgr. [cts]	d-spacing [Å]	Height [cts]	Rel. Int. [%]	Integral Breadth [°2Th.]
T=20°C	1	5.5389	0.9446	35.48	199.36	15.95582	38.08	23.06	0.93184
	2	12.2459	0.1181	18.92	140.6	7.22785	162.47	98.38	0.11648
	3	12.992	0.1574	10.42	139.56	6.81438	67.11	40.64	0.155307
	4	13.7652	0.1574	11.51	138.48	6.43329	74.13	44.89	0.155307
	5	16.2586	0.4723	11.61	142.02	5.45188	24.91	15.08	0.46592
	6	25.4948	0.3149	14.42	185.9	3.49388	46.41	28.1	0.310613
	<u>7</u>	<u>30.0497</u>	<u>0.059</u>	<u>9.62</u>	<u>160.07</u>	<u>2.97385</u>	<u>165.15</u>	<u>100</u>	<u>0.05824</u>
	<u>8</u>	<u>48.1144</u>	<u>0.4723</u>	<u>6.82</u>	<u>80.56</u>	<u>1.89118</u>	<u>14.65</u>	<u>8.87</u>	<u>0.46592</u>
Fed-Batch pH=7	1	12.7576	0.3149	11.36	167.2	6.93907	36.56	100	0.310613
T=30°C	<u>2</u>	<u>29.965</u>	<u>0.2362</u>	<u>8.06</u>	<u>202.89</u>	<u>2.98207</u>	<u>34.61</u>	<u>94.66</u>	<u>0.23296</u>
Fed-Batch pH=7	1	12.9155	0.4723	8.17	185.7	6.85458	17.53	25.58	0.46592
T=40°C	2	16.4745	0.9446	17.31	185.36	5.38091	18.57	27.1	0.93184
	<u>3</u>	<u>24.015</u>	<u>0.4723</u>	<u>18.18</u>	<u>221.95</u>	<u>3.70572</u>	<u>39.02</u>	<u>56.93</u>	<u>0.46592</u>
	<u>4</u>	<u>30.0321</u>	<u>0.1181</u>	<u>7.98</u>	<u>194.28</u>	<u>2.97556</u>	<u>68.53</u>	<u>100</u>	<u>0.11648</u>
Fed-Batch pH=7	1	16.4791	0.9446	18.2	228.71	5.37941	19.53	2.36	0.93184
T=50°C	<u>2</u>	<u>24.0714</u>	<u>0.3542</u>	<u>233.64</u>	<u>239.07</u>	<u>3.69716</u>	<u>668.61</u>	<u>80.66</u>	<u>0.34944</u>
	<u>3</u>	<u>30.3478</u>	<u>0.1574</u>	<u>128.74</u>	<u>216.55</u>	<u>2.94533</u>	<u>828.94</u>	<u>100</u>	<u>0.155307</u>
	<u>4</u>	<u>41.8053</u>	<u>0.551</u>	<u>59.12</u>	<u>165.12</u>	<u>2.16081</u>	<u>108.76</u>	<u>13.12</u>	<u>0.543573</u>
	<u>5</u>	<u>44.4287</u>	<u>0.551</u>	<u>45.17</u>	<u>159.12</u>	<u>2.03912</u>	<u>83.1</u>	<u>10.03</u>	<u>0.543573</u>
	<u>6</u>	<u>45.8166</u>	<u>0.6298</u>	<u>64.22</u>	<u>155.94</u>	<u>1.98053</u>	<u>103.37</u>	<u>12.47</u>	<u>0.621227</u>
	<u>7</u>	<u>48.1603</u>	<u>0.6298</u>	<u>12.77</u>	<u>152.22</u>	<u>1.88949</u>	<u>20.55</u>	<u>2.48</u>	<u>0.621227</u>
	<u>8</u>	<u>52.1542</u>	<u>0.2362</u>	<u>20.07</u>	<u>145.72</u>	<u>1.7538</u>	<u>86.17</u>	<u>10.4</u>	<u>0.23296</u>
	<u>9</u>	<u>56.6462</u>	<u>0.4723</u>	<u>16.02</u>	<u>138.51</u>	<u>1.62493</u>	<u>34.38</u>	<u>4.15</u>	<u>0.46592</u>
	<u>10</u>	<u>62.224</u>	<u>0.6298</u>	<u>21.63</u>	<u>132.87</u>	<u>1.492</u>	<u>34.81</u>	<u>4.2</u>	<u>0.621227</u>
	<u>11</u>	<u>65.5224</u>	<u>0.7872</u>	<u>30</u>	<u>134.65</u>	<u>1.42466</u>	<u>38.63</u>	<u>4.66</u>	<u>0.776533</u>
Fed-Batch pH=6	1	7.9764	0.551	49.06	134.52	11.08449	90.26	100	0.543573
T=30°C	2	16.1219	0.9446	14.3	140.84	5.49781	15.35	17	0.93184
	<u>3</u>	<u>29.9787</u>	<u>0.4723</u>	<u>11.9</u>	<u>167.79</u>	<u>2.98074</u>	<u>25.55</u>	<u>28.31</u>	<u>0.46592</u>
Fed-Batch pH=8	1	12.9083	0.1574	7.76	168.51	6.85838	49.99	8.29	0.155307
T=30°C	2	18.5467	0.3149	10.01	175.05	4.78412	32.24	5.35	0.310613
	<u>3</u>	<u>24.0594</u>	<u>0.3936</u>	<u>234.13</u>	<u>209.47</u>	<u>3.69898</u>	<u>603.01</u>	<u>100</u>	<u>0.388267</u>
	<u>4</u>	<u>30.0057</u>	<u>0.0984</u>	<u>38.43</u>	<u>166.66</u>	<u>2.97812</u>	<u>395.93</u>	<u>65.66</u>	<u>0.097067</u>
	<u>5</u>	<u>30.3138</u>	<u>0.1574</u>	<u>28.86</u>	<u>165.29</u>	<u>2.94855</u>	<u>185.8</u>	<u>30.81</u>	<u>0.155307</u>
	<u>6</u>	<u>41.9688</u>	<u>0.7872</u>	<u>54.41</u>	<u>106.98</u>	<u>2.15277</u>	<u>70.07</u>	<u>11.62</u>	<u>0.776533</u>
	<u>7</u>	<u>45.9117</u>	<u>0.4723</u>	<u>14.46</u>	<u>103.32</u>	<u>1.97665</u>	<u>31.03</u>	<u>5.15</u>	<u>0.46592</u>
	<u>8</u>	<u>48.155</u>	<u>0.4723</u>	<u>7.51</u>	<u>97.32</u>	<u>1.88968</u>	<u>16.13</u>	<u>2.67</u>	<u>0.46592</u>
	<u>9</u>	<u>52.2245</u>	<u>0.6298</u>	<u>17.01</u>	<u>91.01</u>	<u>1.75161</u>	<u>27.38</u>	<u>4.54</u>	<u>0.621227</u>
	<u>10</u>	<u>65.6017</u>	<u>0.4723</u>	<u>15.46</u>	<u>83.67</u>	<u>1.42313</u>	<u>33.19</u>	<u>5.5</u>	<u>0.46592</u>
Fed-Batch pH=9	1	5.324	0.4723	18.3	239.51	16.59943	39.29	20.36	0.46592
T=30°C	2	12.8445	0.2362	7.95	176.64	6.8923	34.12	17.68	0.23296
	3	16.2858	0.9446	15.42	170.77	5.44285	16.55	8.58	0.93184
	<u>4</u>	<u>24.011</u>	<u>0.2362</u>	<u>36.75</u>	<u>203.8</u>	<u>3.70633</u>	<u>157.73</u>	<u>81.75</u>	<u>0.23296</u>
	<u>5</u>	<u>29.9574</u>	<u>0.1574</u>	<u>29.97</u>	<u>186.32</u>	<u>2.98281</u>	<u>192.95</u>	<u>100</u>	<u>0.155307</u>
	<u>6</u>	<u>41.7238</u>	<u>0.6298</u>	<u>16.82</u>	<u>110.64</u>	<u>2.16484</u>	<u>27.07</u>	<u>14.03</u>	<u>0.621227</u>
	<u>7</u>	<u>45.64</u>	<u>0.7872</u>	<u>12.4</u>	<u>106.69</u>	<u>1.98778</u>	<u>15.97</u>	<u>8.28</u>	<u>0.776533</u>
	<u>8</u>	<u>52.1311</u>	<u>0.4723</u>	<u>10.19</u>	<u>93.21</u>	<u>1.75453</u>	<u>21.87</u>	<u>11.34</u>	<u>0.46592</u>

*Italic and underline lines correspond with hexagonal selenium peaks according reference pattern 96-901-2502, according to the software used. FWHM =Full width at half maximum.*



**Table B-3: Peak in the XRD diffractogram during the particle stability tests**

stability test	No.	Pos. [°2Th.]	FWHM Left [°2Th.]	Area [cts*°2Th. ]	Backgr.[ct s]	d-spacing [Å]	Height [cts]	Rel. Int. [%]	Integral Breadth [°2Th.]
pH=9 T=30°C	1	5.3462	0.9446	31.12	171.65	16.5305	33.4	3.28	0.93184
	2	16.371	0.0984	98.97	136.59	5.41472	1019.62	100	0.097067
	<u>3</u>	<u>30.0499</u>	<u>0.4723</u>	<u>10.7</u>	<u>170.12</u>	<u>2.97384</u>	<u>22.96</u>	<u>2.25</u>	<u>0.46592</u>
	4	32.4442	0.1378	9.59	149.53	2.75964	70.56	6.92	0.135893
	5	33.8214	0.0984	15.73	137.69	2.65035	162.09	15.9	0.097067
	<u>6</u>	<u>77.623</u>	<u>0.1181</u>	<u>0.71</u>	<u>54.19</u>	<u>1.23004</u>	<u>6.12</u>	<u>0.6</u>	<u>0.11648</u>
stability test pH=8 T=30°C	1	45.3162	0.672	4.53	74.16	1.99957	5.06	100	0.896
stability test pH=7 T=30°C	1	16.1483	0.768	14.87	136.17	5.48434	14.52	100	1.024
stability test pH=7 T=40°C	<u>1</u>	<u>23.7301</u>	<u>0.9446</u>	<u>17.93</u>	<u>194.07</u>	<u>3.74957</u>	<u>19.24</u>	<u>91.87</u>	<u>0.93184</u>
	<u>2</u>	<u>29.9505</u>	<u>0.6298</u>	<u>13.01</u>	<u>164.32</u>	<u>2.98348</u>	<u>20.94</u>	<u>100</u>	<u>0.621227</u>
stability test pH=7 T=50°C	<u>1</u>	<u>23.8565</u>	<u>0.6298</u>	<u>19.92</u>	<u>180.66</u>	<u>3.72998</u>	<u>32.06</u>	<u>55.1</u>	<u>0.621227</u>
	<u>2</u>	<u>30.1703</u>	<u>0.3149</u>	<u>18.07</u>	<u>152.54</u>	<u>2.96225</u>	<u>58.19</u>	<u>100</u>	<u>0.310613</u>

*Italic and underline lines correspond with hexagonal selenium peaks according reference pattern 96-901-2502, according to the software used. FWHM =Full width at half maximum.*



## **Chapter 4**

### **Selenate reduction to produce recoverable elemental selenium at 50°C by granular sludge from an anaerobic reactor**

This chapter has been prepared for submission as:

Selenate reduction to produce recoverable elemental selenium at 50°C by granular sludge from an anaerobic reactor

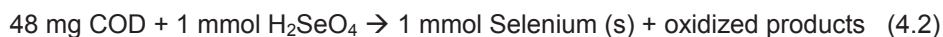
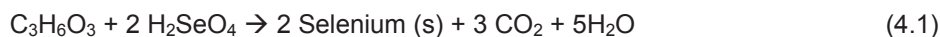
Simon P. W. Hageman,  
Renata D. van der Weijden,  
Alfons J.M. Stams,  
Cees J.N. Buisman.

## **Abstract**

Selenate can be removed from wastewater streams by microbial reduction to form insoluble elemental selenium particles. Selenate is potentially highly toxic at low concentrations and selenium is a valuable element that can be recovered. The size and density of the bio-selenium particles are crucial to enable a viable solid liquid separation process. Until now most biologically produced amorphous selenium particles have been smaller than the micro-organisms. This study focused on producing crystalline bio-selenium particles in the micrometre range. A continuous anaerobic gas lift loop reactor with an internal settler for solid liquid separation inoculated with methanogenic granular sludge was used. Selenate feed of 1 mM with a daily loading rate of 43 mg selenium equivalent was reduced with lactic acid as the electron donor at 50°C and a pH of 7. Hydraulic retention time was around 8.5 days and the experiment was performed over months to allow selenium particles to grow in size. The selenium particles had an acicular needle shape and were about 10 µm in length and about 1 µm in width. They were often surrounded by biomass. The selenium particle size is comparable to those observed in the previous three-week experiments. This means that the selenium particles did not grow further during the long-term experiment. Nevertheless, the selenium acicular particles were sometime concentrated and occurred as larger clusters, which offers promising perspectives for selenium recovery. Microbial selenate reduction activity in the bioreactor was monitored over the months; the biomass reduced around 5% of the selenate that entered the reactor, resulting in limited selenium particle formation. This low reduction capacity might be due to the low electron donor concentration used or the sludge type. In future, the selenate reduction capacity in the reactor could be increased by using more electron donor or by using a thermophilic sludge.

## 4.1 Introduction

Selenate in wastewater streams can be hazardous due to possible toxic accumulation effects (Högberg and Alexander 2007). This is why selenate must be removed from wastewater streams. This can be done by biological reduction followed by solid liquid separation (Staicu et al. 2015). Biological reduction is an environmentally friendly technique that can be used to remove and recover selenium. In the process, organic compounds are oxidized and soluble selenate is reduced to insoluble elemental selenium by microbes (eq 4.1 and eq 4.2).



The selenium particles thus produced can be removed from the wastewater to yield selenium-free water and a pure solid selenium product. The latter is also beneficial, because selenium is a useful element in many industries. It is crucial that the bio-selenium particles have properties that enable a practical solid liquid separation process. The morphology of biological solid selenium particles, which were obtained from selenate bio-reduction by Eerbeek sludge, can be controlled by pH and temperature: a relatively high pH (8-9) and/or a relatively high temperature (40°C and 50°C) resulted in more acicular particles (Chapter 2). Acicular particles often consist of hexagonal selenium. Hexagonal selenium grew to larger crystals and seems to be less attached to biomass than amorphous particles (Chapter 4). However, previous experiments only lasted for weeks and this could have prevented the selenium particles from growing further, which is essential to improve solid liquid separation. This is why a long-term continuous bio-reduction experiment was carried out under process conditions in which acicular selenium particles can be formed.

Selenate reduction at a combination of high temperature and a high pH should be within the limits of the biomass so it will still be able to reduce selenate. Experiments at either 50°C or pH=9 promoted hexagonal particle formation, but reduced the selenate reduction rate (Chapter 2). The 50°C has several advantages: (1) When selenium particles have been produced, a temperature of 50°C promotes the

formation of acicular selenium particles more than a pH of 9 (Chapter 3), (2) temperature control is more suitable than pH control of pH-buffered aqueous wastewater streams, (3) in aqueous solutions at 50°C, selenium nanoparticles can crystallize to the more acicular structure in about 45 minutes (Wu and Ni 2012). This means that with an HRT of 8.5 days the amorphous structure is not maintained, and (4) crushed Eerbeek sludge has the ability to bio-convert several substrates, including CO and SO<sub>4</sub> at 55°C (Sipma et al. 2004). Although previous described fed-batch experiments demonstrate that the selenate reduction activity using Eerbeek sludge was much lower at 50°C than at 30°C (Chapter 2), the loss in selenate reduction capacity might be compensated with a hydraulic retention time of 9 days (Fujita et al. 2002) and the addition of yeast extract (Zhang et al. 2003). A combination of 50 degrees and pH 9 is expected to reduce the selenate reduction capacity too much. For this reason, a temperature of 50°C and a pH=7 was chosen to operate the reactor.

Theoretically, the biomass yield from selenate reduction using lactate is higher than that using fermentation. This might result in a positive selection for selenate-reducing bacteria and these bacteria might outcompete the methanogenic archaea. This energetic selection advantage was demonstrated for *Enterobacter cloacae* SLD1a-1 by Leaver et al. 2008 (Leaver et al. 2008). Less non-selenate-reducing biomass is wanted, because it is suggested by Tejo Prakash 2009 that biomass has the ability to act as a stabilizing agent for amorphous selenium particles (Tejo Prakash et al. 2009). To emphasize the positive selection of selenate reducing bacteria, the electron donor should be balanced with the amount of selenate (eq 4.1 and eq 4.2).

The aim of this research was to grow larger bio-selenium particles in a continuous air lift loop reactor at 50°C. The gas lift loop reactor was chosen because selenium particles and the biomass can be retained in the bioreactor by an internal settler. Granular anaerobic sludge was used as inoculum. To allow reduction of selenate to elemental selenium and to give the selenium thus produced time to form particles in the reactor a hydraulic retention time of 9 days was used. The experiment was performed for almost 230 days to allow the particles to grow.

## **4.2 Material and methods**

### **4.2.1 Biomass and medium**

Eerbeek sludge has been described and characterized in several studies (Roest et al. 2005) (Janssen et al. 2009) and has been used in selenate reduction experiments (Astratinei et al. 2006, Lenz et al. 2008a). Eerbeek sludge was used as biocatalyst because it is able to reduce selenate at 50°C (Chapter 2) and it was successfully used in long-term selenate reduction experiments (months) at 30°C and pH=7 (Lenz et al. 2008a). Unless otherwise stated, medium composition is based on Stams et al (Stams et al. 1992), with the following additions: 1 mM selenate, 0.55 mM lactic acid as electron donor and carbon source and 0.1 g/L yeast extract. Influent was flushed with nitrogen gas prior to leading it into the reactor with a Stepdos pump. During the experiments modifications of the medium were made (see Table 4.1).

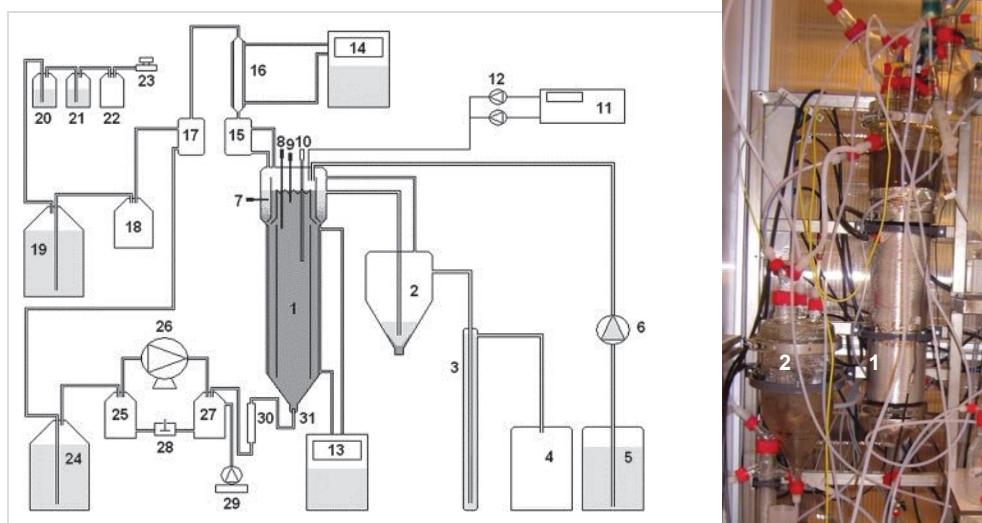


Figure 4.1: Schematic overview of the gas lift loop reactor with internal and external settler (adapted and modified from Hol et al (Hol et al. 2010)): 1. Gas lift loop reactor; 2. External settler (reactor effluent); 3. Water lock; 4. Water lock overflow; 5. Influent; 6. Influent pump; 7. Temperature sensor; 8. Redox electrode; 9. pH electrode; 10. Sample tube (Titanium); 11. pH controller; 12. Acid/base addition; 13. Water bath (heating); 14. Water bath (cooling); 15. Condense back flush; 16. Condenser; 17. Gas effluent split off; 18. Gas wash back flush bottle; 19. (not used) 20. Wash bottle ethyl glycol. 21. Wash bottle base. 22. Ritter back flush; 23. Ritter (gas meter); 25. Recycle bottle; 26. Recycle gas pump; 27. Pressure bottle; 28. valve; 29. N<sub>2</sub> addition; 30. Sho-rate (flow rate); 31. Sparger.

During the experiment adaptations were made to the gas wash systems. Washing recycle gas: The experiment started without washing the recycle gas. At day 77, 1 L ethyl glycol was used as a washing system, including a back-flush bottle. At day 81, the washing system was replaced by 5L 1M Nitric acid. Gas out: Washed with pure ethylglycol to trap methylated compounds, 3 M NaOH to trap selenide.



#### **4.2.2 Reactor conditions and operation**

The design of the anaerobic gas loop reactor (fig. 4.1) was based on Hol. et al 2010 studying the bio-reduction of pyrite (Hol et al. 2010). The working volume of the reactor liquid was 4.7L. The temperature was controlled and set at 50°C and the external settler temperature was uncontrolled and to be around 30°C. The feed was 0.55L per day and this resulted in a HRT of 8.5 days. The feed was monitored by volume and weight of the storage vessel (s) and effluent by the liquid volume in the external settler. The inoculum was 50 g wet weight, unadapted granular Eerbeek sludge. Redox potential was measured with a 210 mm glass S8 Pt-billet redox electrode against Ag/AgCl and monitored with a PHM 210 Radiometer. The pH was measured with a 210 mm glass S8 pH electrode (QP181X/210) and controlled with 0.1 M KOH and kept at pH=7. During the experiment the base feed was measured by noting the differences in weight of the KOH storage containers.

At the start of the experiment, the reactor was filled with the complete medium but without selenate and lactic acid. Later, the selenate-containing medium flow was 550 mL/day. Lactic acid solution and yeast solutions were added to the reactor in certain periods and this is shown with operational modifications in Table 4.1.

**Table 4.1: Modifications in reactor operation**

Period (#)	Time (days)	Adaption	Remark	Result
I	0	Start-up	Start-up was without washing of the recycle gas	Selenate in the reactor diluted to 0.98 mM due to base addition. HRT=8.3 days.
II	57	Influent	Lactic acid separate: influent increases with 25 mL per day	Selenate in the reactor diluted to 0.95 mM, due to separate lactic acid addition. HRT = 8.1 days
	77	Gas recycle	Ethylglycol washing system (To improve the trapping of methylated selenium if produced)	
	81	Gas recycle	Stripping with Nitric Acid (Winkel et al. 2009) (To improve the trapping of methylated selenium if produced)	
III	92	Influent	Influent omitted yeast extract: No sulphur compound in the influent	Selenate in the reactor diluted to 0,95 mM HRT = 8.1 days
IV	145	Influent	Added lactic acid amount increased 5 times	Selenate in the reactor diluted to 0.97 mM HRT = 8.2 days.
	201	Pump	Replacement of the influent pump	
V	209	Influent	Additional of yeast extraction: total influent increased 8 ml per day	Selenate in the reactor diluted to 0.95 mM HRT = 8.1 days.
	235	Stop		

The nitrogen gas influent was 3 litres per hour. The recirculating gas was manually controlled around 0.5 L/min and monitored with an R-2-15-C Sapphire Sho-rate from Brooks Instruments. The gas stream from the reactor was first cooled by the condenser with a cooling temperature of 4°C. After cooling, the gas was split into two streams: gas for recirculation and gas that leaves the system.

#### 4.2.3 Analytical methods

Fatty acids (acetate and propionate) were analysed by GC (Weijma et al. 2000). Lactic acid was analysed by HPLC on a column for organic acids (OA-1000 Alltech

9046) and detected by differential refractometry (separations). The mobile phase was 0.01 N H<sub>2</sub>SO<sub>4</sub> and 0.6 mL/min. The column temperature was 60°C. Selenite and selenate were analysed by IC (Chapter 2, Lenz et al. 2006). Chemical oxygen demand (COD) was measured with a Hach Lange kit for COD and a Hach Lange Xion 500 spectrophotometer. Selenium in liquids or solids was analysed by ICP-OES and the samples with solid particles were microwave destructed in aqua regia. Reactor samples were also analysed with scanning electron microscope (SEM) and light microscope (LM). SEM settings and sample preparation are described in Chapter 4. Sulphide in the reactor liquid was analysed with a Hach Lange kit.

#### **4.2.4 Calculations**

Feed of the supply barrels was based on the slope of weight loss in time. During the experiment a precipitate was analysed for elements by ICP-OES. The molar amount of oxygen was calculated as four times the molar amount of phosphorous. The weight of the precipitate was calculated from Ca<sup>2+</sup>, Mg<sup>2+</sup>, Na<sup>+</sup> and PO<sub>4</sub><sup>3-</sup>.

### **4.3 Results and discussion**

#### **4.3.1 Selenate concentration**

The selenate concentration in the reactor was measured over time and the results are presented in Figure 4.2. The selenate concentration increased from 0 at the start and achieved a concentration of around 0.9 mM selenate in the first 57 days. If selenate had not been converted, the selenate concentration would be varied between 0.95 and 1.00 mM due to dilution effects caused by for example base addition (Fig. 4.2 and Table 4.1). The concentration measured in the reactor was lower and it varied between 0.90 and 0.95 mM, indicating selenate reduction during the whole experiment (Fig. 4.2). Roughly estimated, an average 5% of the selenate was reduced, which is low compared to other reactors.

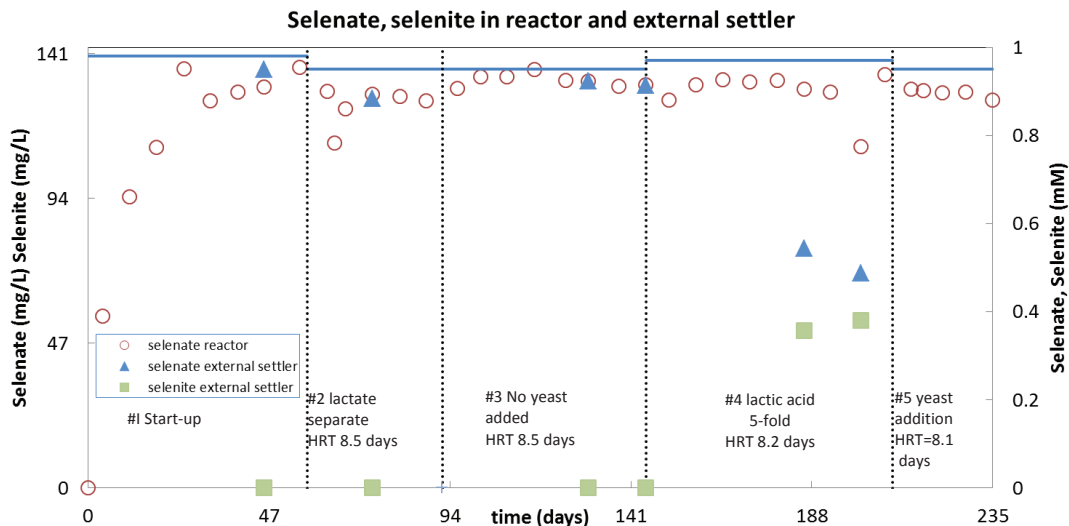


*Figure 4.2: Selenate and selenite concentration in the reactor (pH=7 and T=50°C) and the external settler. The dotted vertical line indicates the start of a new period. The low selenate concentration of 111 mg / L at 201 days is due to a technical failure of the pump. Sulphide was not detected during the experiment.*

Selenate removal efficiency by Eerbeek sludge could be as high as 97% and 99%, as was observed in reactors operated for 132 days at 30°C and pH=7 with 0.1 mM selenate and 13 mM lactic acid in the influent (Lenz et al. 2008a). Removal efficiency of 14% was obtained in fed-batch reactors which operated for three weeks at 50°C and pH=7 with around 25 mM selenate and 12.8 mM lactic acid in the influent (Chapter 2).

It was expected that selenate reducers would grow in the bioreactor over time and the performance of the selenate reduction in the bioreactor would increase. This development of specialised selenate reducers was also suggested by Lenz et al (Lenz et al. 2008a) to explain the improvement of selenate reduction after 58 days in a mesophilic reactor with Eerbeek sludge. However, in our experiment an increase in selenate reduction was not established.

If 5% of the selenate had been converted to elemental selenium, this would accumulate to around 2 mg selenium per day, and around 0.6 g for the total experiment. Selenite was not detected in the reactor during the 270 days and this is in agreement with findings in other 50°C selenate reduction experiments with Eerbeek sludge (Chapter 2).

The selenate concentration in the external settler was equal to the selenate reactor concentration, but this changed in period IV. The increased electron donor addition to the reactor also resulted in more electron donor in the external settler. As a result, around 40% of the selenate was converted to selenite in the external settler at 30°C (fig. 4.2). Selenite production was also observed in fed-batch experiments with Eerbeek sludge at 30°C (Chapter 2).

#### **4.3.2 COD concentration**

The electron donor load was 27 mg lactate per day in the first three periods and 136 mg COD per day in period IV. The measured starting concentration COD in the reactor was around 162 mg COD/L (Fig. 4.3). This COD, which was added to the reactor by the inoculum, did not contain acetate and propionate. Lactic acid was not detected in the reactor during the experiment. The conversion of lactic acid leads to acetate and propionate formation; acetate was around 55 mg COD/L at 12 days and propionate around 10 mg COD/L (Fig. 4.3), i.e. the lactic acid was oxidized.

During period II the COD concentration in the reactor was around 50 mg COD/L, although there were some fluctuations. In period II, the yeast extract was removed from the influent, the COD concentration decreased further, and as a result the measured total COD concentration represented only acetate (Fig. 4.3).

In the last two periods, the COD concentration in the effluent increased due to the addition of extra substrate. The concentration of acetate fluctuated and was not directly related to the COD measured (Fig. 4.3). Lenz et al. 2008a, used a molar ratio of 1 selenate to 130 lactic acid and achieved a 97% to 99% selenate removal efficiency at 30°C in a 150-day experiment, and after 16 days of start-up all of the

COD was removed (Lenz et al. 2008a). In ideal situations 1 mM lactic acid conversion is equivalent to 2 mM selenate conversion to elemental selenium. In our experiment the molar ratio was 1 selenate to 0.55 lactic acid at the start of the experiment. This ratio might have been too low for complete selenate reduction at 50°C, but the electron donor was not completely depleted. In fed-batch experiments at 50°C the selenate reduction still continued at COD concentrations of around 0.3 g L<sup>-1</sup> (Chapter 2).

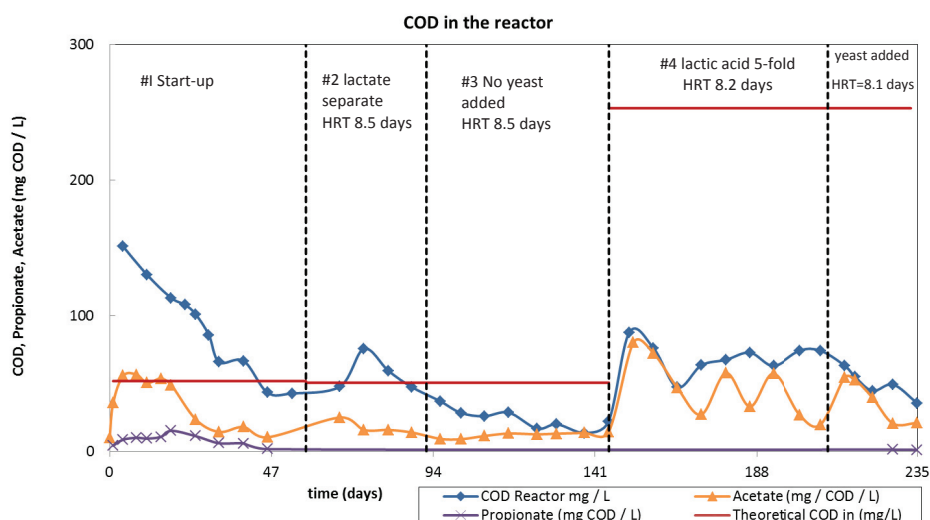


Figure 4.3: COD, acetate and propionate in the gas lift loop reactor. A dotted line indicates the start of a new period.

Comparing Figure 4.3 with Figure 4.4 show that a higher measured COD corresponds to a more negative redox potential. We can conclude from the redox potential that the biomass was still active and had reducing capacity during the whole experiment causing the low redox potential (Fig. 4.4). The measured redox potential in this experiment is comparable to that measured in a former fed-batch experiment for selenate reduction at 50°C (Chapter 2). Due to the addition of yeast extract in period 5, the redox potential became more negative and more stable during the sampling (Fig. 4.4). Probably more conversions took place from the COD in the yeast extract.

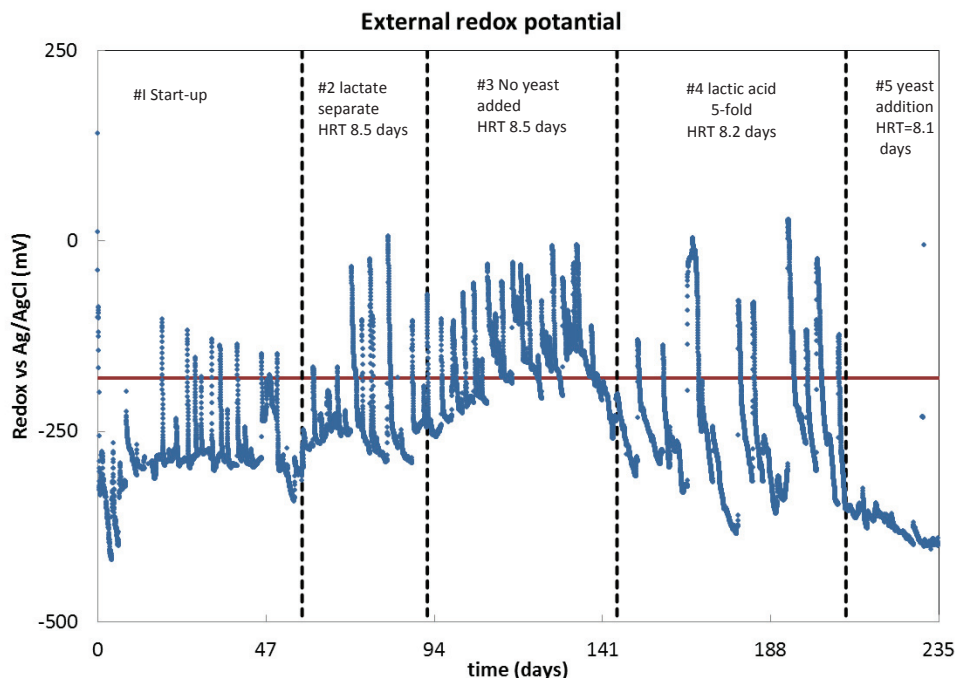


Figure 4.4: Redox potential during the experiment. The horizontal line indicates the redox potential between selenite and elemental selenium; -180 mV vs Ag/AgCl. The redox potential for selenate to selenite conversion is around 100 mV vs Ag/AgCl (Redox potential values were calculated with software HSC chemistry 6 (Ourtotec))

#### 4.3.3 Particle formation and biomass activity

Though selenate reduction was slow, selenium particles were detected. The reactor liquid turned red-brown in 10 days, which was mainly due to the formation of solid selenium particles (Fig. 4.5A). This colour was comparable to the liquid colour in the fed-batch reactor at 50°C (Chapter 3).

In the first period, the acicular selenium particles in the reactor were studied using light microscopy, biomass and other materials surrounded the particles. The size of the acicular structures was 10  $\mu\text{m}$  long and several  $\mu\text{m}$  thick (Fig. 4.5B). The selenium particles were mixed with the biomass, but biomass without selenium particles was also

present. The particle morphology was acicular, as in fed-batch experiments at 50°C in Chapter 2. Further, during this experiment it seemed that the biomass and particles in the liquid, with passing of time, stuck more and more onto the inner surface of the reactor and became less and less suspended.

In period II the reactor liquid became more transparent and the biomass activity had moved from the liquid to the internal surface of the reactor. The original granular sludge particles were almost invisible. Probably the granules were instable in this medium at a pH of 7, 50°C and low COD load.

From period III onwards, samples from the reactor liquid contained little dispersed biomass and selenium particles. For that reason, prior to sampling, the internal gas recirculation was accelerated for several seconds to remove the biomass and particles from the internal reactor surface. As a result of the rough mixing, acicular particles moved to the external settler. In addition, we observed biofilms in our sampling liquid and this means that biofilms were formed in the bioreactor. Probably due to the mixing some biofilm parts entered the sampling port. The biomass film, which had a thickness of several  $\mu\text{m}$ , contained selenium particles (Figure 4.5C). The detection of selenium particles in the biofilms is important since it indicates biomass growth and that selenium needles are probably formed within the active biofilm.

In period IV, some selenium needle clusters were detected (Figures 4.5D and 4.5E). It is likely that selenium needles are produced locally (on a microscale) in this experiment, suggesting that during bacterial development colonies of elemental selenium-producing bacteria exist. On the other hand, perhaps these selenium needles cluster together after formation. The latter indeed seemed to be the case, because clustering was observed when 103 mg selenium powder was added to the 250 mL medium (without lactic acid and selenate) at 50°C. The powder stayed compact and several selenium clusters existed, displaying hydrophobic behaviour.

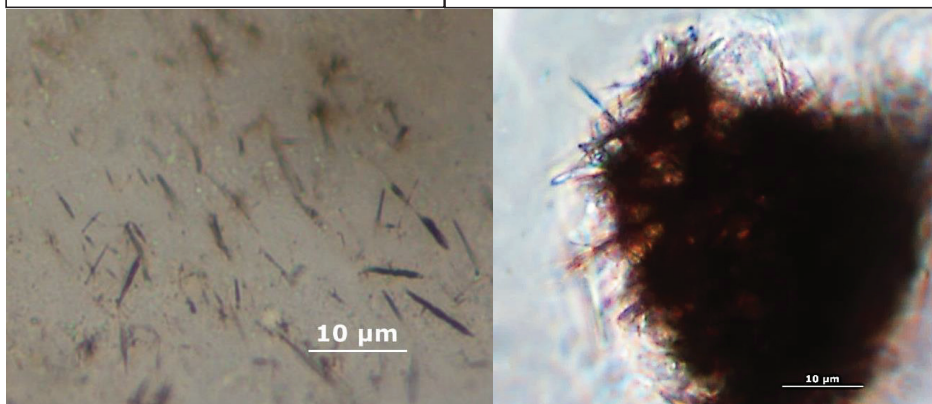
After opening the reactor at the end of the experiment, a biofilm that covered all of the internal surfaces of the reactor was seen. Biomass was also analysed by LM and SEM and again acicular-like structures were detected (Figures 4.6C and 4.6E).





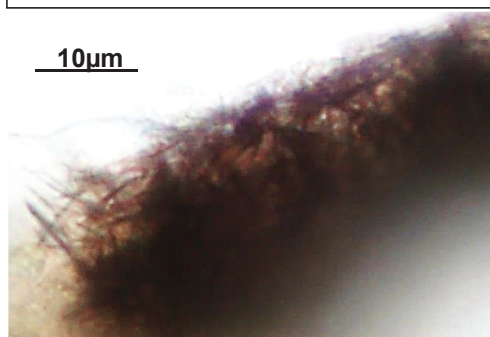
4.5A, Red-brown particle suspension in the reactor, visible at the inner wall at 39 days.

4.5B, biomass with acicular selenium particles at 41 days.



4.5C, Selenium particles in biofilm at 137 days

4.5D, Cluster selenium particles at 195 days.



4.5E, cluster of selenium particles at 164 days.

Figure 4.5 Visible solid selenium nanoparticles obtained during the experiment..

#### 4.3.4. CaPO<sub>4</sub> precipitates

During the experiment CaPO<sub>4</sub> precipitates accumulated on the internal reactor surface (Fig. 4.6A). The CaPO<sub>4</sub> precipitates (Figures 4.6B) were further investigated by SEM and an amorphous structure was visible (Figures 4.6D). During the experiment a precipitate had grown in months in the order of grams and the size was in the order of centimetres. It consisted mainly of the elements Ca, Mg, Na, P and a minor amount of Se could also be detected, 0.1% g/g (Table 4.2). This means that a minority of the selenium had interacted with this CaPO<sub>4</sub> precipitate. So when CaPO<sub>4</sub> precipitates are formed when comparing wastewater treatment processes, it could be contaminated with Se.

**Table 4.2: Elements in the “CaPO<sub>4</sub>” precipitate**

92.2 mg precipitate destroyed	Main elements detected:				Selenium		
(mg)	Ca	Mg	Na	P	Se	O (calculated from PO <sub>4</sub> <sup>3-</sup> )	Total (mg)
(mmol)	23.9	2.4	1.2	15.9	0.1	32.7	73.3
	0.6	0.1	0.1	0.5	0.0	2.0	

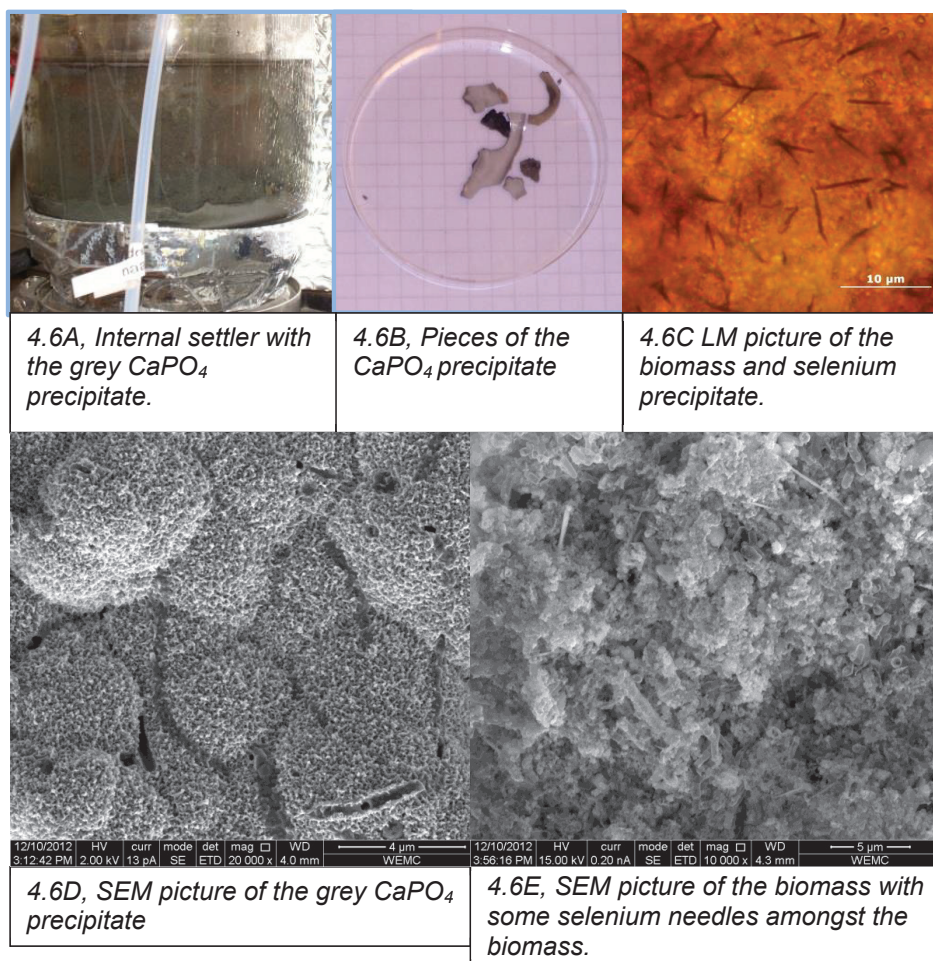


Figure 4.6: Selenium and  $\text{CaPO}_4$  at the end of the experiment. All pictures are from the sampling at  $t_{\text{end}} = 235$  days.

#### 4.4 Conclusion

The production of larger biologic selenium particles during long-term experiments was not observed, though the selenium particles produced were over 10  $\mu\text{m}$  long. The selenium nanoparticles were formed as acicular structures. Further growth of selenium particles was limited due to poor selenate reduction. On the other hand, selenium particle clusters were detected. It is not clear if these acicular selenium particle clusters appeared after formation or that these selenium needles were

produced close to each other. However, these clusters could also result in a better separation process compared to single selenium particles. It was observed that biofilms with selenium particles developed during the reduction process. Two side-effects were observed. Precipitation of calcium phosphate occurred with this medium at 50°C, and biological activity in the settler resulted in partial selenate reduction (conversion of selenate to selenite). The acicular selenium did not reach the settler, but stayed in the reactor. This is important for recovery of selenium. Although the reactor settings for the reduction capacity of selenate were not optimal for Eerbeek sludge. The experiment has proven that it is possible to reduce selenate over 235 days at 50°C.

## **Chapter 5**

### **Microbial selenium sulphide reduction for selenium recovery from wastewater**

This chapter has been prepared for submission as:

Microbial selenium sulphide reduction for selenium recovery from wastewater

S.P.W.Hageman  
R.D. Van der Weijden  
A.J.M. Stams  
P. Van Cappellen  
C.J.N Buisman

## ***Abstract***

Microbial reduction of selenium sulphide ( $\text{SeS}_2$ ) is a key step in a new treatment process that can be used to recover selenium from selenate and selenite streams. In this process, selenate is first reduced to selenite, and subsequently selenite is reduced by sulphide and precipitates from the solution as  $\text{SeS}_2$ . The latter is bio-reduced, resulting in elemental selenium and regenerating sulphide. Anaerobic granular sludges (Eerbeek and Emmtec) were tested for their efficiency in reducing the sulphur compound from a commercially purchased crystalline  $\text{SeS}_2$ . Emmtec sludge had the highest reducing capacity with commercial  $\text{SeS}_2$  and was therefore also used for laboratory synthesised amorphous  $\text{SeS}_2$ . Laboratory  $\text{SeS}_2$  was formed with a sulphide solution and effluent containing selenite. With both  $\text{SeS}_2$  solids, Emmtec sludge produced sulphide and a solid consisting of hexagonal elemental selenium. The crystalline structure suggests the absence of biomolecules, which stabilizes amorphous selenium bio-particles under comparable process conditions ( $T=30^\circ\text{C}$ , and a pH between 6 and 7). Selenium particles were unattached to the biomass, suggesting an extracellular formation. The results support the use of the  $\text{SeS}_2$  bio-reduction process for recovering selenium from water.

## 5.1 Introduction

The bio-reduction of selenium sulphide ( $\text{SeS}_2$ ) offers opportunities for the bio-recovery of selenium from wastewater streams. Selenate and selenite removal from such streams is sometimes essential for environmental safety (Lemly 2004). The recovery of selenium is also of interest because of its value and use in industries. An advantage of biological processes is its selectivity for substrates. Selenate can be bio-reduced to selenite (Chapter 2), which can then be precipitated with sulphide to form  $\text{SeS}_2$  (Geoffroy and Demopoulos 2011). If sulphur can be further bio-reduced from the  $\text{SeS}_2$ , a new biological selenium removal and recovery process was designed (Figure 5.1).

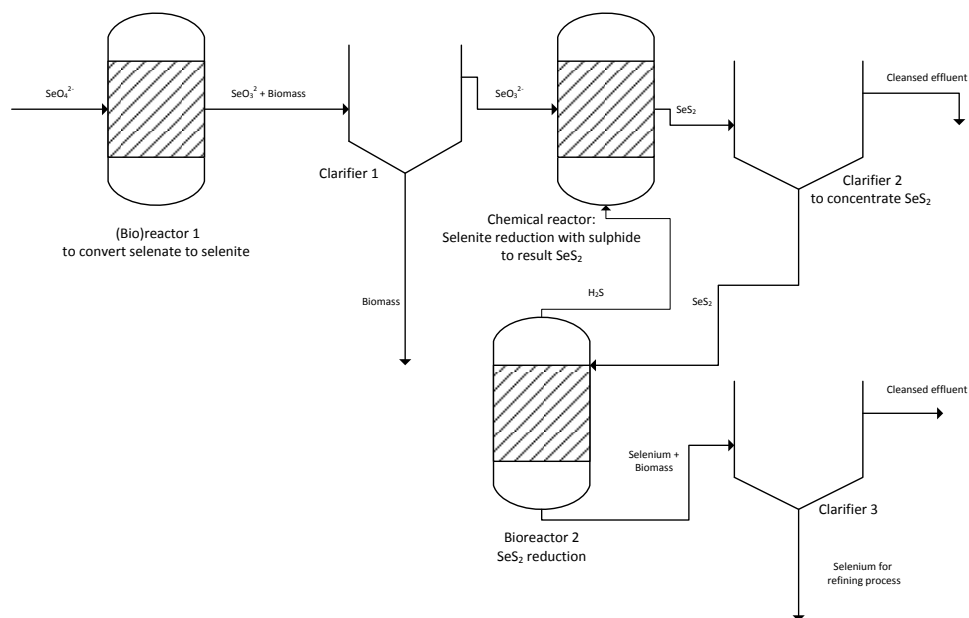


*Figure 5.1 Selenium bio-recovery from selenate via selenite and  $\text{SeS}_2$ . Produced sulphide in bioreactor #2 is re-used to remove selenite in reactor #3. Cleansed effluent from clarifier #3 can be re-used in bioreactor #2. Clarifiers could be integrated in the (bio)reactors.*

Abiotic selenite reduction with sulphide results in the formation of Se-S bonds in  $\text{SeS}_2$ . In  $\text{SeS}_2$  both elemental redox states are 0 (Geoffroy and Demopoulos 2011).

The S:Se ratio in  $\text{SeS}_2$  depends on the precipitation conditions; for example, variation in pH may result in S:Se ratios ranging between 1.7–2.2 (Geoffroy and Demopoulos 2011).

Selenite reduction with (bio)molecules containing thiol-groups such as glutathione (Kessi and Hanselmann 2004, Ganther 1971) and cysteine (Gennari et al. 2014) also resulted in Se-S bonds. However, the Se-S bonds thus produced were further (bio)processed resulting to produce elemental selenium among other products (Kessi and Hanselmann 2004). In a previous study, abiotic leaching tests of  $\text{SeS}_2$  resulted in a stable product (Geoffroy and Demopoulos 2011), thus raising the question as to whether  $\text{SeS}_2$  can also be further bio-processed into elemental selenium.

While in principle both selenium and sulphur can serve as the electron acceptor in reducing  $\text{SeS}_2$ , sulphur is thermodynamically the more favourable electron acceptor (compare the Gibbs energy yields of reactions 1 and 2 in Table 5.1). Thus, in mixed microbial communities reduction of  $\text{SeS}_2$  will result in the production of elemental selenium plus sulphide. As methanogenesis (reaction 6 in Table 5.1) generates comparable Gibbs free energy per electron as  $\text{SeS}_2$  reduction, methane production should be avoided by choosing adequate process conditions, e.g. by removing  $\text{CO}_2$ .



**Table 5.1: Standard Gibbs free energy change of selenium reactions and methane formation at 30°C and pH=7**

Number	Reaction	$\Delta G^\circ$ per reaction (KJ/ mol)	$\Delta G^\circ$ Per electron (KJ/ electron mol)
(1)	$2\text{H}_2(\text{aq}) + \text{SeS}_2^{\text{a}} \rightarrow \text{Se} + 2\text{HS}^- + 2\text{H}^+$	-95.4	-23.8
(2)	$\text{H}_2(\text{aq}) + \text{SeS}_2^{\text{a}} \rightarrow \text{HSe}^- + 2\text{S} + \text{H}^+$	-17.2	-8.6
(3)	$2\text{HSe}^- + \text{SeS}_2^{\text{a}} \rightarrow 3\text{Se} + 2\text{HS}^-$	-66.8	-16.7
(4)	$\text{HS}^- + \text{SeS}_2^{\text{a}} \rightarrow 3\text{S} + \text{HSe}^-$	29.0	14.5
(5) <sup>a</sup>	$\text{SeS}_2^{\text{a}} \rightarrow \text{Se} + 2\text{S}$	-2.9	n/a
(6)	$\text{CO}_2(\text{aq}) + 4\text{H}_2(\text{aq}) \rightarrow \text{CH}_4(\text{aq}) + 2\text{H}_2\text{O}(\text{l})$	-193.1	-24.1
(7)	$\text{HSeO}_3^-(\text{aq}) + 2\text{HS}^-(\text{aq}) \rightarrow \text{SeS}_2^{\text{a}} + 3\text{HO}^-$	-202.3	-50.6
(8)	$\text{HSe}^- + \text{S} \rightarrow \text{HS}^- + \text{Se}$	-32.0	-16.0

Data calculated from Amend and Shock (Amend and Shock 2001) at 30°C and pH=7.  $\Delta G^\circ$  line 5 is estimated using binding energies. Bonds in  $\text{SeS}_2$ : 1/9 Se-Se; 4/9 Se-S; 4/9 S-S).

n/a = not applicable

We postulate that the selenium can be purified and recovered from  $\text{SeS}_2$  by bio-reducing the sulphur in  $\text{SeS}_2$  to sulphide. Besides commercially pure  $\text{SeS}_2$ , synthesised  $\text{SeS}_2$  produced with selenite effluent from a selenate to selenite converting bioreactor (Chapter 2) was also tested for bio-reduction. The latter  $\text{SeS}_2$  may contain impurities that affect the biological reduction.

## 5.2 Material and methods

### 5.2.1 Biomass

Eerbeek sludge originates from a bioreactor that treats paper waste streams. Eerbeek sludge contains 16.1 (+/- 3.1) mg sulphur in the total suspended solid (d'Abzac et al. 2009). Emmtec sludge originates from a reactor in which sulphate is reduced to sulphide with ethanol as the electron source. Emmtec sludge contains 19.9 (+/- 12.3) mg sulphur in the total suspended solid (d'Abzac et al. 2009). Characteristics of both sludges are described by d'Abzac et al. (D'Abzac et al. 2010). Dry weight (dw) was determined in triplicate by drying 5 g washed biomass at 105°C

for 3 days.

### 5.2.2 Medium

Crimp-seal flasks of 118 mL were filled with 5 mL 100 mM sodium lactate and 50 mL medium. Medium was based on Stams et al. (Stams et al. 1992), and consisted of (g L<sup>-1</sup>): Na<sub>2</sub>HPO<sub>4</sub>·2H<sub>2</sub>O (0.53), KH<sub>2</sub>PO<sub>4</sub> (0.41), NH<sub>4</sub>Cl (0.3), CaCl<sub>2</sub>·2H<sub>2</sub>O (0.11), MgCl<sub>2</sub>·6H<sub>2</sub>O (0.10), and trace elements and vitamin solution (Stams et al. 1992). Sodium selenite, sodium hydrogen carbonate and sodium sulphide were not added, (Chapter 2.). Medium pH was set to 7 with NaOH.

### 5.2.3 Reduction of commercial SeS<sub>2</sub>

The electron acceptor was commercial crystalline SeS<sub>2</sub> from Sigma Aldrich. Experiments were performed in batch bottles (#1-1 to #1-8) and overview is given in Table 5.2. The following three controls were added; #1-3, without any biomass; #1-4, Eerbeek sludge without SeS<sub>2</sub>, and #1-7, Emmtec sludge without SeS<sub>2</sub>. Wet sludge density was assumed to be 1 g/L and the SeS<sub>2</sub> volume was insignificant. The headspace was replaced by N<sub>2</sub> (1500 mbar). The bottles were incubated onto a horizontal shaker (100 rpm) at 30°C for 36 days.

During the experiment samples were taken with a needle and syringe. Liquid samples were centrifuged at 10,000 RPM for 10 minutes (Microlite Thermo ICE) and the supernatant was analysed for total sulphide concentration in the liquid (S<sup>2-</sup><sub>T(aq)</sub>) (=H<sub>2</sub>S(aq)+HS<sup>-</sup>(aq)+S<sup>2-</sup>(aq)). Pellets of Emmtec bottles with SeS<sub>2</sub> were analysed on ratio S/Se. For SEM and EDX analyses a part of a pellet was redispersed in MilliQ water and air dried.

At day 36 the headspace was analysed for pressure, CO<sub>2</sub> and methane at room temperature (by GC). A liquid sample was used to measure the final S<sup>2-</sup><sub>T(aq)</sub> and a sample of around 4 ml was directly stored in the freezer at -20°C.

After opening the bottle, the pH was measured immediately and the liquid was stored in a closed 50 mL tube for 14 hours at 4°C. Next, granular biomass particles used as inoculum were separated with a sieve (1 mm). The liquid was centrifuged (2395 RPF

3660 RPM 20°C 10 minutes) and the pellet was disposed in 20 mL milliQ. Pictures of the precipitate were taken with a Nikon SMZ 800 macroscope and a Nikon Eclipse E400 microscope. Next, the 20 mL liquid was again centrifuged as described above and the pellet was air dried at room temperature. After three days drying, some samples still contained liquid and the drying process was accelerated by heating (estimated to be 60°C) for some hours. The colour of the pellet did not change during drying. One fraction of the dried pellet was used to determine the sulphur and selenium content.

Another fraction of the dried pellet was re-suspended in MilliQ and dried on an object glass (VWR ECN 631-1550 76×26×1 mm) at room temperature for X-ray powder diffraction (XRD) analyses. The 60°C during pellet drying might have resulted in crystalline selenium, so 4 mL liquid samples (only Emmttec samples) immediately stored at -20 °C on day 36 were also analysed using XRD. Defrosted samples were washed with MilliQ, then the pellets were dissolved in <100µL MilliQ and finally dried at room temperature on an object glass.

**Table 5.2: Overview of the SeS<sub>2</sub> reduction experiments**

Bottle no.	Label	Lactate	Fresh medium	Eerbeek	Emmtec	Commercial Se-S	synthesised Se-S	Se-S	Total V
#		(mL)	(mL)	(g ww)	(g ww)	(mg)	(mL old medium)	(mM Se)	(mL)
<b>sequence #1: commercial crystalline SeS<sub>2</sub></b>									
#1-1	Eerbeek Commercial SeS <sub>2</sub>	5	50	0.5		72.0		9.1	55.5
#1-2	Eerbeek Commercial SeS <sub>2</sub> duplicate (1-1)	5	50	0.5		73.6		9.3	55.5
#1-3	Control Commercial SeS <sub>2</sub>	5	50			71.5		9.1	55.0
#1-4	Control Eerbeek	5	50	0.5				0.0	55.5
#1-5	Emmtec Commercial SeS <sub>2</sub>	5	50		0.5	70.6		8.9	55.5
#1-6	Emmtec Commercial SeS <sub>2</sub> duplicate (1-5)	5	50		0.5	73.0		9.2	55.5
#1-7	Control Emmtec	5	50		0.5			0.0	55.5
#1-8	Emmtec & Eerbeek Commercial SeS <sub>2</sub>	5	50	0.25	0.25	706.8		89.1	55.5
<b>Sequence #2: synthesised amorphous SeS<sub>2</sub></b>									
#2-1	Emmtec prepared SeS <sub>2</sub>	5			0.5		50	9.5 <sup>1</sup>	55.5
#2-2	Emmtec prepared SeS <sub>2</sub> duplicate (2-1)	5			0.5		50	9.5 <sup>1</sup>	55.5
#2-3	Control Prepared SeS <sub>2</sub>	5					50	9.6 <sup>1</sup>	55.0
#2-4	Emmtec Control	5	50		0.5			0.0 <sup>1</sup>	55.5

1) Selenium content in synthesised Se-S solution was measured by ICP and corrected for the dilution 50 mL/total Volume mL).

## 5.2.4 Synthesised SeS<sub>2</sub>

Effluent from a bioreactor converting selenate to selenite at pH=6 and T=30°C was stored at -20°C. The reactor performance is described in (Chapter 2). After defrosting this effluent, solid particles were removed by centrifugation at 45000 RPM for 20 min with Firlabo SW12 centrifuge. The supernatant was filtered (Schleicher & Schuell Ref.no. 300012) and analysed for total selenium and selenite in duplicate, 11.6 ±0.2 mM Se and 11.3 ±0.1 mM selenite. This solution (226 mL) was mixed in seconds with 1.22 g Na<sub>2</sub>S·9H<sub>2</sub>O dissolved in 10 mL milliQ water. The sulphide beaker was rinsed

with 5 mL milliQ water and this water was added to the reaction mixture. The solution changed from colourless to red/brown and subsequently to an orange suspension. The pH rose to 12 and was adjusted by adding 3 mL 25% HCl, but an overshoot was created (pH=3.53) and this was compensated for with 0.6 mL 0.1 M NaOH to arrive finally at a pH of 5.9 at  $t=23$  minutes. The solution was aerobically stored for 19 hours in a fume hood to remove unreacted sulphide. Orange precipitates were detected and some orange spheres floated at the meniscus of the reaction liquid (pH=6.1). The reaction solution contained  $10.49 \pm 0.42$  mM Se and the supernatant (45000 RPM 20 min Firlabo SW12) contained  $1.14 \pm 0.00$  mM Se. Selenite and sulphide were not detected in the supernatant. The pellet was washed twice and the ratio of S/Se was  $2.09 \pm 0.01$ . The solid liquid separation (by centrifugation) was difficult: the pellet was partly fragile, and a part was stuck to the bottom of the centrifuge tube and was therefore difficult to suspend in the water. Consequently, 50 mL synthesised SeS<sub>2</sub> suspension was directly used in the reduction experiments. Emmtec sludge was used since it had sufficient SeS<sub>2</sub> reducing capacity with commercial SeS<sub>2</sub>. Synthesised SeS<sub>2</sub> reduction experiments were performed as described in the procedure for commercial SeS<sub>2</sub> reduction. An overview of these is listed in Table 5.2 (bottle #2-1 to #2-4).

### 5.2.5 Analysis

Dr Lange LCK-653 was used to measure S<sup>2-</sup><sub>T</sub>(aq) in (mg/L). Results were obtained with a Hach Lange Xion 500 spectrophotometer.

Prior to ICP-OES measurements, pellets or liquids were transferred to 10 mL aqua regia. This mixture was heat destructed (ETHOS 1; Advanced Microwave Digestion system, milestone. In 4 minutes to 90°C; in 5 minutes to 130°C; in 4 minutes to 160°C and 15 minutes at 160°C). Subsequently, the volume was set to 100 mL with milliQ and resulted in 10% aqua regia. Samples were analysed using VARIAN VISTA-MPX CCD – Simultaneous ICP.

XRD was performed with a PHILIPS SR 4160, 40 kV 30mA and data was analysed with HighScore (Plus) software. Method for peak search: 2nd derivate; Minimum

significance 1.00; Minimum tip width ( $^{\circ}2\theta$ ) 0.01; Max. tip width ( $^{\circ}2\theta$ ) 1.00 and peak base width ( $^{\circ}2\theta$ ) 2.00. Peaks were analysed in Search and Match with the following settings: No restrictions, data source: peak data, multi-phase, demote unmatched strong and allow pattern shift.

Samples were attached to scanning electron microscope (SEM) sample holders with spectral grade carbon adhesive tabs (EMS Washington USA) and coated with about 10 nm of carbon (Emitech K950X, Quorum Technologies, East Grinstead, UK). Imaging was done with SE detection in a field emission scanning electron microscope (Magellan 400, FEI, Eindhoven, the Netherlands) at 2 KV, 13.2 pA and WD of about 4 mm. Energy dispersive X-ray (EDX) analyses were accomplished using an Aztec X-ray analyser (Oxford Instruments Analytical, High Wycombe, England) at an acceleration voltage of 15 KV.

The IC system consisted of Autosampler AS-50, a Dionex ICS-2100 with an IonPac AS19 column (4mm 250 mm) at 30°C, an ASRS 4mm suppressor (75 mA) and an electrochemical conductivity detector at 35°C. Flow rate was 1.0 mL min and sample loop was 10 $\mu$ L, but used was partial loop mode, injecting 5  $\mu$ L.

The GC system consisted of a Shimadzu 2010 GC equipped with a Porabond Q (50m x 0.53mm; 10 $\mu$ m; Varian; Part.no. CP7355) Molsieve 5A (25m x 0.53mm; 50 $\mu$ m; Varian; Part.no. CP7538) with a thermal conductivity detector. Helium was carrier gas (pressure – 1bar) and loop injections of 1.5 mL were used. GC oven temp 75°C, Inlet temp 120°C; Detector temp 150°C.

### 5.2.6 Calculations

Methane, CO<sub>2</sub> and H<sub>2</sub>S in the gas phase were calculated according to the gas law. The amount of sulphide and CO<sub>2</sub> were also calculated with the equilibrium between the gas and water phase and between the first dissociation steps for H<sub>2</sub>CO<sub>3</sub> and H<sub>2</sub>S in the liquid.

The following constants are used:

$$T_{\text{measurement}} = 293 \text{ (K)} ;$$

$$K_a \text{H}_2\text{S} = 6.86 \cdot 10^{-8} ;$$

$$\text{Henry coefficient for } \text{H}_2\text{S} = 0.0987 \text{ mol} \cdot \text{L}^{-1} \text{ Pa};$$

$$\text{Henry coefficient for } \text{CO}_2 = 0.03888 \text{ mol} \cdot \text{L}^{-1} \text{ Pa};$$

$$K_a \text{H}_2\text{CO}_3 = 5.3 \cdot 10^{-7}$$

$$\Sigma \text{H}_2\text{S} = \text{sulphide gas phase} + \text{sulphide liquid phase (mmol)}.$$

$$\text{S}\% \text{ or } \text{Se}\% = \text{fraction of element determined by ICP-OES (mg/mg pellet)}$$

$$\text{Ratio S/Se} = \frac{\text{S}\%/32}{\text{Se}\%/79} (-) \quad (8)$$

## 5.3 Results

### 5.3.1 Reduction of commercial SeS<sub>2</sub>

Commercial SeS<sub>2</sub> was insoluble at the start. Some orange coloured SeS<sub>2</sub> floats at the meniscus and some remains on the bottom. Commercial SeS<sub>2</sub> is smooth in structure (Fig 5.4A) and crystalline according to XRD (Fig 5.5). The XRD pattern resembles the one observed by Geoffroy and Demopoulos (Geoffroy and Demopoulos 2011).

During the experiment, commercial SeS<sub>2</sub> starts to decolourise and almost all the material from the meniscus moved to the bottom. Already on day 15 orange and grey/black spots appeared on the SeS<sub>2</sub> particles treated with Emmtec sludge and the particles in the control without biomass were only slightly less bright compared to the start (Fig 5.2). At 36 days, most of the orange or produced grey SeS<sub>2</sub> was at the bottom of the bottles and the liquid was relatively clear. At the end of the control experiment without added biomass the SeS<sub>2</sub> was darkened but still yellow to orange (Fig 5.3a). The decolouring effect from orange to black with Emmtec sludge is stronger than with Eerbeek sludge (Fig 5.3bc). The size of the particles is estimated from SEM and LM pictures to be in the range of 1-100 µm (Fig 5.2, 5.3 and 5.4).

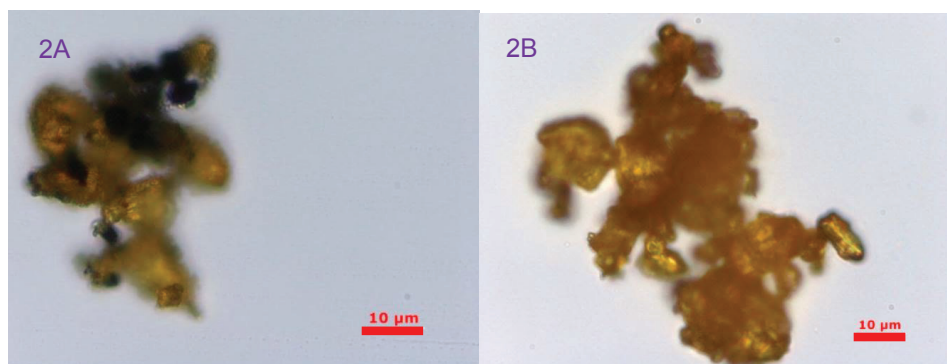


*Figure 5.2: Microscope pictures of the commercial  $\text{SeS}_2$  reduction experiment at 15 days. 2A Treatment with Emmtec sludge (#1-6) 2B Without biomass.; The brightness of the pictures is increased 25%.*

Without added biomass it seems that the  $\text{SeS}_2$  surface is roughened during 36 days of incubation and the ratio S:Se at 36 days is comparable to the ratio S:Se of the starting material (Fig 5.4B). The treatment with Emmtec also resulted in a roughened structure. Moreover some angular structures were also visible and the ratio S:Se had decreased (Fig 5.4c). The particles in Figure 5.4C were in the range of 5  $\mu\text{m}$ , however particles of over 10  $\mu\text{m}$  can also be seen (no EDX result), see Appendix 5A

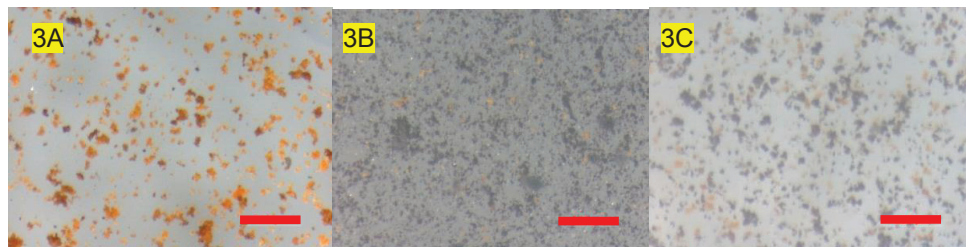
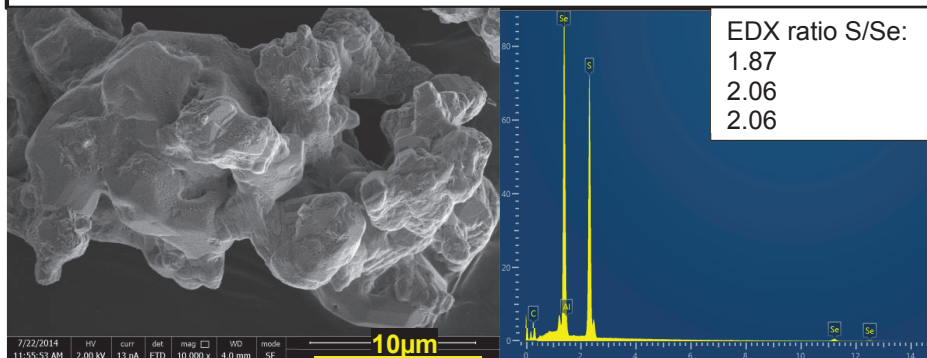


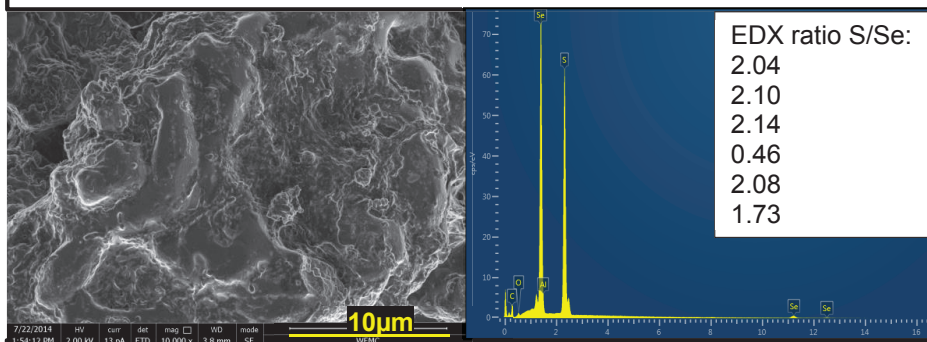
*Figure 5.3 Macroscopic pictures of the commercial  $\text{SeS}_2$  precipitates at 36 days. 3A Without biomass, 3B Emmtec (#1-6), 3C Eerbeek (#1-1). The brightness of the pictures is increased 25%. The scale bar is 250  $\mu\text{m}$ .*



5.4A, Commercial  $\text{SeS}_2$  at the start of the experiment.



5.4B,  $\text{SeS}_2$  treated without added biomass at 36 days.



5.4C, Commercial  $\text{SeS}_2$  treated with Emmtec sludge for 36 days.

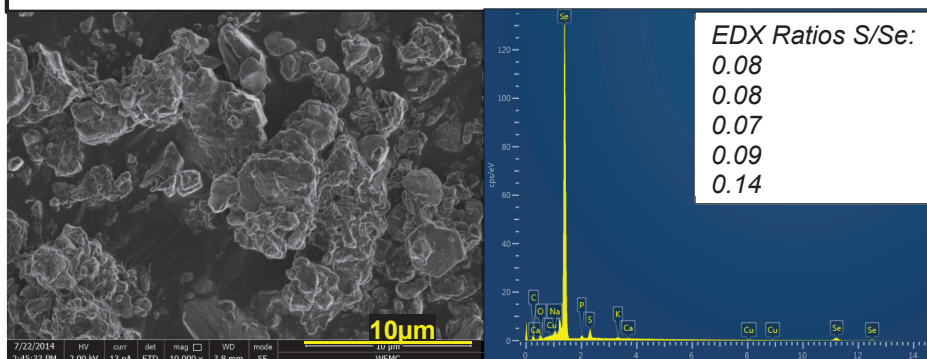
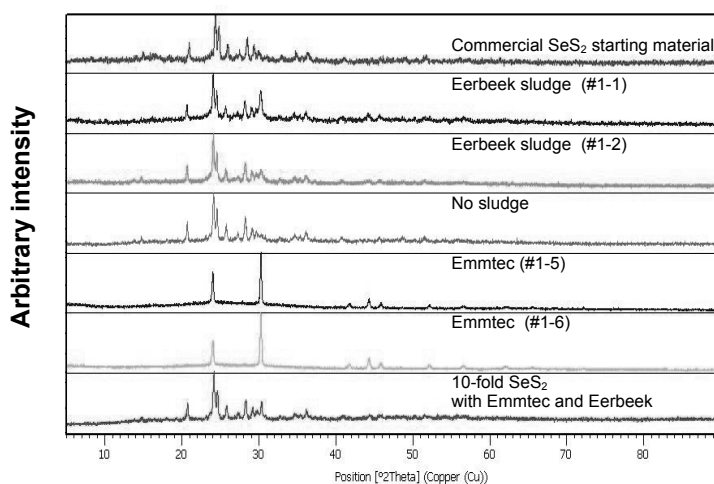


Figure 5.4 SEM and EDX of commercial  $\text{SeS}_2$  reduction: All EDX results and their exact location in the SEM pictures are given in the Appendix 5A.

At 36 days, both precipitates from  $\text{SeS}_2$  reduction with Emmtec as solely biocatalysts resulted in a XRD pattern of hexagonal selenium, all other precipitates have the

same XRD pattern as the commercial starting  $\text{SeS}_2$  material (Fig 5.5). The hexagonal structure might be formed by drying at  $60^\circ\text{C}$ , therefore unheated samples of both Emmtec experiments were also investigated using XRD (as a control). One of the control pellets was crystalline and the XRD software confirmed 77% hexagonal selenium. The XRD pattern of the other control pellet #1-5 was visually comparable with the reference selenium XRD pattern, but the software did not confirm the presence of hexagonal selenium.



*Figure 5.5, XRD results of commercial available  $\text{SeS}_2$  bio-reduction. Except for the starting material, all XRD results were obtained from samples at 36 days.*

The ratio S/Se of the solids in the experiments with Emmtec sludge was followed (Fig 5.6). It is clear from the figure that the sulphur content in the particles decreased during the 36 days of incubation, and this is in accordance with the EDX results (Fig 5.4).

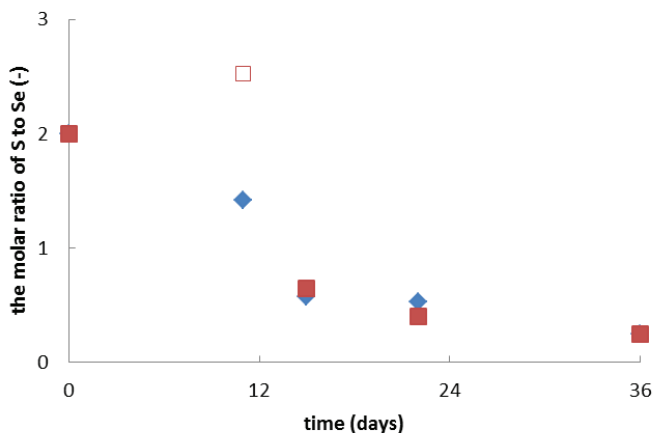


Figure 5.6 The molar ratio S to Se in commercial  $\text{SeS}_2$  during reduction with Emmtec. Both series, ( $\blacklozenge$  #1-5) and ( $\blacksquare$  #1-6), are from bottles that contain Emmtec and commercial  $\text{SeS}_2$ . At  $t=0$  the theoretical value S to Se of 2 was assumed. At  $t=11$  days one measurement exceeded the theoretical ratio S/Se.

### 5.3.2 Sulphide production during commercial $\text{SeS}_2$ reduction

The average  $\text{S}^{2-}_{\text{T}}(\text{aq})$  of the two bottles with Emmtec sludge reached  $250 \pm 19 \text{ mg S}^{2-}/\text{L}$  on  $t=36$  days. The sulphide production resembles linearity over 36 days, though at day 28 a lower value was measured (see Fig 5.7a). For Emmtec, based on duplicate measurements at 36 days, an estimated linear  $\text{S}^{2-}_{\text{T}}(\text{aq})$  production rate of  $7 \text{ mg S}^{2-}/\text{L} / \text{day}$  was determined. When Eerbeek sludge was used the average final  $\text{S}^{2-}_{\text{T}}(\text{aq})$  of the two bottles was  $35 \pm 5 \text{ mg S}^{2-}/\text{L}$  only. Bottles with  $>0.3 \text{ mmol } \Sigma\text{H}_2\text{S}$  ( $\approx 9.6 \text{ mg}$ ) production at  $t=36$  days revealed black/grey precipitates and bottles with  $<0.3 \text{ mmol } \Sigma\text{H}_2\text{S}$  ( $\approx 9.6 \text{ mg}$ ) production revealed a mixture of black and orange (spotted) particles (Table 5.3).

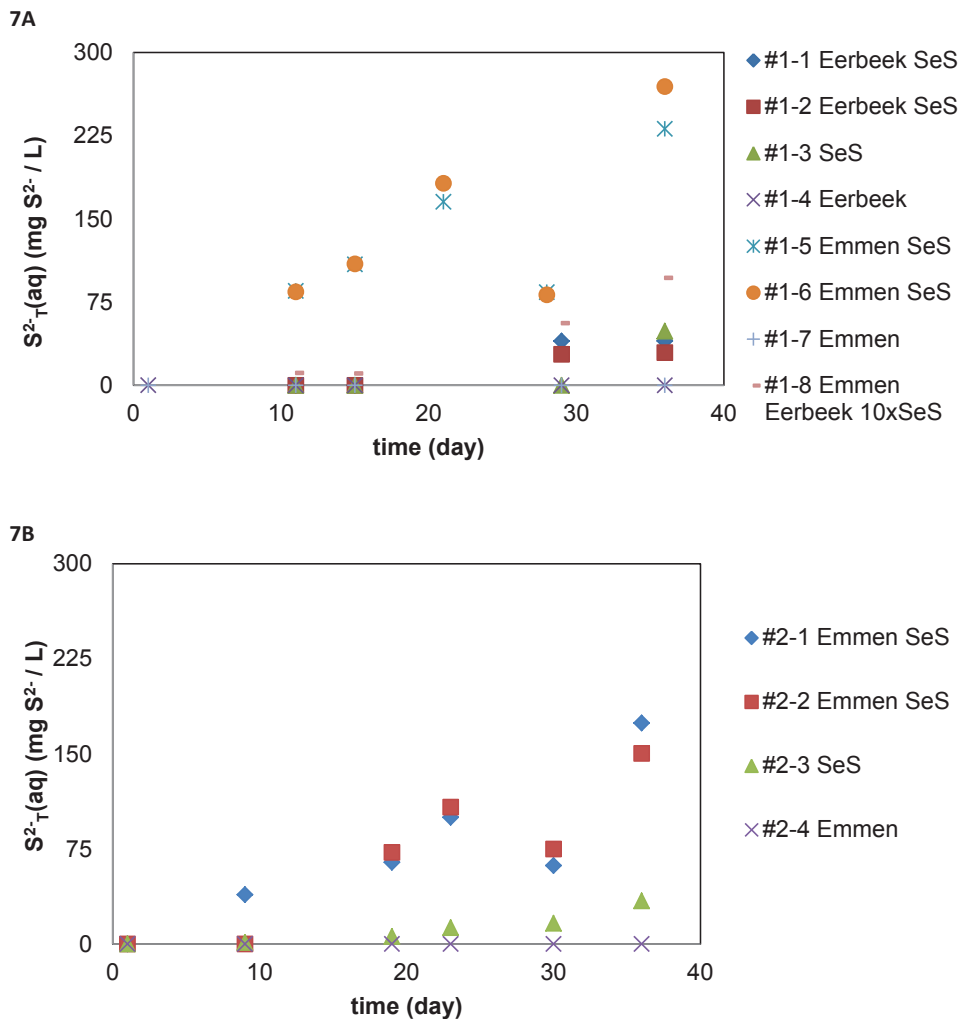


Figure 5.7:  $S^{2-}_T(aq)$  accumulation during the experiments. 7A reduction of commercial  $SeS_2$ . 7B reduction of synthesised  $SeS_2$ .

Sulphide production in controls without added  $SeS_2$  but with Eerbeek and Emmtec sludge was insignificant. Only with Eerbeek sludge was a  $S^{2-}_T(aq)$  amount of 0.119

$S^{2-}$  mg/L detected after 24 hours, but during further incubation no sulphide could be detected. The Emmtec dry weight was 0.08 g per g wet weight and Eerbeek dry weight was 0.12 g per g wet weight. This means that the amount of sulphur added with the inoculum was <0.1 mg S for both sludges and this could contribute to a  $S^{2-}_T$  (aq) of maximum 2 mg  $S^{2-}$  /L in 50 mL of liquid.

However, the control – without addition of any sludge – resulted in a  $S^{2-}_T$ (aq) amount of 49 mg  $S^{2-}$  / L at t=36 day. This was probably due to biological contamination that can reduce  $SeS_2$ , since the medium and the bottles were not sterilised. This contamination is probably present in all bottles with  $SeS_2$  and could have contributed to some  $H_2S$  production.

### **5.3.3 Bioreduction of synthesised $SeS_2$**

Synthesised  $SeS_2$  had a similar orange colour to commercial  $SeS_2$  and a smaller particle size than commercial  $SeS_2$ . Dried synthesised  $SeS_2$  had an amorphous structure according to XRD (Fig 5.9). During the experiment the discolouration was stronger in the bottle with added biomass. At 36 days, the batch bottle solution was not as clear as with commercial  $SeS_2$  reduction.

The particle size of the synthesised  $SeS_2$  was estimated by SEM to be smaller than 1  $\mu m$  (Fig 5.8A). The synthesised  $SeS_2$  particles were not stable and modifications in particle shape were detected in 24 hours (Fig 5.8B). At 36 days, acicular structures were detected both in the bottle with and without Emmtec sludge (Fig 5.8C and 5.8D).

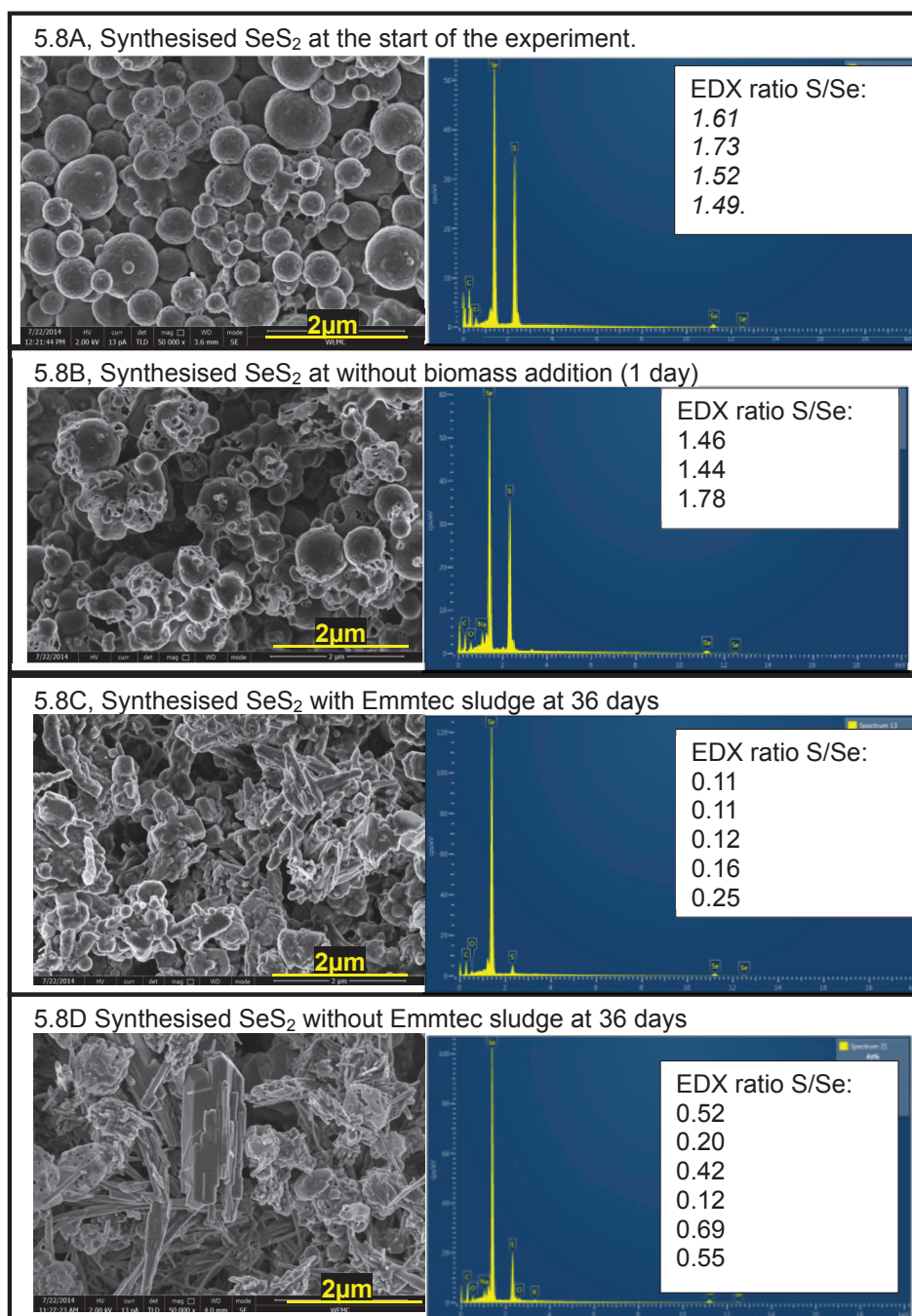
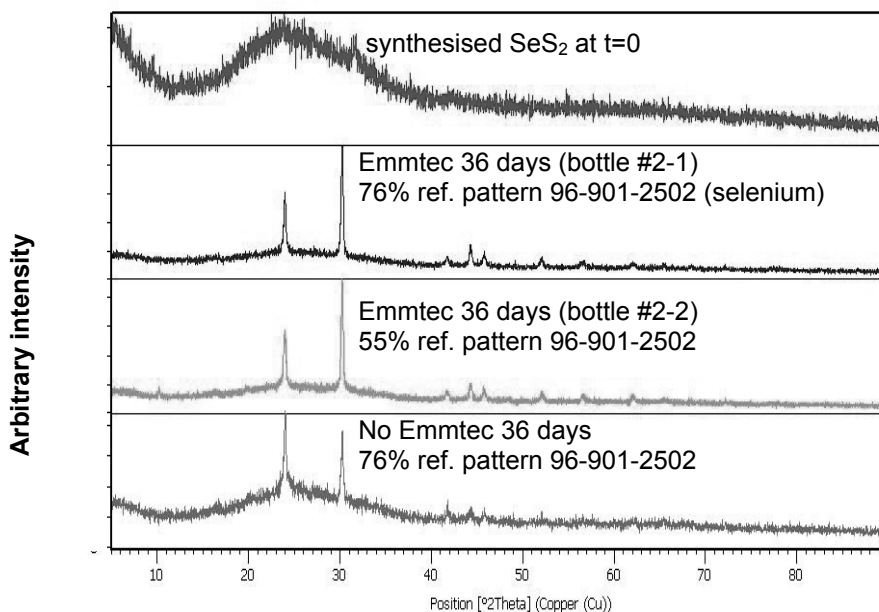


Figure 5.8: SEM and EDX results of synthesised  $\text{SeS}_2$  bio-reduction experiments. EDX spots combined with the SEM pictures are given in Appendix 5B.

XRD analysis of bio-reduced synthesised  $\text{SeS}_2$  indicated a hexagonal selenium structure (Fig 5.9). To investigate that the crystallinity was not due to heating, unheated samples were also analysed using XRD. The control pellet without Emmtec was crystalline and the XRD program confirmed the presence of hexagonal selenium (77%). The pellet with Emmtec also resulted in a visible diffraction pattern for crystalline selenium, but the pattern was not recognized by the software as elemental selenium.



*Figure 5.9: The XRD patterns of the synthesised  $\text{SeS}_2$  reduction experiments*

With synthesised  $\text{SeS}_2$  and Emmtec sludge an average  $\text{S}^{2-}_{\text{T(aq)}}$  of 162 mg  $\text{S}^{2-}$  / L was produced over 36 days (Fig 5.7B). Roughly this is 4.5 mg  $\text{S}^{2-}$  / L / day. The measurements showed that the sulphide concentration increased over this 36-day period with the exception of at day 30 (Fig 5.7B). In the control – with no added synthesised  $\text{SeS}_2$  – no sulphide is detected. The control – with synthesised  $\text{SeS}_2$  and without added biomass – revealed sulphide production from  $t=23$  days and the

production continued till t=36 days (Fig 5.7B). Probably this bottle was contaminated with micro-organisms that can reduce SeS<sub>2</sub> to sulphide.

**Table 5.3** Overall results

Bottle no.	Bottle label	SeS <sub>2</sub> added at t=0	$\Sigma H_2S$	Colour	% Se in pellet	CH <sub>4, gas</sub>	$\Sigma CO_2$ (mmol)	pH	Ratio S/Se
(-)	(-)	(mmol Se)	(mmol)	(-)	(% W/W)	(mmol)	(mmol)	(-)	(-)
#1-1	Eerbeek SeS <sub>2</sub> A	0.50	0.09	Red black	59	0.71	0.88	6.85	1.42
#1-2	Eerbeek SeS <sub>2</sub> B	0.51	0.06	Red black	56	0.71	0.69	6.78	1.67
#1-3	Blank SeS <sub>2</sub>	0.50	0.10	orange	51	0.00	0.24	6.76	1.89
#1-4	Blank Eerbeek	0.00	0.00	-	-	0.74	0.73	7.05	-
#1-5	Emmtec SeS <sub>2</sub> A	0.49	0.52	black	75	0.03	0.48	6.49	0.24
#1-6	Emmtec SeS <sub>2</sub> B	0.51	0.61	black	85	0.02	0.50	6.44	0.35
#1-7	Blank Emmtec	0.00	0.00	-	-	0.29	0.38	7.10	-
#1-8	Emmtec & Eerbeek 10 times SeS <sub>2</sub>	4.94	0.20	orange	40	0.56	0.82	6.88	1.95
#2-1	Emmtec + SeS <sub>2</sub>	0.53	0.40	black/brown	77	0.00	0.55	6.27	0.31
#2-2	Emmtec + SeS <sub>2</sub> (Duplicate)	0.53	0.35	black/brown	80	0.00	0.58	6.29	0.16
#2-3	SeS <sub>2</sub>	0.53	0.08	red/brown/black	64	0.00	0.27	6.23	1.42
#2-4	Emmtec	0.00	0.00	-	-	0.56	0.57	6.76	-



## 5.4 Discussion

### 5.4.1 Mechanism to bio-reduce $\text{SeS}_2$ to hexagonal selenium particles

The results show that commercial and synthesised  $\text{SeS}_2$  are bio-reduced to sulphide and the remaining selenium transforms to hexagonal selenium at  $T=30^\circ\text{C}$  and a pH between 6 and 7. Prior to hexagonal selenium formation the sulphur and the selenium are segregated from each other. The micro-organisms are able to drive the process with electron donor oxidation. For a summary of the process see Fig 5.10.

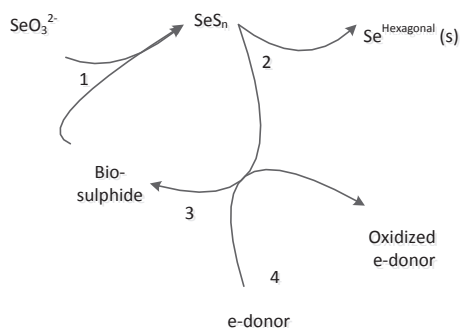


*Fig 5.10. Selenium production process via  $\text{SeS}_2$ . Selenite is reduced by (bio-) sulphide to  $\text{SeS}_n$  (1). From  $\text{SeS}_n$  sulphur is bio-reduced to sulphide, the remainder selenium transforms to hexagonal selenium (2). To be able to reduce the sulphur (3), the micro-organism uses an electron donor (4)*

### 5.4.2 Explanation formation of hexagonal selenium

The formation of crystalline selenium as a result of the high selenium purity has been confirmed by others: Xu and Barton discovered that the bio-removal of sulphur at  $\text{pH}=7.4$  and  $T=35^\circ\text{C}$  in biological selenium and sulphur micro-particles resulted in poly-crystalline selenium particles (Xu and Barton, 2013). Geoffroy and Demopolous showed that with an abiotic stability test at  $\text{pH}=12.2$  and  $T=23^\circ\text{C}$   $\text{SeS}_2$  segregated in elemental sulphur and hexagonal elemental selenium (Geoffroy and Demopoulos

2011). Bector and Kullerud demonstrated a crystalline selenium structure at roughly more than 83% molar Se and a temperature of  $>25^{\circ}\text{C}$  in a condensed Se-S system (Bector and Kullerud 1987). However, instead of the formation of crystalline selenium as a result of high selenium purity, several researchers (Wang et al. 2010, Tejo Prakash et al. 2009) observed that bio-selenium particles from selenate and selenite bio-reduction stay amorphous. It has been suggested that the amorphous structure is stabilized by biomolecules (Wang et al. 2010). In our study high purity selenium and the absence of biomolecules allowed the formation of hexagonal selenium. Moreover, it allowed selenium particles to grow to larger crystals, which is beneficial for the recovery of selenium.

#### **5.4.3 Possible $\text{H}_2\text{Se}$ production**

$\text{SeS}_2$  is available for micro-organisms near the surface of the  $\text{SeS}_2$  particles and in the water phase. The latter is confirmed by leaching tests with  $\text{SeS}_2$  carried out by Geoffrey and Demopoulos (Geoffroy and Demopoulos 2011). They indicate that  $\text{SeS}_2$  slowly dissolves at  $\text{pH}=3$  and  $\text{pH}=5$  but remains stable at  $\text{pH}=7$  ( $<0.005$  mg Se/L)(Geoffroy and Demopoulos 2011). When the bioavailable sulphur is reduced by micro-organisms, the leaching equilibrium of  $\text{SeS}_2$  probably restores and as a result  $\text{SeS}_2$  instability increases. So the leaching process continues. Additionally, though the production of bio-selenide from elemental selenium has been reported (Herbel et al. 2003, Nelson et al. 1996), the production of sulphide is more likely in  $\text{SeS}_2$  bio-reduction. The reason for this is that bacteria gain more energy from sulphide production (Table 5.1: lines 1 and 2). Also it has been noticed that in some cases of microbial reduction, hexagonal selenium was less bio-reactive compared to amorphous selenium (Herbel et al. 2003). In our experiment selenide production could not be excluded because selenide is a substitute for the remaining sulphur atoms in the  $\text{SeS}_2$  particles. As a result solid selenium forms (Nelson et al. 1996) (Table 5.1:lines 3 and 4).

#### **5.4.4 Selenium and sulphur exchange reactions (flux)**

The separation of selenium and sulphur clusters in  $\text{SeS}_2$  is energetically a spontaneous process at  $30^{\circ}\text{C}$  (Table 5.1), but without biological interference this

separation process is slow (Geoffroy and Demopoulos, 2011). During biological treatment of  $\text{SeS}_2$ , biomolecules with thiol and selenol groups can be produced. These groups can substitute for sulphur or selenium with other selenium or sulphur compounds. Several exchange reactions have been described in detail (Kessi and Hanselmann 2004, Steinmann et al. 2010, Wessjohann et al. 2007). This implies that these sulphur and selenium substitute reactions probably result in an exchange flux between S and Se in  $\text{SeS}_2$ . This increases the probability of sulphur and selenium separation and the probability of crystallization to hexagonal selenium. Possibly the black selenium parts appearing in our  $\text{SeS}_2$  particles (Fig 5.2) are the result of separation and crystal formation. With commercial  $\text{SeS}_2$  it seems unlikely that the particles would have passed the cell membrane because of their size. This confirms extracellular selenium particle formation.

#### **5.4.5 Biological $\text{H}_2\text{S}$ production rate**

The biological sulphide production rate of Emmtec sludge was estimated to be 7 mg  $\text{S}^{2-}$  / L / day for commercial  $\text{SeS}_2$  and 4.5 mg  $\text{S}^{2-}$  / L / day for synthesised  $\text{SeS}_2$ . The difference in rate can be explained by three factors. 1. The dissimilarity between commercial and synthesised  $\text{SeS}_2$  such as the size, the (non)crystallinity, the morphology, the hydrophobicity and the ratio S to Se. These  $\text{SeS}_2$  properties affect the bioavailability and thus the bioconversion rate. 2. The difference in medium: the synthesised  $\text{SeS}_2$  medium was already altered during selenite production from selenate (Chapter 2) and by the  $\text{SeS}_2$  synthesis reaction, whereas the commercial  $\text{SeS}_2$  medium was fresh. Components that might affect biological activity could therefore be present in different concentrations. 3. The pH in both experiments differed and this could have affected the biological activity and the bioavailability of  $\text{SeS}_2$ .

#### **5.4.6 $\text{SeS}_2$ reduction and methane production**

Emmtec sludge tended to reduce  $\text{SeS}_2$  rather than produce methane (Table 5.3: compare lines 1#5, 1#6 with 1#7 and compare 2#1, 2#2 with 2#4), The calculated Gibbs free energy per electron for  $\text{SeS}_2$  reduction to sulphide is comparable with methane formation (Table 5.1). This tendency with Emmtec sludge is important,

because methane formation costs electron donor. With Eerbeek sludge the presence or absence of  $\text{SeS}_2$  (Table 5.3) appears not to change the amount of methane produced. Additionally, the microbial community composition of the inoculum had an impact on the metabolism in these short-term experiments.

#### **5.4.7 The importance of $\text{SeS}_2$ synthesis**

In the precipitation step selenite can quickly be removed from the wastewater stream to form a selenium concentration of 0.005 mg Se / L (Geoffroy and Demopoulos, 2011). Adequate process conditions for reducing selenite by sulphide have to be determined to minimize selenium losses and to produce a bio-convertible  $\text{SeS}_2$  product.  $\text{SeS}_2$  bio-convertibility can be affected by among other factors, rate of precipitation, stoichiometry and particle size.  $\text{SeS}_2$  is unstable at high pH and colloidal selenium and sulphur particles might have been formed (Geoffroy and Demopoulos 2011) during our synthesis (temporarily pH=12). Selenium was detected in our supernatant (<11% of starting Se). This indicated the presence of selenium bearing particles that are difficult to remove. Because of the high pH level and the sulphide, other components in our medium (Chapter 2) could also have co-precipitated and thus have affected the  $\text{SeS}_2$  precipitate properties and bioavailability. For example, EDX scans of precipitation mixtures by Hocking and Gadd (Hockin and Gadd 2003) confirmed the presence of S, Se, Ca, and Fe. In general, the waste stream properties and precipitation settings are important steps in designing a biological  $\text{SeS}_2$  reduction process.

### **5.5 Conclusion**

Selenium from wastewater streams containing selenate or selenite can be recovered through  $\text{SeS}_2$  bio-reduction. Commercial  $\text{SeS}_2$  is crystalline (as shown by XRD) and has poor solubility in water, whereas in our experiment synthesised  $\text{SeS}_2$  was amorphous and remained suspended. Commercial  $\text{SeS}_2$  and synthesised  $\text{SeS}_2$  were bio-reduced by Emmtec sludge to sulphide and selenium. Sulphide can be re-used for  $\text{SeS}_2$  synthesis. Selenium transforms to a hexagonal structure at  $T=30^\circ\text{C}$  and a pH around 6 to 7. The atomic S/Se ratio in commercial  $\text{SeS}_2$  decreased from 2 to 0.24 in 36 days. The reduction of synthesised  $\text{SeS}_2$  proves the possibility of bio-

reducing  $\text{SeS}_2$  originating from an aqueous stream. The main advantage is a crystalline, extracellular elemental selenium product. This is important to implement  $\text{SeS}_2$  bio-reduction in the treatment of wastewater streams containing selenite. The pure and expected high yield of selenium makes this bio-reduction process suitable for bio-recovery of selenium.

Appendix 5A: Commercial SeS<sub>2</sub> bio-reduction

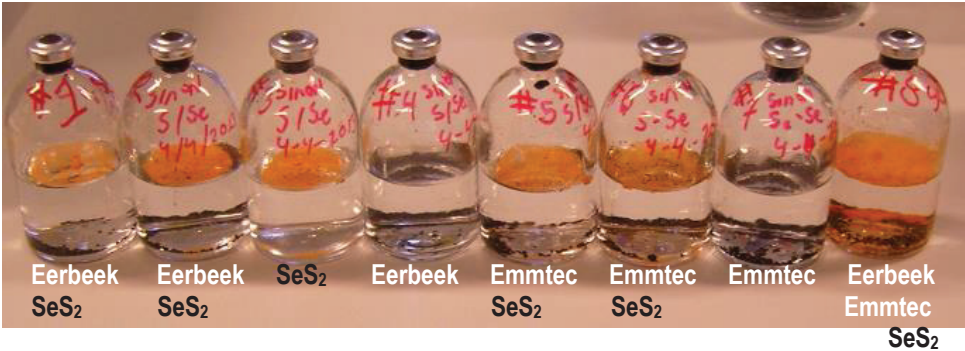


Photo of the start of the experiment.

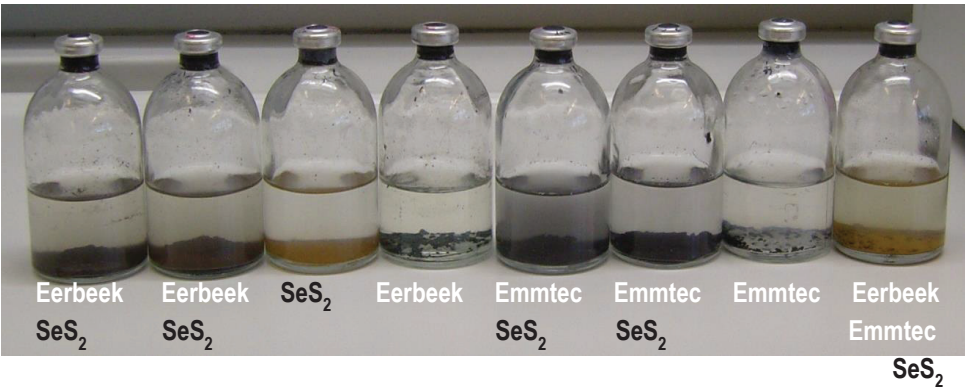
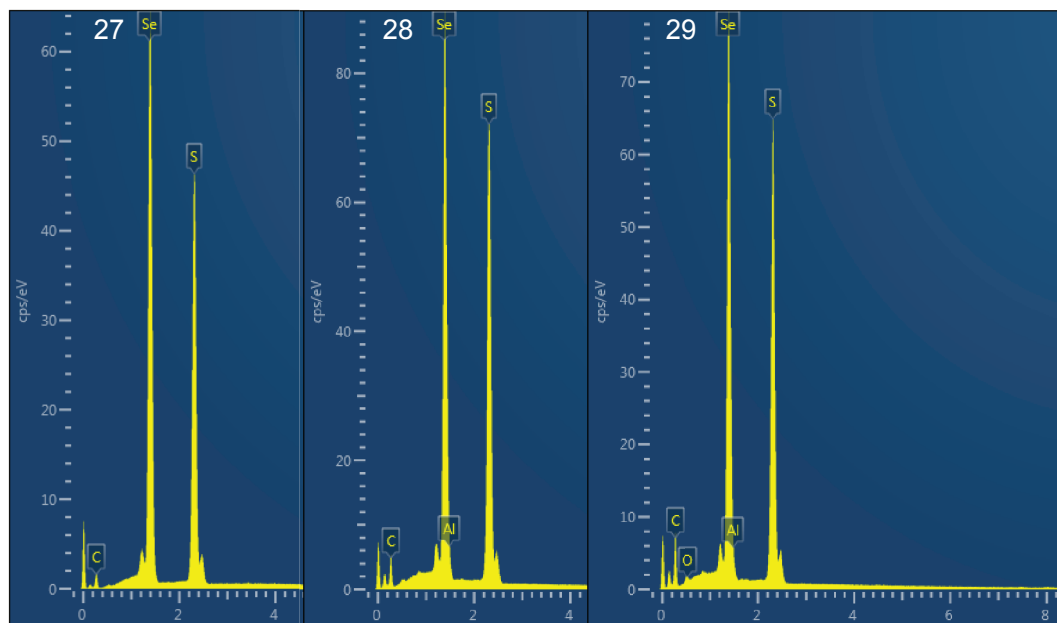
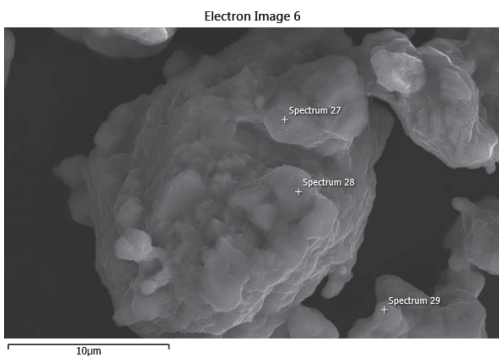
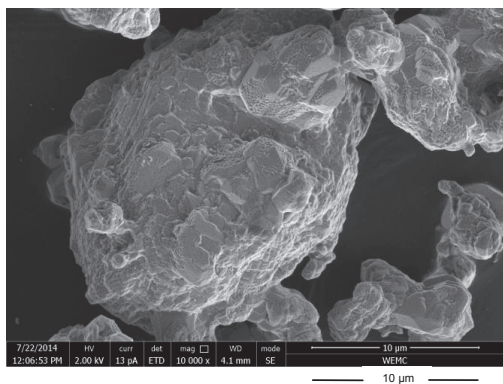
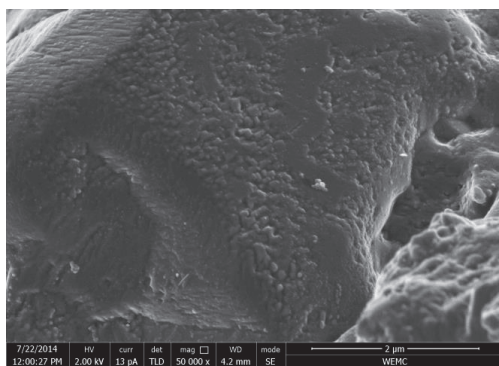
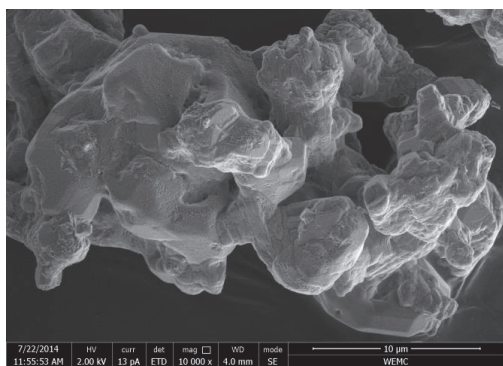
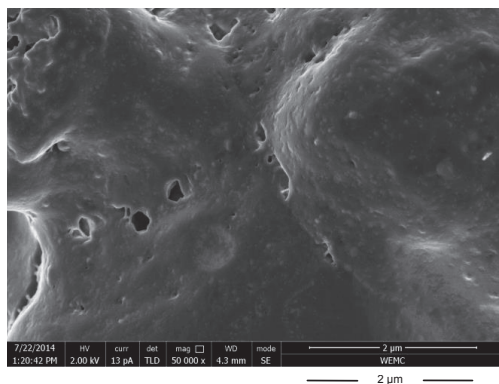
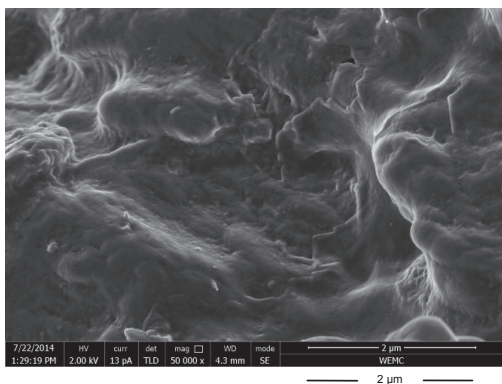
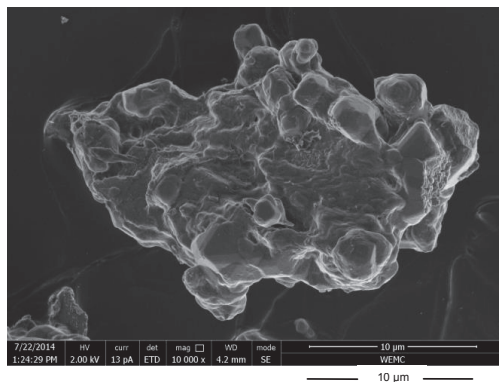
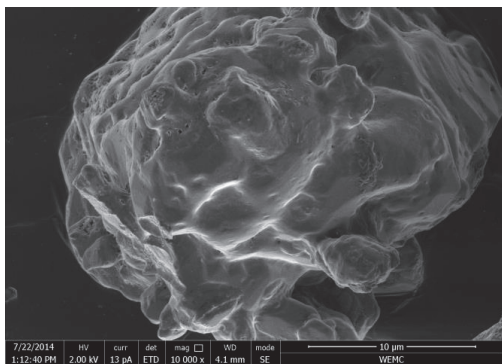


Photo of the end of the experiment at 36 days.

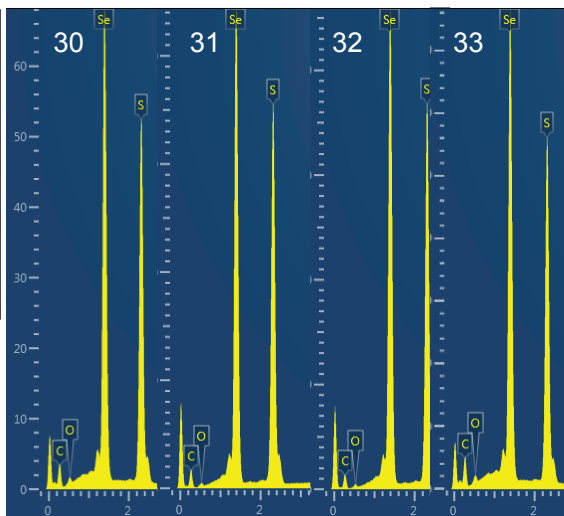
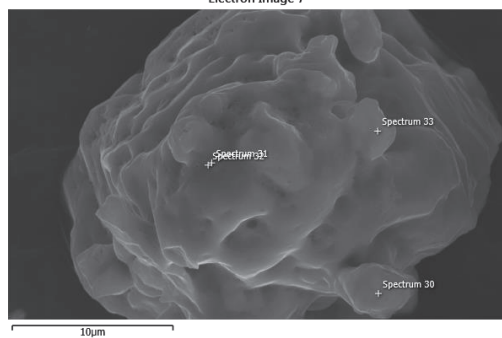


**SEM and EDX of commercial  $\text{SeS}_2$  mixed in MilliQ and dried in air at room temperature.**



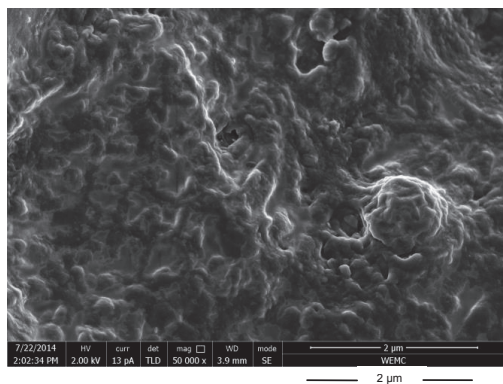
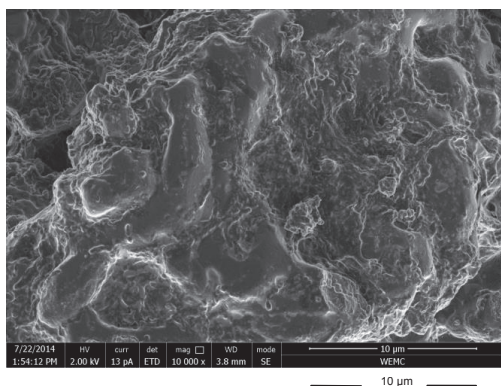
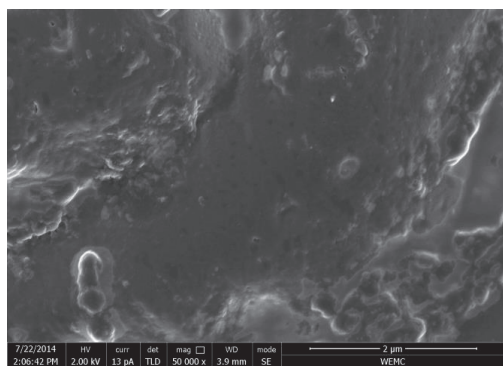


Electron Image 7

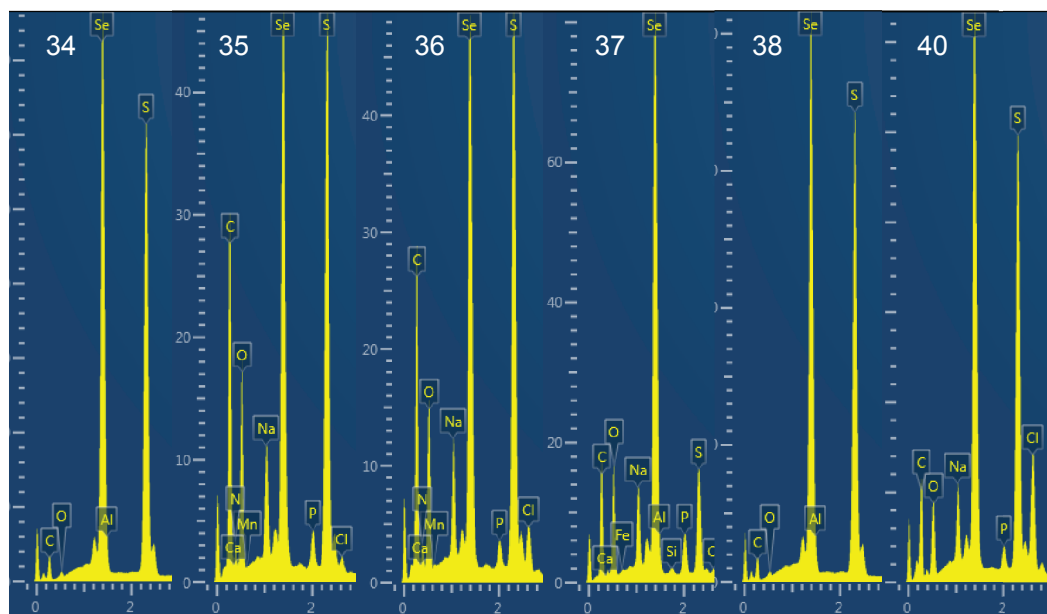
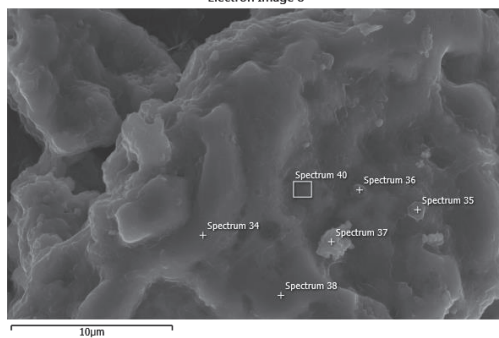


SEM and EDX of commercial  $\text{SeS}_2$  at  $t = 1$  day. (bottle 1-8)

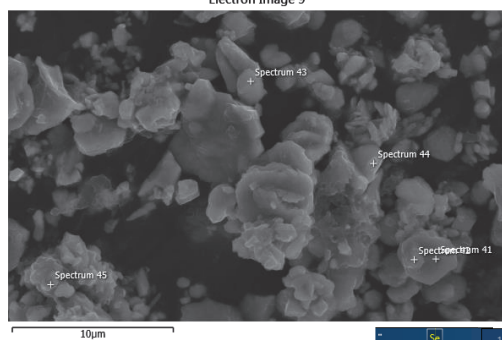
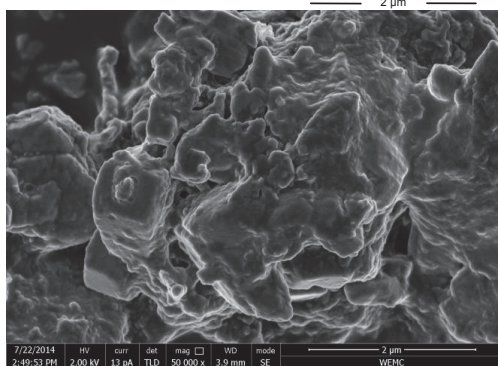
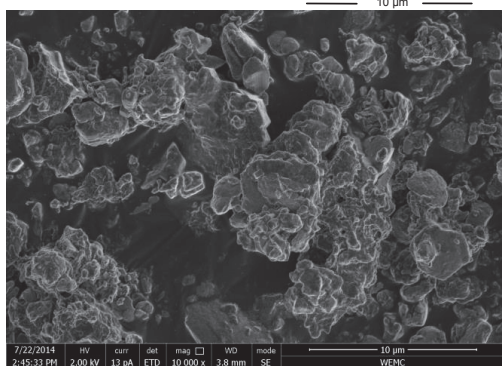
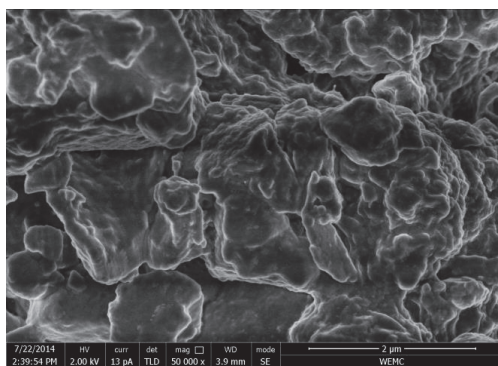
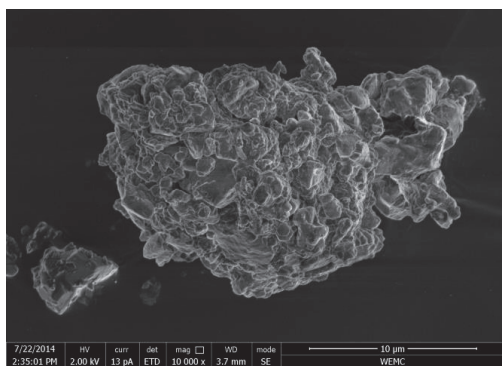




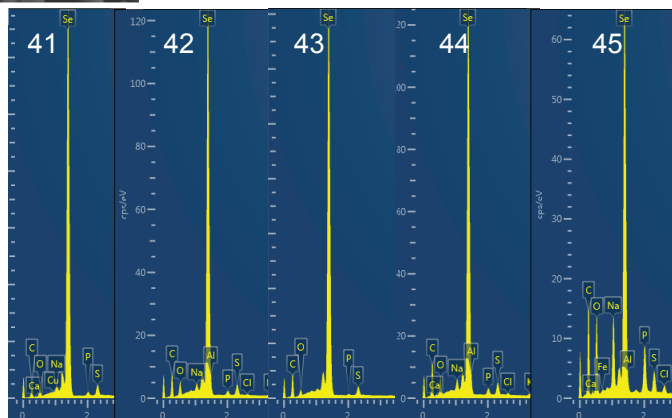
Electron Image 8



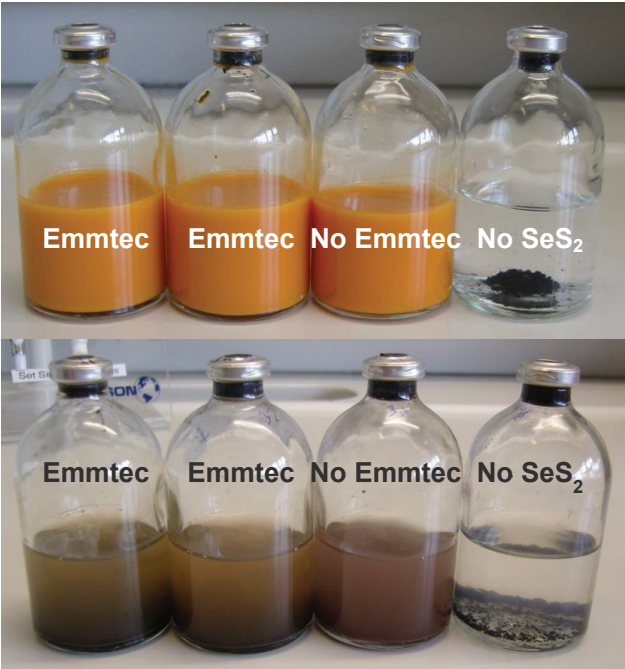
SEM and EDX of commercial  $\text{SeS}_2$  without sludge at 36 days



SEM and EDX of commercial  $\text{SeS}_2$  and Emmtec at 36 days (#1-6)

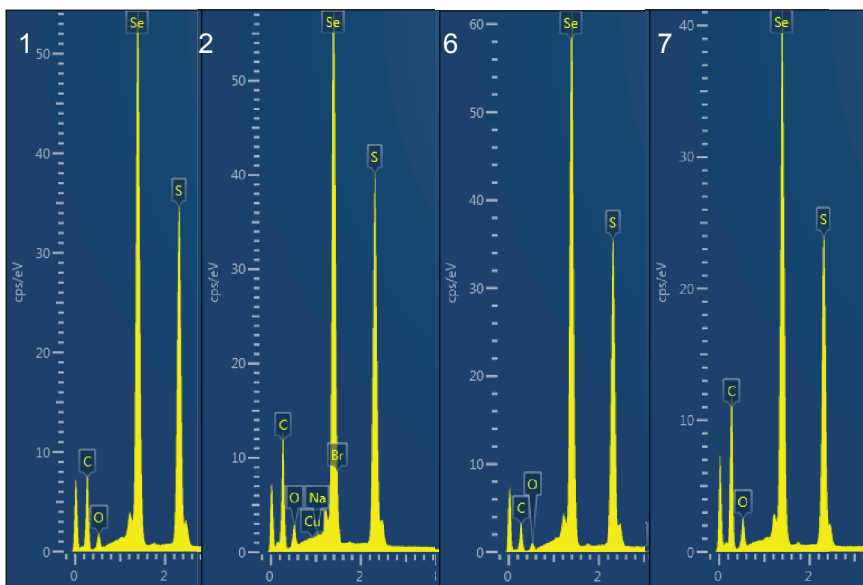
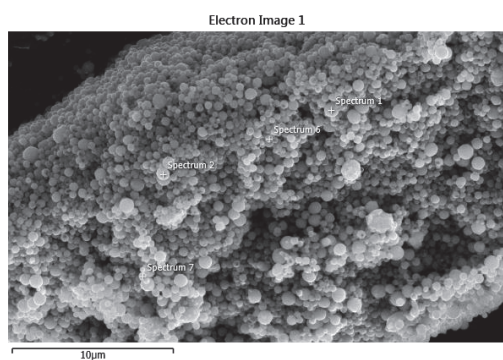
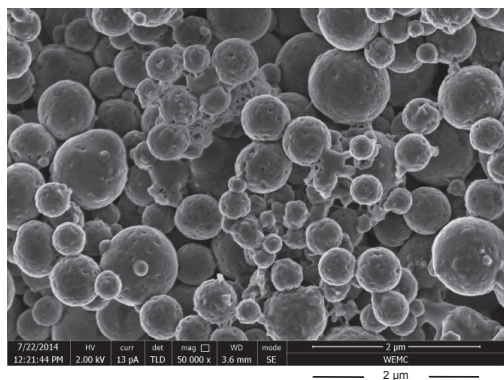
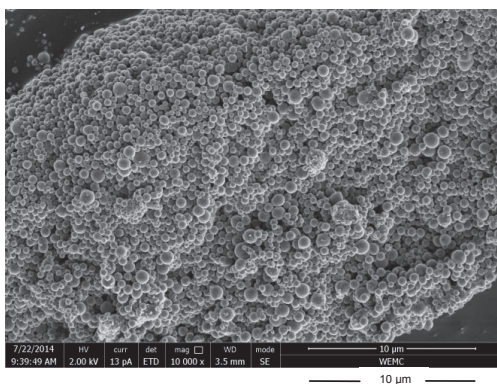
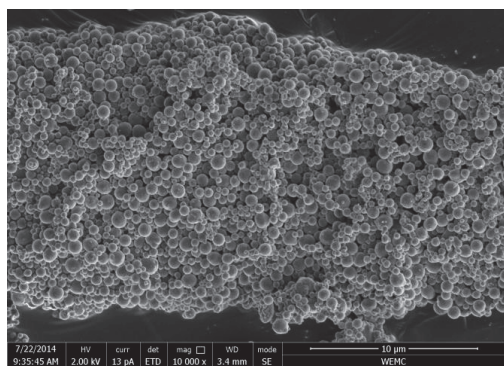


**Appendix 5B: Synthesised  $\text{SeS}_2$  bio-reduction**

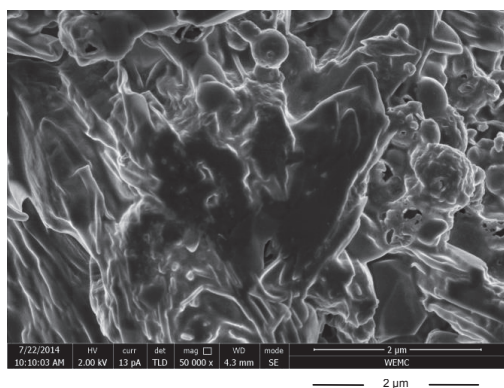
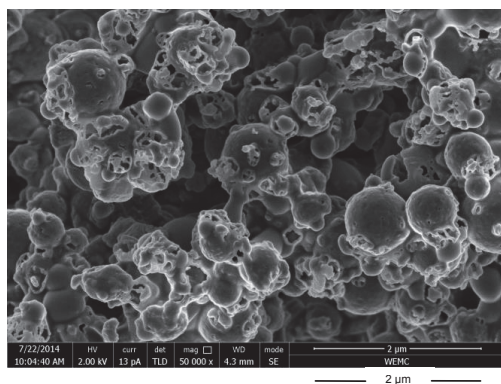
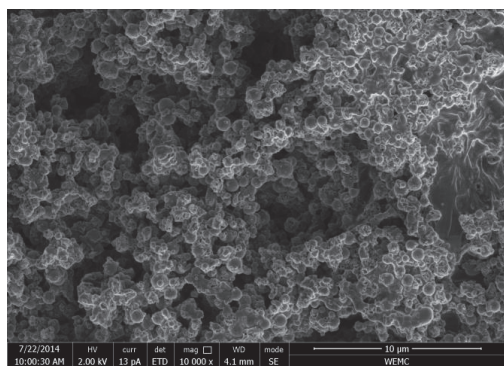


Start and end of the experiment with synthesised  $\text{SeS}_2$ . The upper photo shows the start and the lower photo shows the end of the experiment.

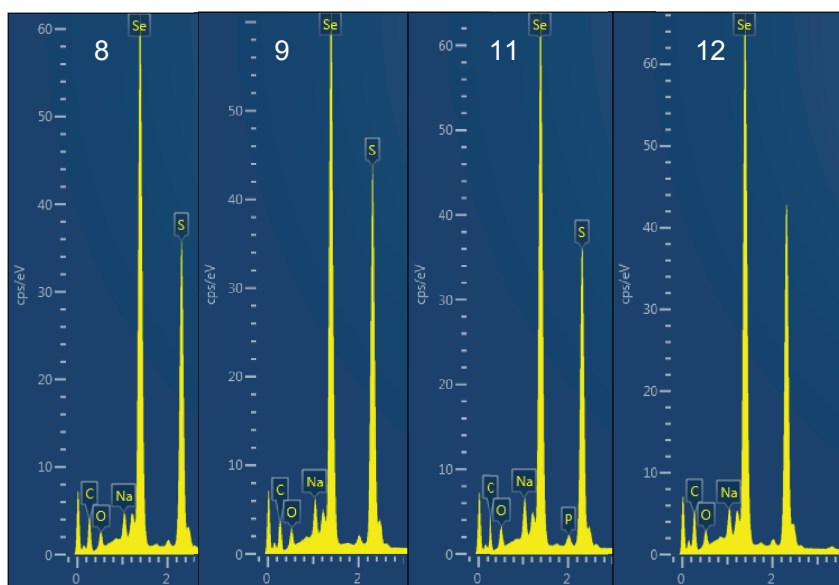
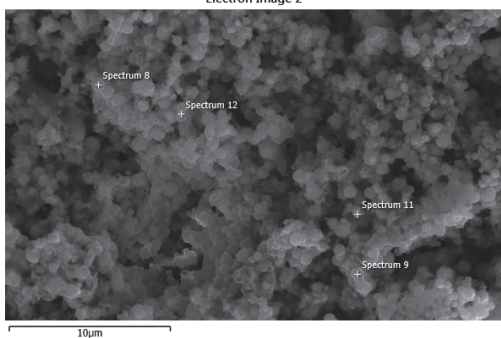




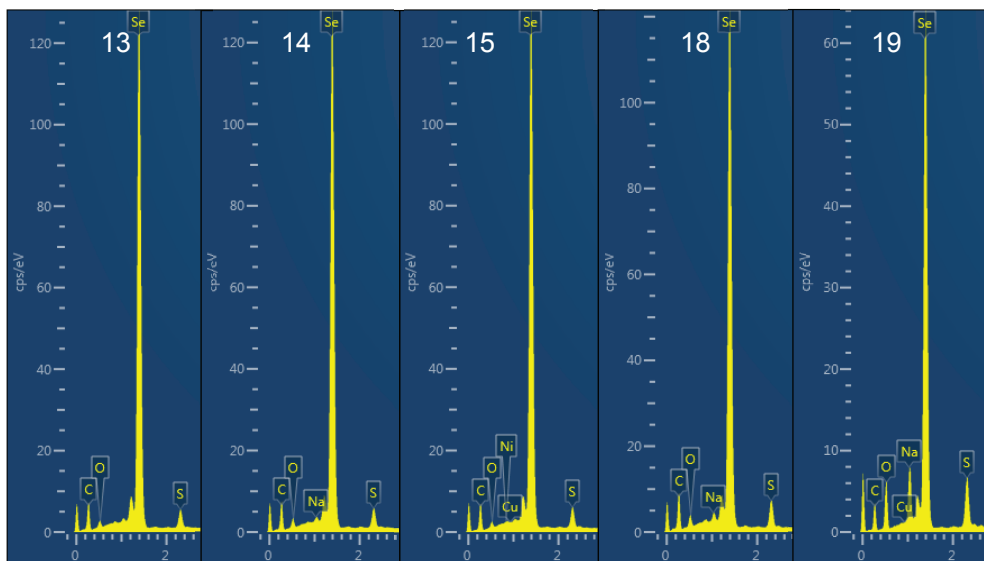
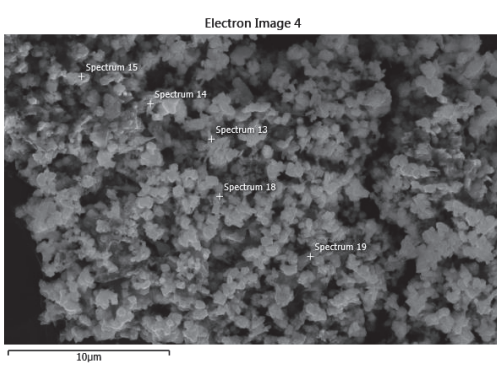
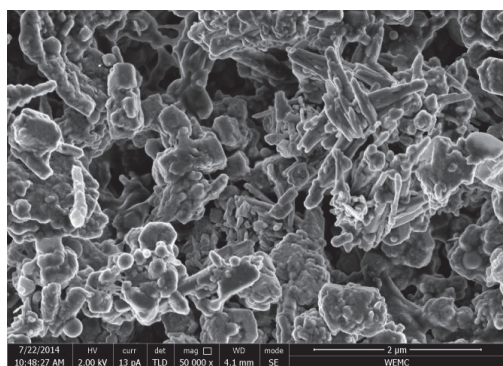
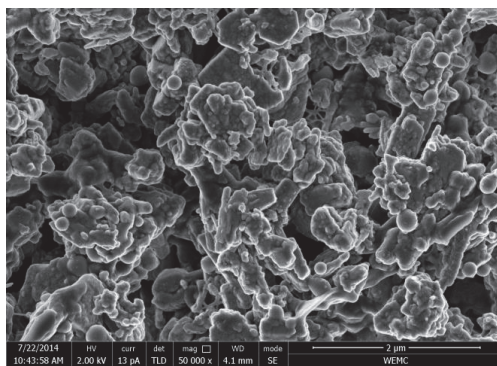
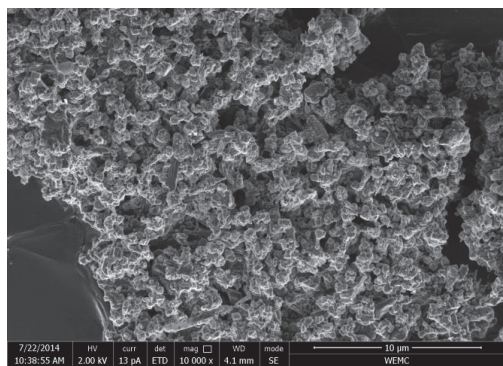
**SEM and EDX of synthesised  $\text{SeS}_2$  at the start of the experiment**



Electron Image 2

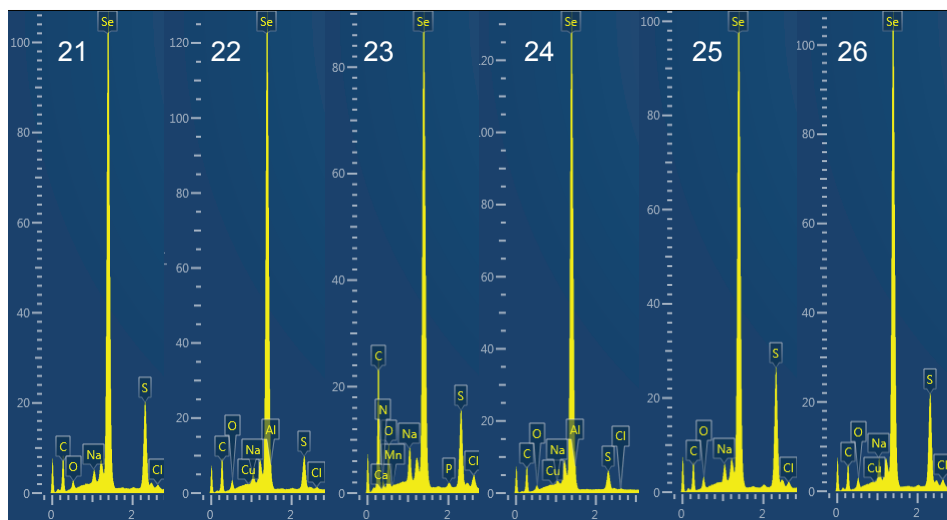
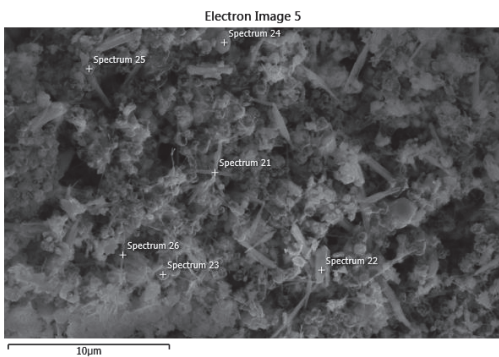
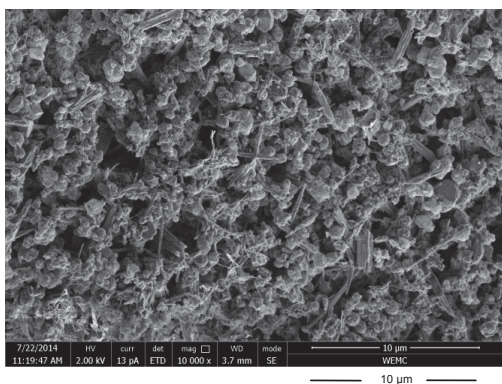
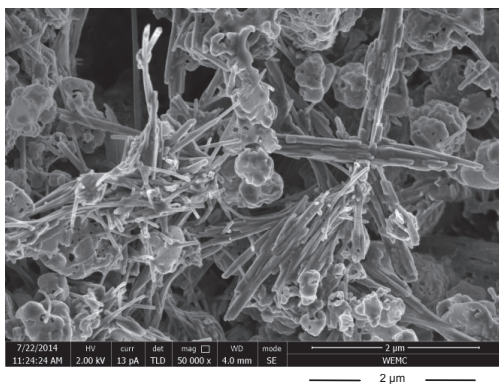
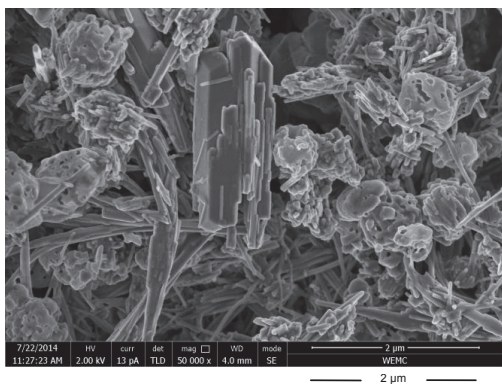


SEM and EDX of synthesised  $\text{SeS}_2$  with no biomass at  $t = 1$  day



**SEM and EDX of synthesised  $\text{SeS}_2$  reduced by Emmtec at  $t=36$  days (#2-1)**





**SEM and EDX of synthesised  $\text{SeS}_2$  without biomass at  $t = 36$  days**





## **6 General Discussion and Outlook**

The process of biological removal of selenium from wastewater has previously been researched by Lenz in the sub-department of Environmental Technology at Wageningen University (2008c). As a follow-up to that work, this thesis focuses on improving the volume of recoverable solid selenium particles in a biological way. As a basis for the discussion, I first summarize the main findings of this thesis. Then the following paragraphs highlight results and reflections on improvement. Further, in 6.6 the two reduction systems are compared and paragraph 6.7 gives main recommendations for further research. The chapter closes with the concluding remarks.

### **6.1 Summary of main results**

Chapter 1 describes the complexity of biological and chemical control of selenium reduction processes. Besides biological reduction, product formation (selenite or solid selenium) should be stable and controlled. The selenite or selenium produced should also be recoverable. Control of biological selenium production is limited by process conditions: temperature and pH. The process is challenged by the following factors: the reactivity of selenite, the particle formation of selenium, and the discharge limits of the different selenium waste streams such as total selenium concentration.

Chapter 2 demonstrates that it was possible to convert selenate to (mainly) selenite at relatively low electron donor concentrations. The yield was relatively high (79-95%).

Chapter 3 shows that selenium particle properties can be influenced by temperature and pH and that at a higher pH and higher temperature more acicular crystalline hexagonal selenium can be produced (fig 6.1 BC). The effect of the pH and temperature on the formation of particles was more effective during the selenium particle formation than post modification (fig 6.1 D).

In an attempt to increase the size of acicular selenium particles at 50°C in a

continuous system (Chapter 4), acicular selenium particle clusters appeared (Fig 6.1E). Unfortunately, the selenate-reducing biomass did not develop at 50°C and selenate reduction capacity remained poor. It was also clearly not possible to grow the selenium particles to a larger size than the particles obtained during the experiments as described in chapter 3.

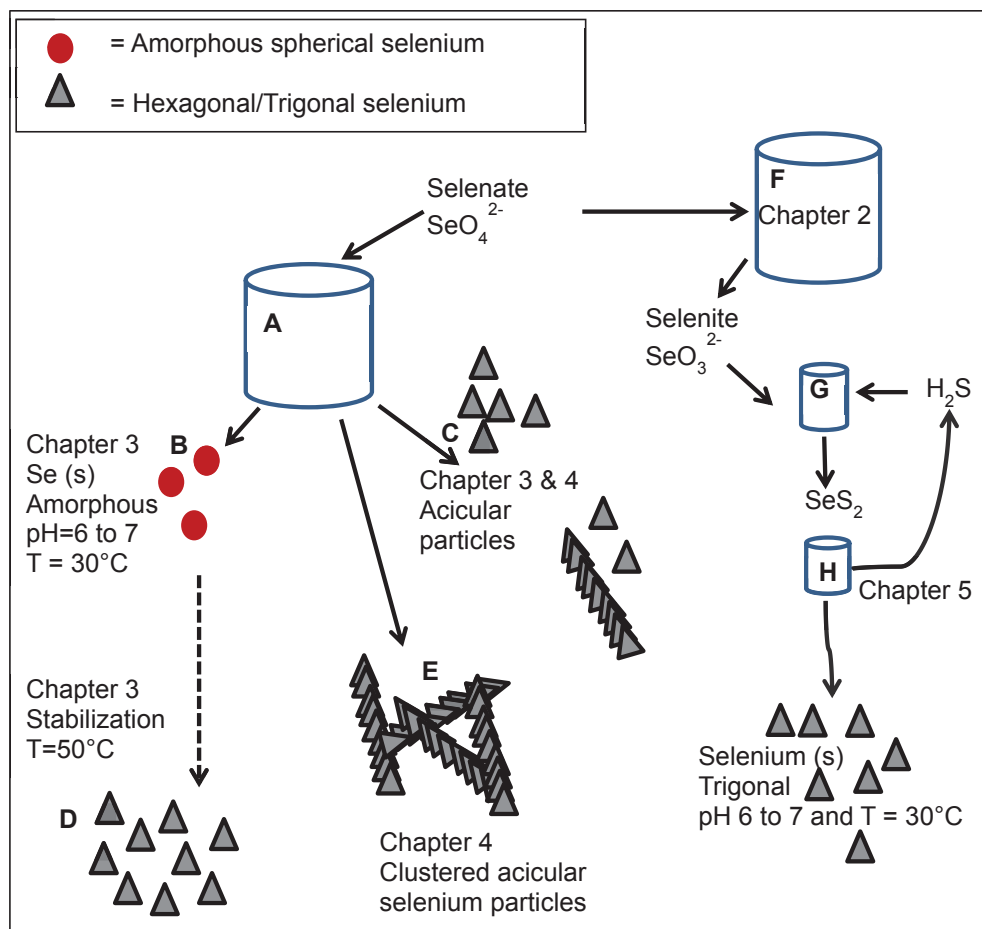


Figure 6-1: Two routes for recovering selenium from wastewater. Selenate containing wastewater starts with biological selenate reduction to either elemental selenium or selenite. Reactor A, conversion of selenate to solid elemental selenium. B, red amorphous particles. C, hexagonal acicular particles. D, crystalline selenium particles formed by post-treatment. E, acicular selenium clusters. F, conversion of selenate to selenite. G, reactor chemical selenite precipitation with sulphide. Reactor H, biomass converts  $\text{SeS}_2$  to sulphide and selenium (hexagonal).

Produced selenite (Chapter 2) reacts with sulphide to form amorphous  $\text{SeS}_2$ . In Chapter 5, the produced amorphous  $\text{SeS}_2$  and a commercially purchased crystalline  $\text{SeS}_2$  were both reduced to selenium and sulphide by bacteria present in Emmtec sludge, resulting in a viable recovery system for selenium (Chapter 5).

In conclusion, two routes for recovering bio-selenium are possible. One involves direct reduction of selenate to elemental selenium (Fig 6.1 reactor A) and the other route is to produce selenium via  $\text{SeS}_2$  (Fig 6.1 reactors FGH). Both routes have advantages in terms of product stability, selenate reduction rate and electron donor costs.

## **6.2 properties of the produced selenium particles**

### **6.2.1 Comparing the properties of the produced selenium particles**

After biological reduction of selenate to elemental selenium, different kinds of selenium particles were detected: acicular particles and spherical particles (Chapter 3). Intermediate particles were also detected and these were mostly observed under process conditions in which acicular selenium particles were also formed. The acicular particles were made visible by light microscopy, and the size of these particles (around 10  $\mu\text{m}$  long) suggests that these were extracellular. The amorphous spherical particles were smaller (roughly estimated to be up to half a micron in diameter, SEM pictures (Chapter 3)).

In some cases, selenium acicular particle clusters were detected (Chapter 4 and Fig. 6-1). The clustering of these selenium particles might stimulate transformation or particle growth, because the selenium particles are close together.

Hexagonal selenium particles were formed at  $T=30^\circ\text{C}$  and  $\text{pH}=7$  via  $\text{SeS}_2$  and amorphous spherical particles were formed via direct reduction of selenate to elemental selenium. This implies that the mechanism or route affects the stability of the non-hexagonal particles with high selenium content. The amorphous selenium is stabilized by biomolecules such as proteins from, for example, *Geobacter*

*sulfurreducens* (Pierce et al. 2009). These biomolecules might prevent the phase transformation to the hexagonal selenium structure and selenium particles via  $\text{SeS}_2$  were not stabilized by these molecules.

### **6.2.2 Biomass attached to selenium particles**

In most of the experiments in which the amorphous selenium spherical particles were identified by SEM and XRD, light microscopy showed that the whole micro-organism was coloured red. It was thus clearly not possible to see separate amorphous selenium particles. This suggests that the amorphous selenium particles were very tightly connected to the biomass, whereas the bigger selenium acicular particles were detected extracellularly.

Selenite can be precipitated with  $\text{S}^{2-}$  to  $\text{SeS}_2$  and an average particle size of  $6.3\ \mu\text{m}$  can be obtained (Geoffroy and Demopoulos 2011). Regarding the size of some  $\text{SeS}_2$  particles, it appears that the particle formation of the hexagonal selenium compounds is extracellular. The black spots on the  $\text{SeS}_2$  particles suggest this (Chapter 5, Fig. 2A).

### **6.2.3 The effect of the particle properties on the recovery**

Amorphous spherical selenium particles are up to  $0.5\ \mu\text{m}$  in diameter and this corresponds with a globular volume of about  $0.07\ \mu\text{m}^3$ . The biggest acicular particles are in the range of  $10\ \mu\text{m}$  in length and  $0.5\ \mu\text{m}$  thick, corresponding with a cylindrical volume of about  $2\ \mu\text{m}^3$ . This means that the particles in the reactors were more or less equal in volume (30-fold). In the  $\text{SeS}_2$  reduction experiment the selenium particles were sometimes over  $125\ \mu\text{m}^3$  (cube  $5\ \mu\text{m}$ ). (Particles over  $10\ \mu\text{m}$  could also be detected; however in this case no EDX result is available, see Appendix 5A.) See particle volumes and sedimentation velocities in Table 6.1. The amorphous spherical compared with a crystalline  $125\ \mu\text{m}^3$  particle resulted in much increased sedimentation velocity (over 150-fold) and increased particle volume (over 1750-fold).

Table 6-1: Sedimentation velocities of the particles produced

Process conditions	Particle description	Volume ( $\mu\text{m}^3$ )	Radius according to spherical particle ( $\mu\text{m}$ )	Sedimentation velocity (according Appendix 1A) ( $\text{m s}^{-1}$ )
1 Amorphous particles using Eerbeek sludge at $T=30^\circ\text{C}$ and $\text{pH}=7$ (Chapter 3)	Amorphous Spherical	0.07	0.3	$5.9 \cdot 10^{-7}$
2 Crystalline particles no mass growth in the calculation. (Chapter 3) (Stability test)	Crystalline Spherical	0.06	0.2	$7.8 \cdot 10^{-7}$
3 Crystalline particles at $T=50^\circ\text{C}$ and $\text{pH}=7$ or $T=30^\circ\text{C}$ and $\text{pH}=9$ (Chapter 3 and 4)	Acicular (long cylindrical)	2	0.8	$3,5 \cdot 10^{-5}$
4 Crystalline particles at $T=30^\circ\text{C}$ and $\text{pH}=7$ (Chapter 5)	via $\text{SeS}_2$ (rock-like)	125	3.1	$8.4 \cdot 10^{-5}$

In line 1 amorphous density is used, whereas in lines 2, 3 and 4 crystalline density is used.

#### 6.2.4 Possibility to avoid the formation of red amorphous selenium

Since elemental selenium is insoluble, the reduction rate of selenate and selenite to elemental selenium equals the precipitation rate. In all of the experiments it seemed to be impossible to skip the red phase of amorphous selenium. Even in the batch experiments at  $50^\circ\text{C}$  and a high pH (Chapter 3), a red phase was noticed. This shows that the formation of red amorphous selenium is fast compared to the transformation to a hexagonal structure in our biological experiments.

In the chemical reduction experiment performed by Harańczyk et al. (2002) at a temperature of  $84^\circ\text{C}$  no red colour was detected at a high initial pH of 8.3. This indicates that the amorphous selenium phase was skipped in this chemical experiment. A lower pH in this chemical reduction led to a red phase during the process. Skipping the formation of red-coloured selenium in Harańczyk's chemical (selenite reduction with  $\text{HSO}_3^-$ ) experiments is partially explained by the fact that a

higher pH reduces the reaction rate and consequently changes the morphology of the selenium deposits. However, Harańczyk et al. (2002) used 250 mM of  $\text{Se}^{4+}$  at 357K and the reaction lasted 300 minutes. Thus, the reaction rate was much higher than in our biological experiments. The difference in the chemical reaction rate cannot explain the difference in particle structure and morphology in our experiments. However, both our experiments and those carried out by Harańczyk confirm that the red phase of selenium formation is less noticeable at a higher pH.

Now the question arises as to whether it is possible to skip the red amorphous phase in biocrystallisation, since it is limited by the temperature of the water and the pH value at which the micro-organisms can reduce selenate or selenite. At the borders of these conditions (a higher temperature and higher pH) selenate reduction might be limited, but the transformation can be stimulated. This would perhaps result in direct crystalline hexagonal selenium particle formation.

## **6. 3 Reflection on lactic acid as electron donor**

### **6.3.1 Electron donor balance**

In nearly all experiments the molar ratio lactic acid to selenate was 0.55 to 1. In the continuous reactor (Chapter 4) around 5% of the selenate is converted and around 80% of the electron donor is used. This means that the yield of selenium on electron donor is roughly 6%. The fed-batch experiments yielded 14% elemental selenium from the selenate at 50°C. This difference (5% and 14%) can be explained by the fact that there was proportionally more inoculum in the continuous reactor (50 g for the continuous reactor and 5 g for the fed-batch reactor). The electron donor concentration was 0.55 mM for the continuous reactor and 13.75 mM for the fed-batch reactor. Probably relatively more electron donor was used for biomass maintenance in the continuous experiment.

In fed-batch systems at 30°C around 20% of the selenate was converted to elemental selenium (Chapter 2, Table 2.2). This means that roughly 20% of the

electron donor was effectively used for selenium recovery since the amount of electron donor was balanced with the amount of selenate.

In the route via  $\text{SeS}_2$ , a maximum of 40% of the electron donor was effectively used in the first step to convert selenate to selenite (Chapter 2, Table 2.2). In the next step 0.5 mmol lactic acid was used to reduce 0.5 mmol of  $\text{SeS}_2$ . Roughly 75% of the sulphur was removed from the  $\text{SeS}_2$ . This means that 25% of the lactic acid was used for sulphur reduction. However, regarding the carbon balance with  $\text{CO}_2$ ,  $\text{CH}_4$  and lactic acid, it is likely that more electron donor was still present in the  $\text{SeS}_2$  reduction bottles. Only one third of the carbon was converted to  $\text{CO}_2$  (Emmtec bottles table 5.3). This means that in the  $\text{SeS}_2$  reduction process the electrons from the electron donor were used very effectively.

Overall, comparing the electron donor costs based on the experiment performed the production of selenium directly cost an equivalent 5 times the electron donor. Via  $\text{SeS}_2$  this would now be 2.5 times only. Still the yield on electron donor should be improved for both systems and reactor design and electron donor type could be specialised.

### **6.3.2 Usage of lactic acid as electron donor for selenate to elemental selenium reduction**

In almost all experiments in Chapter 2 and most of the time during the long-term experiment described in Chapter 4, lactic acid and selenate was added in the molar ratio 0.55 to 1. In both reactors propionic acid was detected, thus it seems that lactic acid was first reduced instead of oxidized and this oxidation step could not have contributed to selenate reduction. An alternative might be to use propionic acid and acetic acid directly in the bioreactor. Astratinei et al., 2006 tested 0.5 mM selenate reduction using Eerbeek sludge with several electron donors at 20 mM. The selenium removal rate of soluble selenium to insoluble selenium increases with the electron donor in the following order: acetate, propionate, lactate and ethanol. So apparently, lactate has a positive effect on the selenium reduction rate compared with propionate and acetate. However, 20 mM ethanol resulted in the best selenium removal according to Astratinei et al., 2006 experiments with Eerbeek sludge. This means that

the type of electron donor influences the recovery on electron donor.

During this PhD research, ethanol was also tested as an electron donor for selenium removal in the fed-batch reactors (Chapter 2). The molar ratio ethanol to selenate was 0.55 to 1. However, selenate reduction using Eerbeek sludge was poor in our experiments with ethanol as the electron donor. This was probably caused by the gas removal system in the reactors used. This result suggests that the combination of electron donor type and reactor design must be optimised.

## 6.4 Options for optimizing selenite production

### 6.4.1 Effect of selenite on the particle formation

Selenate was originally used as a substrate and selenite had been accumulating during the reduction process (Chapter 2). Acicular particles were produced both with (pH=8 and T=30°C) and without selenite accumulation (pH=9 and T=30°C). In the Fed-batch experiments (chapter 3) at which amorphous particles were produced, selenite was detected. One question I considered is whether selenite production affects particle formation. When yeast extract was added to a solution with selenite an orange colour appeared at 25 and 30°C, but not at 50 and 70°C (Fig. 6-2). This implies that selenite (when produced) can chemically react with organic compounds from biomass or that it reduces relatively fast compared to biological selenate reduction. This could perhaps result in selenium seeds and this affects particle formation. As a result, more – and smaller – selenium particles can be obtained, and also selenite yield is reduced.

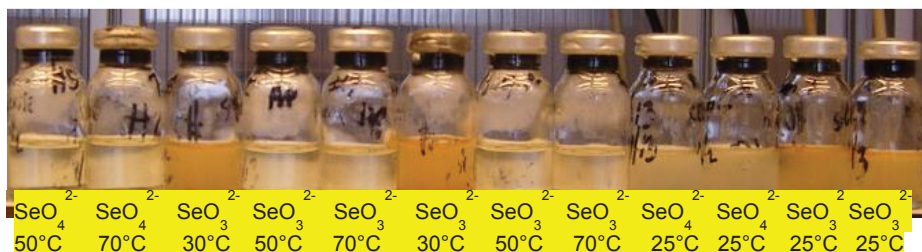


*Fig 6-2: Preliminary results after 19 hours: selenite and selenate addition with yeast extract. pH ranges between 6.1 and 7.1, The medium was as used in all chapters, with 3 mM selenate or selenite and 0.25 g/L yeast extract.*



### **6.4.2 Acetate as possible electron donor for selenate to selenite conversion**

In this research, the selenite yield from selenate was relatively high (chapter 2), but the yield of selenite reduction on the electron donor could have been improved. It would be interesting to repeat the experiments with propionic acid or acetate acid to determine whether propionic or acetate oxidizing bacteria are responsible for the selenate reduction. Moreover, lactic acid, which is converted rapidly in these experiments, can contribute to the selenate reduction. For example, this was demonstrated by Oremland et al., 1994 for *Sulfurospirillum barnesii* strain SES-3 that converts lactate to acetate and CO<sub>2</sub> via dissimilatory selenate to selenite.

Interestingly, after increasing the COD concentration in the continuous experiment (Chapter 4), around 40 mg/L of COD (mainly acetate) and around 0.9 mM of selenate was collected in the external settler. When half of the selenate is reduced to selenite in the external settler, then one third of the electron donor was used to convert selenate to selenite (eq 4.1 and 4.2). With this in mind, it would be interesting to research the use of acetate as an electron donor to convert selenate to selenite.

### **6.5 Recovery from waste streams with low concentrations of selenium**

Probably selenium removal has a threshold, like at relatively high electron donor concentrations, the total amount of selenium removed is limited. The selenium effluent concentration in a sulphate-reducing reactor was 0.24 µg/L and in a methanogenic reactor it was 8 µg/L, (Lenz et al., 2008a).

In this research (see Chapters 2, 3 and 4) relatively high selenium concentrations of 10 to 1 mM were used, so it would also be interesting to obtain acicular selenium particles at low selenate concentrations.

To grow selenium particles (for example particles of 2 µm<sup>3</sup>) for recovery of selenium, the ratio of biomass to selenium should be as low as possible to enhance the crystallization process. So in waste water with low selenium concentrations also a small amount of biomass should be used. But this probably means that the bioreactor will have a lower volumetric selenium reduction capacity and it can become difficult to remove all the selenium. The question raises now when the concentration is too low for efficient bio-recovery through growing selenium particles.

## 6.6 Comparing the two recovery systems

The two routes for selenium bio-recovery are summarized in Table 6.2 and Fig. 6.1. Selenium waste streams may vary in composition and nature such as groundwater, metal processing wastewater, and oil and coal wastewater. The two systems are compared in terms of several wastewater properties with a focus on selenium recovery from selenate (Table 6-2).

**Table 6-2: Selenium recovery from selenate, both directly and via  $\text{SeS}_2$**

	Direct	Via $\text{SeS}_2$	Remark
Equipment			
Reactors and settlers	1 bioreactor 1 settler	2 bioreactors 1 settler and 1 $\text{H}_2\text{S}$ mixer 1 sludge treatment	via $\text{SeS}_2$ the reactor size is smaller, due to a fast reaction
Electron donor costs	Selenate to elemental selenium costs 6 electrons	- selenate reduction to selenite costs 2 electrons - converting S in $\text{SeS}_2$ to $\text{S}^{2-}$ costs 4 electrons for one $\text{Se}^0$	Equal in both situations under optimal conditions
HRT (reactor size)	Long HRT up to days	HRT expected to be shorter since selenite can accumulate during selenate to selenium reduction	Short HRT means smaller reactors
Product quality			
Product size	Amorphous or crystalline particles up to $2\ \mu\text{m}^3$	crystalline particles $125\ \mu\text{m}^3$	
Product concentration	Depends on nuclei and selenium concentration in the waste stream	Concentrated selenium stream due to sedimentation steps	

### 6.6.1 Comparing Equipment costs

The equipment cost of the two processes is based on reactors and settlers or other solid liquid separation processes (Table 6-2). A single bioreactor is used for direct conversion to elemental selenium, while two bioreactors and one mixing step with  $\text{H}_2\text{S}$  are needed for selenate conversion via  $\text{SeS}_2$ . Because of the gaseous hydrogen sulphide used, safety requirements are also an issue. On the one hand, it seems that

the total equipment costs of the  $\text{SeS}_2$  removal system represent a disadvantage. On the other hand, the HRT of biological selenate reduction could be shorter for selenite production compared to elemental selenium production. The HRT of the selenite waste stream is also short due to the fast reaction of selenite with sulphide. These short HRTs result in smaller chemical and biological reactor size and reduce the investment costs for selenium removal systems using  $\text{SeS}_2$ .

### **6.6.2 Control of process conditions**

Selenate removal starts with biological conversion in both processes. So the effect of process conditions on the process routes is more or less the same. Often the temperature and the pH conditions are limited by control options. This means that the use of hyperthermophilic bacteria stimulates selenium particle formation, but it increases the heating cost. The presence of nitrate and sulphate or other elements is estimated to have the same effect on the first biological reduction. The elements  $\text{Zn}^{2+}$ ,  $\text{Fe}^{2+}$ ,  $\text{Ag}^+$ ,  $\text{Pb}$ ,  $\text{Hg}^{2+}$ ,  $\text{Hg}^+$  and  $\text{Cu}^{2+}$  will be precipitated by sulphide.

### **6.6.3 $\text{SeS}_2$ recovering has an advantage regarding equipment and product quality**

Overall, from Table 6-2, it can be concluded that selenium as selenate can be recovered with  $\text{SeS}_2$ . The first biological step, selenate reduction to selenite is faster than selenate to selenium reduction under certain process conditions (Chapter 3). The main advantages are a higher product quality and a higher concentration, as the selenium product is larger and more dewatered. After both of the biological treatment steps, selenium is obtained. To re-use the selenium thus obtained, a percentage of 5-25% of selenium is required. This is the amount that is also used in selenium refinement industries (Hoffmann 1989). With particles over  $125\mu\text{m}^3$  in size these concentrations must be feasible.

## **6.7 Main recommendations for further research**

### **Direct selenium particle formation**

Selenate reduction using Eerbeek sludge was sometimes inhibited by the process

conditions we chose. Temperatures were 20°C and 50°C (Chapters 2, 3 and 4), and pH range limits were 6 and 9 (Chapter 2 and 3). The electron donor concentration in the reactor could have been limited for the reduction processes. In follow-up research it is advised to use another sludge that can handle a higher temperature or higher pH and to see if pH and temperature could be raised further during the selenium reduction experiments to directly promote acicular selenium particle formation.

### **Selenium particle formation via $\text{SeS}_2$**

The selenium particles obtained in the direct route for selenium production are in the range of several tenths of  $\mu\text{m}$  long. It would be interesting to study the recrystallisation process from  $\text{SeS}_2$  to Se. It would also be interesting to determine whether  $\text{SeS}_2$  can adsorb low concentrations of selenite. The main challenge is the rigorous requirements: removal efficiency (5ppb) and low concentrations (1000ppb) combined with Se recovery.

### **Selenium particle formation at high ethanol concentrations**

Since the addition of compounds can alter the selenium particles, the electron donor could have the same effect. This means that the electron donor itself can act as a stabilizing agent. However, it is known that ethanol has a positive effect on selenium recrystallization (Li et al., 2006). Thus, when relatively high concentrations of ethanol are used in a selenium reduction process, crystallisation towards the hexagonal structure can be stimulated.

## **6.8 Concluding remarks**

To remove selenate, the first step should be biological, because of the microbes' selectivity. Reducing selenate to elemental selenium, directly or indirectly via  $\text{SeS}_2$ , results in different selenium particle properties under comparable pH and temperature conditions. Finally, the selenium particles in the route via  $\text{SeS}_2$  resulted in the largest crystalline selenium product free from biomass. For re-use the route via  $\text{SeS}_2$  therefore seems to be the most promising approach.

## 7 References

- d'Abzac, P., Bordas, F.O., Joussein, E., Hullebusch, E.v., Lens, P.N. and Guibaud, G. (2009) Characterization of the mineral fraction associated to extracellular polymeric substances (EPS) in anaerobic granular sludges. *Environmental science & technology* 44(1), 412-418.
- D'Abzac, P., Bordas, F., Van Hullebusch, E., Lens, P.N. and Guibaud, G. (2010) Extraction of extracellular polymeric substances (EPS) from anaerobic granular sludges: comparison of chemical and physical extraction protocols. *Applied microbiology and biotechnology* 85(5), 1589-1599.
- de Almeida, C.M.S., Ribeiro, A.S., Saint'Pierre, T.D. and Miekeley, N. (2009) Studies on the origin and transformation of selenium and its chemical species along the process of petroleum refining. *Spectrochimica Acta Part B: Atomic Spectroscopy* 64(6), 491-499.
- Amend, J.P., Shock, E.L., 2001. Energetics of overall metabolic reactions of thermophilic and hyperthermophilic Archaea and Bacteria. *FEMS Microbiology Reviews* 25(2), 175-243.
- Astratinei, V., Hullebusch Van, E., Lens, P., 2006. Bioconversion of selenate in methanogenic anaerobic granular sludge. *Journal of Environmental Quality* 35 (5), 1873.
- Bajaj, M., Eiche, E., Neumann, T., Winter, J. and Gallert, C. (2011) Hazardous concentrations of selenium in soil and groundwater in North-West India. *Journal of hazardous materials* 189(3), 640-646.
- Ball, S. and Milne, J. (1995) Studies on the interaction of selenite and selenium with sulfur donors. Part 3. Sulfite. *Canadian Journal of Chemistry* 73(5), 716-724.
- Boctor, N. and Kullerud, G. (1987) Phase relations and equilibrium copolymerization in the Se - S system. *Journal of Solid State Chemistry* 71(2), 513-521.
- Brimmer S.P., Fawcett W.R., Kulhavy K.A. (1987) Quantitative reduction of selenate ion to selenite in aqueous samples *Analytical Chemistry* 59(10).1470-1471
- Brozmanová, J., Mániková, D., Vlčková, V. and Chovanec, M. (2010) Selenium: a double-edged sword for defense and offence in cancer. *Archives of toxicology* 84(12), 919-938.
- Butler, C., Debieux, C., Dridge, E., Splatt, P. and Wright, M. (2012) Biomineralization of selenium by the selenate-respiring bacterium *Thauera selenatis*. *Biochemical Society Transactions* 40(6), 1239-1243
- Bye, R. and Lund, W. (1988) Optimal conditions for the reduction of selenate to selenite by hydrochloric acid. *Fresenius' Journal of Analytical Chemistry* 332(3), 242-244.
- Catal, T., Bermek, H. and Liu, H. (2009) Removal of selenite from wastewater using microbial fuel cells. *Biotechnology letters* 31(8), 1211-1216.
- Chasteen, T.G. and Bentley, R. (2003) Biomethylation of selenium and tellurium: micro-organisms and plants. *Chemical reviews* 103(1), 1-26.
- Dauchot, J. and Watillon, A. (1967) Optical properties of selenium sols: I. Computation of extinction curves from Mie equations. *Journal of Colloid and Interface Science* 23(1), 62-72.

Dhanjal, S. and Cameotra, S.S. (2010) Aerobic biogenesis of selenium nanospheres by *Bacillus cereus* isolated from coalmine soil. *Microbial cell factories* 9, 52-52.

Ding, Y., Li, Q., Jia, Y., Chen, L., Xing, J. and Qian, Y. (2002) Growth of single crystal selenium with different morphologies via a solvothermal method. *Journal of crystal growth* 241(4), 489-497.

Dwivedi, S., AlKhedhairy, A.A., Ahamed, M. and Musarrat, J. (2013) Biomimetic synthesis of selenium nanospheres by bacterial strain JS-11 and its role as a biosensor for nanotoxicity assessment: a novel Se-bioassay. *PloS one* 8(3), e57404.

Envirogen (2011) Envirogen Technologies, Treatment of Selenium-containing coal mining wastewater with fluidized bed reactor technology. An Envirogen Technologies Whitepaper. Pages 1-15

Falcone, G., & Nickerson, W. J. (1963). Reduction of selenite by intact yeast cells and cell-free preparations. *Journal of bacteriology*, 85(4), 754-762.

Fernández-Martínez, A. and Charlet, L. (2009) Selenium environmental cycling and bioavailability: a structural chemist point of view. *Reviews in Environmental Science and Biotechnology* 8(1), 81-110.

Frenkel, G.D., Falvey, D. and MacVicar, C. (1991) Products of the reaction of selenite with intracellular sulfhydryl compounds. *Biological trace element research* 30(1), 9-18.

Fujita, M., Ike, M., Kashiwa, M., Hashimoto, R. and Soda, S. (2002) Laboratory scale continuous reactor for soluble selenium removal using selenate reducing bacterium, *Bacillus* sp. SF 1. *Biotechnology and bioengineering* 80 (7), 755-761.

Gates, B., Mayers, B., Cattle, B. and Xia, Y. (2002) Synthesis and characterization of uniform nanowires of trigonal selenium. *Advanced Functional Materials* 12(3), 219-227

Ganther, H.E. (1971) Reduction of the selenotrisulfide derivative of glutathione to a persulfide analog by glutathione reductase. *Biochemistry* 10(22), 4089-4098.

Gennari, F., Sharma, V.K., Pettine, M., Campanella, L. and Millero, F.J. (2014) Reduction of selenite by cysteine in ionic media. *Geochimica et Cosmochimica Acta* 124, 98-108.

George, M.W. (2014) CRC usgs minerals Selenium and Tellurium [advance release]. world, U.s.f.a.c. (ed), U.S. Department of the Interior (2014) U.S. Geological survey. Pages 65.1 - 65.8

Geoffroy, N., Demopoulos, G., 2011. The elimination of selenium (IV) from aqueous solution by precipitation with sodium sulfide. *Journal of Hazardous Materials* 185 (1), 148-154.

Group, R.A. (2014) Retorte., <http://www.retorte.de/english/selen.html> (2014)

Harańczyk, I., Szafirska, B. and Fitzner, K. (2002) The influence of the rate of selenium crystallization from aqueous solutions on its morphology. *Journal of Mining and Metallurgy, Section B: Metallurgy* 38(1-2), 33-48.

He Q. and Yao K., (2010) Impact of alternative electron acceptors on selenium(IV) reduction by *Anaeromyxobacter dehalogenans*. *Bioresource Technology* 2010; 102(3):3578-3580.

Herbel, M.J., Blum, J.S., Oremland, R.S. and Borglin, S.E. (2003) Reduction of elemental selenium to selenide: experiments with anoxic sediments and bacteria that respire Se-oxyanions. *Geomicrobiology Journal* 20(6), 587-602.

Hockin, S.L. and Gadd, G.M. (2003) Linked redox precipitation of sulfur and selenium under anaerobic conditions by sulfate-reducing bacterial biofilms. *applied and environmental Microbiology* 69(12), 7063-7072.

Hoffmann, J.E. (1989) Recovering selenium and tellurium from copper refinery slimes. *JOM* 41(7), 33-38.

Högberg, J., Alexander, J., 2007. Selenium, in: Nordberg, G.F., Fowler, B.A., Nordberg, M., Friberg, L. (Eds.), *Handbook on the toxicology of metals*, Third ed. Academic Press, pp. 783-807.

Hohl, D., Jones, R., Car, R. and Parrinello, M. (1987) The structure of selenium clusters—Se<sub>3</sub> to Se<sub>8</sub>. *Chemical Physics Letters* 139(6), 540-545.

Hol, A., Van der Weijden, R.D., Van Weert, G., Kondos, P. and Buisman, C.J. (2010) Bio-reduction of pyrite investigated in a gas lift loop reactor. *International Journal of Mineral Processing* 94 (3), 140-146.

Iida, Y., Yamaguchi, T., Tanaka, T. and Nakayama, S. (2010) Solubility of selenium at high ionic strength under anoxic conditions. *Journal of nuclear science and technology* 47(5), 431-438.

Janssen, A.J., Lens, P.N., Stams, A.J., Plugge, C.M., Sorokin, D.Y., Muyzer, G., Dijkman, H., Van Zessen, E., Luimes, P. and Buisman, C.J. (2009) Application of bacteria involved in the biological sulfur cycle for paper mill effluent purification. *Science of the total environment* 407 (4), 1333-1343.

Kessi, J. and Hanselmann, K.W. (2004) Similarities between the abiotic reduction of selenite with glutathione and the dissimilatory reaction mediated by *Rhodospirillum rubrum* and *Escherichia coli*. *Journal of Biological Chemistry* 279(49), 50662-50669.

Kice, J.L., Lee, T.W.S. and Pan, S.T. (1980) Mechanism of the reaction of thiols with selenite. *Journal of the American Chemical Society* 102(13), 4448-4455.

Leaver, J.T., Richardson, D.J. and Butler, C.S. (2008) *Enterobacter cloacae* SLD1a-1 gains a selective advantage from selenate reduction when growing in nitrate-depleted anaerobic environments. *Journal of industrial microbiology & biotechnology* 35 (8), 867-873.

Lemly, A.D. (2004) Aquatic selenium pollution is a global environmental safety issue. *Ecotoxicology and Environmental Safety* 59(1), 44-56.

Lenz, M., Gmerek, A. and Lens, P.N.L. (2006) Selenium speciation in anaerobic granular sludge. *International Journal of Environmental Analytical Chemistry* 86 (9), 615-627.

Lenz, M., Hullebusch, E.D.V., Hommes, G., Corvini, P.F.X. and Lens, P.N.L. (2008a) Selenate removal in methanogenic and sulfate-reducing upflow anaerobic sludge bed reactors. *Water Research* 42(8-9), 2184-2194.

Lenz, M., Smit, M., Binder, P., Van Aelst, A.C., Lens, P.N.L., 2008b. Biological alkylation and colloid formation of selenium in methanogenic UASB reactors. *Journal of Environmental Quality* 37, 1691-1700

Lenz, M., Buisman, Dr. Ir. C.J.N. ; Lens, Dr. Ir. P.N.L., (2008C) Biological selenium removal from wastewaters, ISBN 9789085048015

Lenz, M., Van Aelst, A., Smit, M., Corvini, P. and Lens, P.N. (2009) Biological production of selenium nanoparticles from waste waters, pp. 721-724, Trans Tech Publ.

Li, Q. and Yam, V.W.W. (2006) High-yield synthesis of selenium nanowires in water at room temperature. *Chemical Communications* (9), 1006-1008.

Lin, Z.-H. and Chris Wang, C. (2005) Evidence on the size-dependent absorption spectral evolution of selenium nanoparticles. *Materials chemistry and physics* 92(2), 591-594.

Lortie, L., Gould, W., Rajan, S., McCready, R. and Cheng, K.J. (1992) Reduction of selenate and selenite to elemental selenium by a *Pseudomonas stutzeri* isolate. *Applied and Environmental Microbiology* 58(12), 40-42.

Ma, J., Kobayashi, D.Y. and Yee, N. (2007) Chemical kinetic and molecular genetic study of selenium oxyanion reduction by *Enterobacter cloacae* SLD1a-1. *Environmental science & technology* 41(22), 7795-7801.

Maiers, D.T., Wichlacz, P.L., Thompson, D.L. and Bruhn, D.F. (1988) Selenate reduction by bacteria from a selenium-rich environment. *Applied and environmental Microbiology* 54(10), 2591-2593

Mayers, B.T., Liu, K., Sunderland, D. and Xia, Y. (2003) Sonochemical synthesis of trigonal selenium nanowires. *Chemistry of materials* 15(20), 3852-3858.

McCloskey, J., Twidwell, L., Park, B. and Fallon, M. (2008) Removal of Selenium oxyanions from industrial scrubber waters utilizing elemental iron. *Proceedings of the International Conference "Industrial Dust Environmental Protection"*

Meulepas, R.J., Jagersma, C.G., Zhang, Y., Petrillo, M., Cai, H., Buisman, C.J.N., Stams, A.J.M. and Lens, P.N.L. (2010) Trace methane oxidation and the methane dependency of sulfate reduction in anaerobic granular sludge. *FEMS microbiology ecology* 72(2), 261-271.

Mehdi, Y., Hornick, J.-L., Istasse, L. and Dufrasne, I. (2013) Selenium in the environment, metabolism and involvement in body functions. *Molecules* 18(3), 3292-3311.

Minaev, V.S., Timoshenkov, S.P. and Kalugin, V.V. (2005) Structural and phase transformations in condensed selenium. *Journal of Optoelectronics and Advanced Materials* 7(4), 1717-1741

Mishra, R.R., Prajapati, S., Das, J., Dangar, T.K., Das, N. and Thatoi, H. (2011) Reduction of selenite to red elemental selenium by moderately halotolerant *Bacillus megaterium* strains isolated from Bhitarkanika mangrove soil and characterization of reduced product. *Chemosphere* 84(9), 1231-1237.

Mondal, K., Jegadeesan, G., & Lalvani, S. B. (2004). Removal of selenate by Fe and NiFe nanosized particles. *Industrial & engineering chemistry research*, 43(16), 4922-4934.



Mondal, K., Roy, P. and Srivastava, S.K. (2008) Facile biomolecule-assisted hydrothermal synthesis of trigonal selenium microrods. *Crystal Growth and Design* 8(5), 1580-1584.

Murphy, A.P., 1988. Removal of selenate from water by chemical reduction. *Industrial & engineering chemistry research* 27(1), 187-191.

Nelson, D.C., Casey, W.H., Sison, J.D., Mack, E.E., Ahmad, A. and Pollack, J.S. (1996) Selenium uptake by sulfur-accumulating bacteria. *Geochimica et Cosmochimica Acta* 60(18), 3531-3539

Oremland, R.S., Blum, J.S., Culbertson, C.W., Visscher, P.T., Miller, L.G., Dowdle, P. and Strohmaier, F.E. (1994) Isolation, growth, and metabolism of an obligately anaerobic, selenate-respiring bacterium, strain SES-3. *applied and environmental Microbiology* 60(8), 3011-3019.

Oude Elferink, S.J.W.H., Vorstman, W.J., Sopjes, A. and Stams, A.J.M. (1998) Characterization of the sulfate-reducing and syntrophic population in granular sludge from a full-scale anaerobic reactor treating papermill wastewater. *FEMS Microbiology Ecology* 27(2), 185-194.

Pearce, C.I., Coker, V.S., Charnock, J.M., Patrick, R.A.D., Mosselmans, J.F.W., Law N., Beveridge T.J., Lloyd J.R., Microbial manufacture of chalcogenide-based nanoparticles via the reduction of selenite using *Veillonella atypica*: an in situ EXAFS study. *Nanotechnology* 19 (2008) 155603 (13pp).

Pearce, C.I., Patrick, R.A., Law, N., Charnock, J.M., Coker, V.S., Fellowes, J.W., Oremland, R.S. and Lloyd, J.R. (2009) Investigating different mechanisms for biogenic selenite transformations: *Geobacter sulfurreducens*, *Shewanella oneidensis* and *Veillonella atypica*. *Environmental technology* 30(12), 1313-1326.

Pejova, B. and Grozdanov, I. (2001) Solution growth and characterization of amorphous selenium thin films: Heat transformation to nanocrystalline gray selenium thin films. *Applied surface science* 177(3), 152-157.

Pettine, M., Gennari, F., Campanella, L., Casentini, B., Marani, D., 2011. The reduction of selenium (IV) by hydrogen sulfide in aqueous solutions. *Geochimica et Cosmochimica Acta* 83, 37-47.

Pettine, M., Gennari, F. and Campanella, L. (2013) The reaction of selenium (IV) with ascorbic acid: Its relevance in aqueous and soil systems. *Chemosphere* 90(2), 245-250.

Pickett T., and Harwood, J. (2012) Biofiltration systems: answer selenium treatment challenge, *Industrial water world*. March/April 2012

Puranen, A., Jansson, M. and Jonsson, M. (2010) A study on the immobilization of selenium oxyanions by H<sub>2</sub>/Pd (s) in aqueous solution:: Confirmation of the one-electron reduction barrier of selenate. *Journal of contaminant hydrology* 116(1-4), 16-23.

Rauschenbach, I., Narasingarao, P. and Häggblom, M.M. (2011) *Desulfurispirillum indicum* sp. nov., a selenate-and selenite-respiring bacterium isolated from an estuarine canal. *International Journal of Systematic and Evolutionary Microbiology* 61(3), 654-658.

Roest, K., Heilig, H., Smidt, H., de Vos, W.M., Stams, A.J.M., Akkermans, A.D.L., 2005. Community analysis of a full-scale anaerobic bioreactor treating paper mill wastewater. *Systematic and applied microbiology* 28(2), 175-185.

Sanfilippo, A. and English, J. (2006) An overview of medicated shampoos used in dandruff treatment. *P AND T* 31(7), 396.

Scalet, B.M., Slade, S., Kasper, A., Van Marcke, d.L., Gitzhofer, K. and Van Limpt, H. (2006) Selenium emissions from glass melting furnaces: formation, sampling and analysis. A position paper by the Technical Committee 13," Environment", of the International Commission on Glass (ICG). *Glass Technology-European Journal of Glass Science and Technology Part A* 47(2), 29-38.

Shah, C.P., Dwivedi, C., Singh, K.K., Kumar, M. and Bajaj, P.N. (2010a) Riley oxidation: A forgotten name reaction for synthesis of selenium nanoparticles. *Materials Research Bulletin* 45(9), 1213-1217.

Shah, C.P., Singh, K.K., Kumar, M. and Bajaj, P.N. (2010b) Vinyl monomers-induced synthesis of polyvinyl alcohol-stabilized selenium nanoparticles. *Materials Research Bulletin* 45(1), 56-62.

Siddique, T., Arocena, J.M., Thring, R.W. and Zhang, Y. (2007) Bacterial reduction of selenium in coal mine tailings pond sediment. *Journal of Environmental Quality* 36(3), 621-627.

Sipma, J., Meulepas, R., Parshina, S., Stams, A., Lettinga, G. and Lens, P. (2004) Effect of carbon monoxide, hydrogen and sulfate on thermophilic (55 C) hydrogenogenic carbon monoxide conversion in two anaerobic bioreactor sludges. *Applied microbiology and biotechnology* 64 (3), 421-428.

Soda, S., Kashiwa, M., Kagami, T., Kuroda, M., Yamashita, M., Ike, M., 2011. Laboratory-scale bioreactors for soluble selenium removal from selenium refinery wastewater using anaerobic sludge. *Desalination* 279 (1), 433-438.

Song, J.-M., Zhu, J.-H. and Yu, S.-H. (2006) Crystallization and shape evolution of single crystalline selenium nanorods at liquid-liquid interface: From monodisperse amorphous Se nanospheres toward Se nanorods. *The Journal of Physical Chemistry B* 110(47), 23790-23795.

Srivastava, N. and Mukhopadhyay, M. (2013) Biosynthesis and Structural Characterization of Selenium Nanoparticles Mediated by *Zooglea ramigera* Powder Technology.1480-1487

Staicu, L.C., van Hullebusch, E.D. and Lens, P.N. (2015) Production, recovery and reuse of biogenic elemental selenium. *Environmental Chemistry Letters* 13 (1), 89-96.

Stams, A.J.M., Grolle, K.C.F., Frijters, C.T.M. and Van Lier, J.B. (1992) Enrichment of thermophilic propionate-oxidizing bacteria in syntrophy with *Methanobacterium thermoautotrophicum* or *Methanobacterium thermoformicum*. *Applied and Environmental Microbiology* 58(1), 346-352.

Steinberg, N.A. and Oremland, R.S. (1990) Dissimilatory selenate reduction potentials in a diversity of sediment types. *applied and environmental Microbiology* 56(11), 3550-3557.

Steinmann, D., Nauser, T. and Koppenol, W.H. (2010) Selenium and sulfur in exchange reactions: a comparative study. *The Journal of organic chemistry* 75(19), 6696-6699.

Tejo Prakash, N., Sharma, N., Prakash, R., Raina, K.K., Fellowes, J., Pearce, C.I., Lloyd, J.R. and Patrick, R.A.D. (2009) Aerobic microbial manufacture of nanoscale selenium: exploiting nature's bio-nanomineralization potential. *Biotechnology letters* 31(12), 1857-1862.

Sandy T., Disante C., (2010) Review of available technologies for the removal of selenium from water. *North American Metals Council*.(2010) 1-233

Tomei, F.A., Barton, L.L., Lemanski, C.L., Zocco, T.G., Fink, N.H. and Sillerud, L.O. (1995) Transformation of selenate and selenite to elemental selenium by *Desulfovibrio desulfuricans*. *Journal of Industrial Microbiology and Biotechnology* 14(3), 329-336.

Torres, J., Pintos, V., Domínguez, S., Kremer, C. and Kremer, E. (2010) Selenite and selenate speciation in natural waters: Interaction with divalent metal ions. *Journal of Solution Chemistry* 39(1), 1-10.

Wang, S., Weststrom, B. and Fernandez, J. (2003) A novel process for recovery of Te and Se from copper slimes autoclave leach solution. *Journal of Minerals and Materials Characterization and Engineering* 2(1), 53-64.

Wang, T., Yang, L., Zhang, B. and Liu, J. (2010) Extracellular biosynthesis and transformation of selenium nanoparticles and application in H<sub>2</sub>O<sub>2</sub> biosensor. *Colloids and Surfaces B: Biointerfaces* 80(1), 94-102.

Weijma, J., Stams, A.J.M., Pol, L.W.H., Lettinga, G., 2000. Thermophilic sulfate reduction and methanogenesis with methanol in a high rate anaerobic reactor. *Biotechnology and bioengineering* 67, 354-363.

Wessjohann, L.A., Schneider, A., Abbas, M. and Brandt, W. (2007) Selenium in chemistry and biochemistry in comparison to sulfur. *Biological chemistry* 388(10), 997.

WHO (2011) Selenium in drinking water. Selenium in Drinking-water. Background document for development of WHO Guidelines for Drinking-water, Quality © World Health Organization 2011

Winkel, L., Feldmann, J. and Meharg, A.A. (2009) Quantitative and qualitative trapping of volatile methylated selenium species entrained through nitric acid. *Environmental science & technology* 44 (1), 382-387.

Winkel, L.H., Johnson, C.A., Lenz, M., Grundl, T., Leupin, O.X., Amini, M. and Charlet, L. (2011) Environmental selenium research: from microscopic processes to global understanding. *Environmental Science & Technology* 46(2), 571-579.

Wu, Y. and Ni, Y. (2012) Low temperature rapid preparation of selenium nanostructures in the presence of food surfactants. *Chemical Engineering Journal* 187, 328-333.

Xi, G., Xiong, K., Zhao, Q., Zhang, R., Zhang, H. and Qian, Y. (2006) Nucleation-dissolution-recrystallization: a new growth mechanism for t-selenium nanotubes. *Crystal Growth & Design* 6(2), 577-582.

Xu, H., and Barton, L., L. (2013) Se-bearing colloidal particles produced by sulfate-reducing bacteria and sulfide-oxidizing bacteria: TEM study. *Advances in Microbiology* 3, 205-211

Yamada, A., Miyashita, M., Inoue, K. and Matsunaga, T. (1997) Extracellular reduction of selenite by a novel marine photosynthetic bacterium. *Applied microbiology and biotechnology* 48(3), 367-372.

Zehr, J.P., Oremland, R.S., 1987. Reduction of selenate to selenide by sulfate-respiring bacteria: experiments with cell suspensions and estuarine sediments. *Applied and Environmental Microbiology* 53, 1365-1369.

Zhang, N., Lin, L.S. and Gang, D. (2008) Adsorptive selenite removal from water using iron-coated GAC adsorbents. *Water Research* 42(14), 3809-3816.

Zhang, S.-Y., Zhang, J., Wang, H.-Y. and Chen, H.-Y. (2004) Synthesis of selenium nanoparticles in the presence of polysaccharides. *Materials Letters* 58(21), 2590-2594

Zhang, Y., Zahir, Z.A. and Frankenberger, W.T. (2003) Factors affecting reduction of selenate to elemental selenium in agricultural drainage water by *Enterobacter taylorae*. *Journal of agricultural and food chemistry* 51 (24), 7073-7078.

Zhang, W., Chen, Z., Liu, H., Zhang, L., Gao, P. and Li, D. (2011) Biosynthesis and structural characteristics of selenium nanoparticles by *Pseudomonas alcaliphila*. *Colloids and Surfaces B: Biointerfaces* 88(1), 196-201.

## Summary

Selenium in the form of selenate or selenite in wastewater needs to be removed due to its potential toxicity in the environment. Also, selenium is a valuable element that is used in several industries and current selenium resources are likely to be exhausted in less than 50 years. Waste streams containing selenium can therefore be used as a source of selenium. This requires conversion of the selenium in wastewater into a form that can be recovered. Biologically induced selenate reduction to recoverable selenium has the advantage that it uses the selective reduction capacities of biomass and a renewable electron donor.

To improve the recoverability of selenium the conversion of selenate to selenite was seen as an interesting opportunity. Selenite is more reactive than selenate and can be removed in a second step. As described in Chapter 2, it proved possible to convert selenate to mainly selenite at a low electron donor concentration.

Another method which is reviewed in this thesis is direct biological reduction of selenate to elemental selenium. After reduction the solids can be removed by a liquid solid separation process. Previously amorphous selenium particles were produced, which hampered recovery. In this research it is demonstrated that at a higher temperature, around 40 - 50°C, and at a higher pH, around pH 8 - 9, a more hexagonal selenium structure can be produced (Chapter 3). Crystalline acicular selenium particles of different sizes were thus obtained. This implies that selenium particles formation can be controlled and that selenium particles can grow. Large selenium particles make the separation process economic.

To grow larger selenium particles, a long-term experiment was performed at 50°C (Chapter 4). The reduction rate was poor, but selenium acicular particles were produced. These particles were also detected as clusters. These clusters open up new recovery opportunities. With Eerbeek sludge the optimal conditions for selenate conversion are around pH=7 and 30°C. To enlarge the selenium particles it is strongly recommended to use a different sludge since the optimal conditions with Eerbeek sludge do not match the conditions needed for acicular particle formation.

When selenate is converted to selenite, the selenite can be precipitated by sulphide to form selenium sulphide. Emmtec sludge was used to reduce the sulphur compounds to sulphide, leaving selenium as the sole remaining element. This process was performed at T=30°C and a pH between 6 and 7. The selenium thus recovered had a crystalline hexagonal structure (revealed by x-ray diffraction) and the particles were as large as 125µm<sup>3</sup>.

Future research on the two routes that are explored in this thesis can give insights into selenium reduction mechanisms and the formation of large selenium particles. The recoverability of biological selenium particles has also been improved (as discussed in this thesis). In conclusion, this thesis has resulted in a new, bio-selective, renewable selenium recovery method via selenium sulphide.

## **List of publications**

### **Peer reviewed publication**

Hageman, S. P., van der Weijden, R. D., Weijma, J., & Buisman, C. J. (2013). Microbiological selenate to selenite conversion for selenium removal. *Water research*, 47(7), 2118-2128.

### **Conference proceeding**

Hageman, S.P.W., Weijden, R.D. van der, Weijma, J., Buisman, C. J.N., (2011), Control of Biologically Produced Selenium Particle Properties for Selenium Recovery and Re-Use EMC Conference Dusseldorf.





## Acknowledgements

Writing this thesis has been difficult at times and I wouldn't have been able to do this without the support of many. Because it was so difficult, it was probably also a longer trip than planned for my supervisors. Their support was enormous. Renata, all of our conversations about bio-crystallization should be written down, now we only have one PhD-research as a result 😊, thank you for your creative and social support. That has been very important to me. Fons, the enormous amount of knowledge you have about sciences really helped me to go up-hill at the toughest moments in this whole process (winter and spring 2015). Cees, you kept me focussed on the goal of the research: produce the big selenium particles, always believing in me and inspiring me. Thank you all three for being my (co)-promotors. Jan and Philippe, both of you thank you for recognizing opportunities in my research results.

All the people from ETE, I will miss you and also especially the things connected to some persons (for sure I will forget some). First of all I want to thank the Biotechnion for the thick walls and toilet-areas. Alex, "Hé collega", not to forget Vinnies and Bert's back-offices in the Biotechnion (the A-team for getting reactor equipment). Els, thank you for the supporting Bassie and Adriaan lunch walks. Annemiek, thank you for supporting my personal development in research. Ilse, special thanks to the help in the Heavy Metall lab in combination with "Goede dag meneer Jean" "Goede dag meneer Simon", Mieke for the laughter and the weekly puzzle coffee breaks (Boerenbruiloft), Magdalena, thank you for the laughs we had and I think we will win a gold medal in the next mixed bob-sleigh tournaments, but the helicopters are still difficult to get rid of. Christel, Ralph and Tim, thank your general support and lunchwalks around the Biotechnion and the Technotron. Liesbeth and Katja, thank you for helping me out with a lot of questions about the ETE. Ingo, thank you for the beers and being the Canadian roommate. Marjo, thank you for your laughs during the coffee-break and hopefully I will be invited for the Veluwe-loop or other runs. Diego, thank you for saving the environment by walking without shoes and socks.

Iris, it was an honour to mentor you during your internship. Especially your propositions were impressive and they "staan of vallen" bij een goede verdediging.

Paula, ola amiga. We worked a lot together but never in the same project. I think we have to do that some time, since working with you anywhere anytime was always very enjoyable. From Dusseldorf to Praag and from Wageningen to Leeuwarden. Thank you for all your help.

Marieke, my Master is a long time ago, but you helped me to keep up the good things. Scientifically and also as a friend. Thank you for being and supporting me on the stage. It is an honor to have you here as a paranymp.

Pake en Beppe, hartelijk dank voor het oppassen en de ondersteunende gesprekken. Jullie hartelijkheid en duidelijkheid is erg prettig.

Lieve Papa en Mama, ik ga nu straks promoveren in plaats van afstuderen. En eigenlijk is dat thuis al begonnen, jullie hebben me alles meegegeven om te kunnen promoveren. De basis is toch dat ik thuis veel stiekem kon experimenteren, waarvan ik een paar experimenten niet meer durf te herhalen gezien het gevaar. Dank jullie wel voor alle steun.

Marieke en Jurre, wat moet ik schrijven? Het werk is niet altijd makkelijk geweest en dan nam ik het weleens naar huis. Jullie hebben me geforceerd om maar eens meer te ontspannen. Dat is gelukt! Ik ben zo blij met jullie dat dit niet op papier uit te drukken is.

## About the author

Simon Hageman was born in 1977 in Didam, The Netherlands. During his youth he was already a real science wiz kid: using salt water in combination with electric power, breaking open old batteries out of curiosity and doing other “scientific experiments”. After completing the secondary education (VWO) in 1996 he studied Biotechnology at the Wageningen University. During his study he kept a broad interest in several fields, bioreactors, chemistry, microbial conversions and



environment research questions. During the final phase of the study, the production of bio hydrogen and the production of plasmid DNA for gene therapy was researched. Another field of interest has always been education. For that reason he developed education material for secondary schools, of course with a scientific subject. But after that he could not leave the lab for a long time and tried to improve yield during fermentation

processes with a microbial fuel cell. This work was so attractive, that he continued the lab and educational work with a PhD research on selenium biocrystallization. The combination of research and education gives him a lot of positive energy which is why he enjoys his current job: lecturer and researcher for Saxion, University of Applied Sciences, Enschede, in the department of sustainable energy.



*Netherlands Research School for the  
Socio-Economic and Natural Sciences of the Environment*

# D I P L O M A

*For specialised PhD training*

The Netherlands Research School for the  
Socio-Economic and Natural Sciences of the Environment  
(SENSE) declares that

***Simon Petrus Wilhelmus Hageman***

born on 3 November 1977 in Didam, The Netherlands

has successfully fulfilled all requirements of the  
Educational Programme of SENSE.

Wageningen, 23 October 2015

the Chairman of the SENSE board

Prof. dr. Huub Rijnaarts

the SENSE Director of Education

Dr. Ad van Dommelen

*The SENSE Research School has been accredited by the Royal Netherlands Academy of Arts and Sciences (KNAW)*



K O N I N K L I J K E N E D E R L A N D S E  
A K A D E M I E V A N W E T E N S C H A P P E N



The SENSE Research School declares that **Mr Simon Hageman** has successfully fulfilled all requirements of the Educational PhD Programme of SENSE with a work load of 43.9 EC, including the following activities:

#### SENSE PhD Courses

- o Environmental Research in Context (2010)
- o Speciation and Bioavailability (2011)
- o Research in Context Activity: 'Co-developing and organising try out course for OLI software and preparing a Selenium example', Wageningen University (2013)

#### Other PhD and Advanced MSc Courses

- o Teaching and Supervising Thesis Students, Wageningen University (2010)
- o Techniques for Writing and Presenting a Scientific Paper, Wageningen University (2011)
- o Matlab Introductory Course, Wageningen University (2011)
- o Writing Grant Proposals, Wageningen University (2013)
- o OLI Stream Analyzer, Wageningen University (2013)

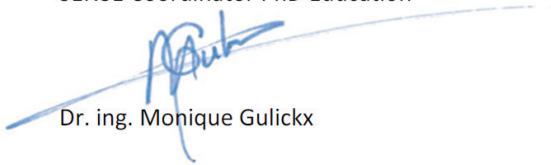
#### Management and Didactic Skills Training

- o Informing students at the Education Convention and Refresher Seminar, Wageningen University (2009-2010)
- o Head of the lab 151 in Biotechnion, Wageningen University (2009-2011)
- o Assisting practicals of the MSc course 'Introduction Environmental Technology' (2009-2012)
- o Organising Mineral Discussion Group, Environmental Technology department, Wageningen University (2009-2012)
- o Supervising internship vocational student (2010-2011)
- o PhD-representative Rehousing Committee of Department Environmental Technology, Wageningen University (2010-2011)

#### Oral Presentations

- o *Control of biologically produced selenium particle properties for selenium recovery and re-use.* Conference EMC 2011, 26-29 June 2011, Dusseldorf, Germany
- o *PhD Bio-selenium recovery.* PhD trip Environmental Technology Department, 2-16 June 2012, Toronto, Canada

SENSE Coordinator PhD Education



Dr. ing. Monique Gulickx

## **Colophon**

Financial support from Wageningen University for printing this thesis is gratefully acknowledged.

The cover of this thesis was provided by Roberto van Zwieten (Famous)

This thesis was printed by Gildeprint Drukkerijen, Enschede, The Netherlands